# Mathematical modeling of tuberculosis epidemiology in Ethiopia.

**Ashenafi Kelemu Mengistu**


UNIVERSITY *of the*
WESTERN CAPE

A thesis submitted in partial fulfilment of the requirement for the degree of Doctor of Philosophy in the Department of Mathematics and Applied Mathematics at the Faculty of Natural Sciences, University of the Western Cape.

**Supervisor: Prof Peter J. Witbooi**

February, 2024

## Keywords

- Tuberculosis;
- BCG vaccination
- Basic reproduction number
- Disease-free equilibrium point
- Endemic equilibrium point
- Local and global stability
- Lyapunov function
- Ethiopia
- Saturated incidence rate
- Optimal control
- Incremental cost-effectiveness ratio
- Prison TB model
- Inflow of infecteds

# List of Publications

Part of this thesis has been published or submitted for publication in the form of the following research articles to international journals.

1. Ashenafi Kelemu Mengistu, Peter J. Witbooi, "Modeling the Effects of Vaccination and Treatment on Tuberculosis Transmission Dynamics", Journal of Applied Mathematics, vol. 2019, Article ID 7463167, 9 pages, 2019. https://doi.org/10.1155/2019/7463167

2. Ashenafi Kelemu Mengistu, Peter J. Witbooi, "Mathematical Analysis of TB Model with Vaccination and Saturated Incidence Rate", Abstract and Applied Analysis, vol. 2020, Article ID 6669997, 10 pages, 2020. https://doi.org/10.1155/2020/6669997

3. Ashenafi Kelemu Mengistu, Peter J. Witbooi, "Tuberculosis in Ethiopia: Optimal Intervention Strategies and Cost-Effectiveness Analysis", Axioms 2022, 11, 343. https://doi.org/10.3390/axioms11070343

4. Ashenafi Kelemu Mengistu, Peter J. Witbooi, "Cost-Effectiveness Analysis of the Optimal Control Strategies for Multi-drug-Resistant Tuberculosis Transmission in Ethiopia", International Journal of Differential Equations, vol. 2023, Article ID 8822433, 15 pages, 2023. https://doi.org/10.1155/2023/8822433

5. Ashenafi Kelemu Mengistu, Peter J. Witbooi, "A model of the disease dynamics of Tuberculosis in a prison system: the case of Ethiopia", Submitted for publication.

# List of abbreviations

- **AIDS**: Acquired immunodeficiency syndrome
- **ANOVA**:Analysis ofVariance
- **BCG**: Bacillus Calmette-Guérin
- **CDC**: Centers for Disease Control and Prevention
- **COVID**: Corona Virus Disease
- **DFE**: Disease Free Equilibrium
- **DS-TB**: Drug-Susceptible Tuberculosis
- **DOT**:Directly observed therapy
- **EEP**: Endemic Equilibrium point
- **HDMR**: High Dimensional Model Representation
- **HIV**: Human Immunodeficiency virus
- **ICER**: Incremental Cost-Effectiveness Ratio
- **INH**: isoniazid
- **IRIS**:Immune Reconstitution Inflammatory Syndrome
- **LHS**: Latin Hypercube Sampling
- **MDR-TB**: multi-drug-resistant tuberculosis
- **Mtb**: Mycobacterium tuberculosis
- **ODE**: Ordinary Differential Equation
- **PRCC** : Partial Rank Correlation Coefficient
- **PSS**: Parameter Sensitivity Spectrum

- **RIF**:rifampin
- **SA**: Sensitivity Analysis
- **SEIL**: Susceptible- Exposed- Infected- Latently infected
- **SEIR**: Susceptible- Exposed- Infected- Recovered
- **SIR**: susceptible-infected- recovered
- **SHM**: Sensitivity Heat Map
- **SVELI**: Susceptible- Vaccinated-Exposed- Latently infected-Infected
- **TB**: Tuberculosis
- **WHO**: World Health Organization

# Declaration

As the author of the mathematical modeling of tuberculosis epidemiology in Ethiopia, I declare that it is completely original, has not been submitted for a degree or examination at any other university, and has been referenced properly.

Ashenafi Kelemu Mengistu

Signed

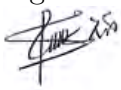

February, 2024

# Acknowledgments

First and foremost, I would like to thank my supervisor, Professor Peter Witbooi, for his invaluable guidance and continual encouragement throughout the research work. His quick understanding of the problem and his suggestions for solutions were very helpful.

Secondly, I would like to thank Woldia University and the Ethiopian Ministry of Education for the financial support I received for my doctoral studies.

I would also like to take this opportunity to thank my mum, Ayehu Gebo, for her unwavering support, which has been the foundation of my educational success from the beginning to the end of my PhD journey. Her tireless efforts and sacrifice were crucial at every stage of my academic career.

Finally, I would like to thank my wife, Yimegn Ayenew. It would not have been possible to complete my PhD without her tireless support and encouragement. Her dedication and belief in my abilities has motivated me to overcome challenges and celebrate successes.

# Abstract

Tuberculosis (TB) is currently one of the most severe public health issues in Ethiopia and many other countries. Despite demanding efforts having been made by governmental and nongovernmental organizations to eliminate tuberculosis, it is still a severe health problem in Ethiopia. It is one of the significant causes of mortality and morbidity.

Scientific studies of the dynamics of tuberculosis play an essential role in eliminating it, and mathematical models contribute significantly to this effort. Mathematical models have been used for decades to study tuberculosis's transmission dynamics and develop strategies to prevent TB spread in various countries. However, there are insufficient intensive studies of TB dynamics using mathematical models in Ethiopia. This thesis aims to develop a modified TB dynamics model and propose an optimal TB prevention and control strategy for Ethiopia. The study examined five different scenarios.

In the first scenario, a mathematical model for the transmission dynamics of TB by including BCG vaccination for newborns is developed. The global stability of the disease-free equilibrium point is determined using the Lyapunov theory. Sensitivity coefficients of the reproductive number are calculated to examine control measures' effectiveness. The results quantify the positive influence of vaccination and the treatment for high-risk latent and active TB patients on tuberculosis control.

The second instance incorporates a saturated incidence rate on the previous model. Positive solutions to the model are shown to exist and be unique. The stability of the equilibria is established. It is found that the most effective methods to control the spread of tuberculosis in Ethiopia are through minimizing the contact between TB-infected and susceptible individuals and increasing access to treatment for latently infected individuals.

Furthermore, three time-dependent controls (distancing, case holding, and case-finding) are introduced into a TB model to find an optimal control strategy that minimizes the number of exposed and infected populations in Ethiopia with minimal cost. The conditions for achieving the optimal controls are derived and solved

numerically using Pontryagin's principle. Besides, a cost-effectiveness analysis is carried out using an incremental cost-effectiveness ratio (ICER). For optimal and cost-effective TB control, it is recommended that the Ethiopian government focuses more on preventative measures such as isolating infected individuals, diagnosing patients with the disease early on, and implementing treatment and education programmes.

The fourth scenario identified the effective strategies for combating MDR-TB in Ethiopia. Among single control strategies, it is found that successful treatment of drug-susceptible tuberculosis (DS-TB) is the most effective control factor for controling MDR-TB transmission in Ethiopia. Furthermore, within the six dual-control strategies, the combination of distancing and successful treatment of DS-TB is less costly and more effective than other strategies. Finally, out of the triple control strategies, the combination of distancing, successful treatment for DS-TB, and treatment for MDR-TB is the most efficient strategy for curbing the MDR-TB disease in Ethiopia.

Finally, a mathematical model is developed to describe the population dynamics of tuberculosis in a prison system. The model includes the inflow of exposed and TB infective inmates. Further, the model parameters are calibrated based on the epidemiological data of Ethiopia.

# List of Figures

# Table of Contents

# Chapter 1

# General Introduction

## 1.1 Tuberculosis

Tuberculosis (TB) is a highly contagious airborne disease caused by Mycobacterium. When an infected person coughs, sneezes, spits, or talks, the bacteria that cause tuberculosis are released into the air and inhaled by others exposed to it [1], in addition to the lungs, TB can affect the kidneys, spine, brain, bones, and joints [2]. The most common symptoms of TB are a persistent cough that lasts up to three weeks, fever, fatigue, night sweats, and weight loss [3].

The early phase of a tuberculosis infection is called the latent phase. An individual at this phase does not show symptoms and is non-contagious to others. According to Cohen et al., [4], one-fourth of the world's population already has latent TB infection. Tuberculin skin tests or blood tests are used to diagnose latent TB. Most latent TB patients will stay long without progressing to the next stage. But persons infected with HIV and other diseases, persons within the first two years after infection, and children are at high risk for progressing from latent TB to the second stage of infection [5].

The second stage of infection is called active TB infection. Individuals show some or all TB symptoms at this stage, which can infect susceptible people. Chest X-ray screening can identify active tuberculosis. Its treatment requires long-term antibiotics for at least six months and is highly effective if the patient takes their treatment properly [6].

Tuberculosis can be classified into two types based on its response to drugs: drug-susceptible TB (DS-TB) and multi-drug-resistant TB (MDR-TB). DS-TB is a type of tuberculosis that can be treated with the usual medicines. MR-TB, on the other hand, is resistant to at least two medications, isoniazid (INH) and rifampin (RIF) [7]. The improper treatment of DS-TB patients and poor management of the supply and quality of drugs can lead to the bacterium acquiring multi-drug-resistant tuberculosis [8, 9].

Multi-drug-resistant tuberculosis is more difficult to treat than drug-resistant tuberculosis. It requires the use of second-line drugs for up to two years. These drugs are more costly and cause more side effects. Additionally, because it takes longer to recover from MDR-TB, this may result in more people being infected [10]. The best way to stop the spread of MDR-TB is to take all DS-TB drugs as directed by physician [7].

## 1.2 Background of Study

Tuberculosis is the leading cause of death from infectious diseases worldwide. Each year, 10 million people are infected with tuberculosis. Even if TB is preventable and treatable, it kills 1.5 million people annually [11]. The spread of the disease is high in Africa, and in 2019, the region had an estimated 2.5 million tuberculosis cases, accounting for 25% of the global burden. Moreover, more than 500,000 Africans die from this disease annually [12].

Ethiopia has a high burden of tuberculosis, with an estimated incidence of 140 per 100,000 and a mortality rate of 21 per 100,000 in 2019. This disease is one of the country's top 10 causes of death [13, 14].

By 2030, the World Health Organisation (WHO) hopes to have eliminated TB globally [14]. Hence, improved research is needed to develop effective control strategies. Understanding the dynamics of TB transmission is essential for predicting the future characteristics of the disease and planning reliable control intervention programs [15]. Mathematical models are one of the tools used to study the dynamics of infectious diseases [16], and they have been used to study the dynamics of TB transmission in different countries (e.g., [17–21]). However, there is no such inten-

sive study of TB dynamics in Ethiopia using mathematical models. Therefore, this thesis aims to develop modified TB dynamics models and propose an optimal TB prevention strategy for Ethiopia.

## 1.3 Literature on the modeling of tuberculosis

Mathematical models for tuberculosis transmission dynamics have become increasingly important in recent years. Waaler developed the first TB model in 1923 [22]. This model was based on a simple mass-action law and provided a basic understanding of the dynamics of TB transmission. Since then, many other mathematical models have been developed for more complex factors, such as the effects of vaccination, treatment, drug resistance, etc. The following are some of the models that were developed based on these factors:

***Age structure***

Purwati et al. [23] developed a discrete age-structured model of tuberculosis transmission. They investigated the existence and stability of the model equilibria based on the basic reproduction number. They also conducted a sensitivity analysis of the model parameters. Finally, they applied an optimal control strategy and found that combining TB prevention and treatment is the most cost-effective strategy.

Lee et al. [24] developed a mathematical model to evaluate the effects of TB management interventions on TB transmission dynamics in Korea. Their model included two age groups ($< 65$ years and $\geq 65$ years). The model parameters were estimated using TB epidemic data from 2001 to 2018. Their results indicated that age-specific interventions are required to reduce the overall incidence of TB. In addition, they recommended that intensive treatment efforts be focused on older people. However, the early detection and treatment rates for latent TB were the most important factor in reducing TB incidence in both age groups.

Zhao et al. [25] developed a susceptible-exposed-infectious-recovered (SEIR) epidemic model by age group that includes three categories: children, middle-aged, and older people, to investigate the role of age in tuberculosis transmission in mainland China from 2005 to 2016. The study findings indicate that different age groups have

distinct effects on TB transmission. The authors recommended two effective measures to achieve the goals of the WHO End TB Strategy: increasing the recovery rate and reducing the infectious rate of the elderly population.

***Vaccination***

Yang et al. [26] used a mathematical model to analyse the impact of treatment and vaccination on the dynamics of TB transmission. Their study incorporated a control term, evaluated the cost of control strategies, and performed an optimal control analysis using Pontryagin's maximum principle. Their study concludes that the vaccination strategy must be implemented at the highest level.

Nkamba et al. [27] evaluated the impact of vaccination on the spread of TB using a deterministic epidemic SVELI model. Using the Lyapunov Lasalle method, they analyzed the stability of the epidemic system around the equilibria (disease-free and endemic). Using TB data from Cameroon, they concluded that vaccination coverage is insufficient to control TB, and effective contact rate significantly impacts the spread of TB.

Aldila et al. [28] constructed a deterministic model for the dynamics of TB transmission with the intervention of vaccination. Ten-dimensional ordinary differential equations were used to develop the model using the SEIR method. They concluded that the vaccination strategy effectively suppresses the spread of tuberculosis.

***HIV-TB co-infection***

To study the effect of TB on the spread of HIV infection, Naresh et al. [29] constructed a nonlinear mathematical model. They found that as the number of TB infections decreases due to recovery, the number of HIV infections also decreases, and the endemic equilibrium approaches the TB-free equilibrium. Their model also revealed that the number of AIDS patients decreases if TB is not associated with HIV infection.

Awoke and Kassa [30] developed a mathematical model to study the transmission of TB-HIV/AIDS co-infection. Their results showed that the optimal combination of prevention and treatment controls would suppress the prevalence of both HIV and TB to below 3% within ten years. Furthermore, they found that the treatment control is more effective than the preventive controls.

To investigate the effects of early and late HIV therapy throughout the TB treatment course on new HIV infections, HIV-related deaths, and IRIS cases, Mallela et al. [31] created a mathematical model. Their findings imply that disease eradication cannot be achieved only through co-infection treatment programmes. Each disease must be treated separately for successful eradication.

***Drug-resistant strains***

Liu et al. [32] developed a mathematical model that includes multi-drug-resistant (MDR) and undetected TB cases. They used the model to simulate and predict the TB epidemic in Guangdong. Their results showed that the undetected rate plays a vital role in the TB trend. They also concluded that TB could not be eradicated if current TB control strategies are continued.

To understand the dynamics of drug-susceptible and multi-drug resistant TB transmission, Kuddus et al. [33] constructed a two-strain TB mathematical model and fitted it to the Bangladesh TB data. Within optimal control, they examined the cost-effectiveness of combinations of the four fundamental control methods of distancing, case finding, case holding, and case finding. According to their study findings, the most cost-effective way to reduce the burden of TB is to employ a quadruple control method that incorporates latent case finding, active case finding, distancing, and case holding.

Trauer et al. [34] presented a model of two strains of drug-resistance and drug-sensitive TB for highly endemic countries of the Asia Pacific. They found that the detection and treatment rate are the most critical determinants of disease rates with each strain, while vaccination rates are less important. Moreover, the finding of their study showed that improved treatment of drug-susceptible TB did not result in decreased rates of MDR-TB through prevention of *de novo* resistance but instead resulted in a modest increase in MDR-TB through strain replacement.

***Effect of migrants***

Jia et al. [35] presented two models to examine how immigration may affect tuberculosis transmission dynamics. They applied the model to reported tuberculosis data from Canada. They indicated that the disease does not disappear and becomes endemic in the host area. They also suggested that immigrants considerably

influence tuberculosis's overall transmission dynamics behavior.

Guo and Wu [36] developed a simple compartmental TB model with constant immigration. They tried to investigate the impact of new immigrants with latent TB on the overall TB incidence. Their result showed that new immigrants in the early latent stage have a much more significant impact on the TB incidence of the foreign-born population in an immigrant country than those in the late latent stage.

***TB in Semiclosed Communities***

The semi-closed communities are enclaves where residents may maintain daily contact for several weeks, months, or even years. These communities can include refugee camps, schools, and prisons. Such settings exacerbate the spread of tuberculosis. Following are some of the studies that have considered these factors.

Vyambwera and Witbooi [37] proposed a two-group epidemic model to study the dynamics of tuberculosis in a prison system. They showed that the disease-free equilibrium is globally stable using a Lyapunov function. Additionally, they applied the model to reported South African data on tuberculosis and found that the model predictions agreed with the data.

Buonomo and Lacitignola [38] studied a four-compartment tuberculosis model that includes exogenous reinfection. They derived sufficient conditions on the parameters of the system that guarantee the occurrence of backward bifurcation. They also discussed the global stability of the endemic equilibrium using a generalization of the Poincaré–Bendixson criterion. They applied the model to the internally displaced people's Camps in North Uganda.

## 1.4 Literature on tuberculosis modeling in Ethiopia

Mathematical models are powerful tools for understanding the factors that contribute to the spread of TB and can be used to design and evaluate interventions to control the disease. However, such studies are rare in Ethiopia.

One of the mathematical models of TB epidemiology in Ethiopia was developed by Debebe et al. [39]. This model was used to quantify the role of geospatial hotspots in the spread of tuberculosis in rural Ethiopia. They found that the role of hotspots in the geospatial spread of tuberculosis in rural Ethiopia is limited,

suggesting that tuberculosis transmission is mainly local. However, the authors did not demonstrate the biological feasibility of the model solutions (i.e., the uniqueness and positivity of the solutions). The long-term behavior of the model (which can be achieved through global equilibrium stability) was not also discussed.

Another mathematical model of TB epidemiology in Ethiopia was developed by Kereyu and Demie [18]. This model was used to study the effect of distancing, case finding, and treatment strategies in controlling tuberculosis in the Haramaya district of Ethiopia. The authors found that combining all control measures (distancing, case finding and treatment) is the most effective strategy to eradicate tuberculosis in the community at an optimal level with minimal intervention costs. Their research was limited to a single Ethiopian district. However, in our thesis, we study the transmission dynamics of TB in the country by using data from Ethiopia as a whole. We also pointed out effective strategies to control the disease.

Sileshi [40] developed a mathematical model to study drug-resistant tuberculosis transmission dynamics in Ethiopia. The researcher found that treatment at early and latent stages stops drug-susceptible tuberculosis. Although the researcher claimed to have studied MDR-TB transmission in Ethiopia, he did not use Ethiopian data to estimate the variables and parameters. However, in our thesis, we estimated the variables and parameters in the model using Ethiopian health data.

The previous studies on the mathematical modeling of TB epidemiology in Ethiopia have the following gaps.

- The models have not been validated using real-world data.
- The models have not been used to study the impact of new TB control interventions.
- The models have not been used to study the cost-effectiveness of different TB control strategies.

Our thesis addresses these gaps by focusing on:

- Validating the models using real-world data.

- Using the models to study the impact of vaccination, distancing, case finding and treatment control interventions.
- Using the models to study the cost-effectiveness of different TB control strategies.

## 1.5 Objectives of the Study

The main objective of this thesis is to develop modified TB dynamics models and propose optimal TB prevention and control strategies for Ethiopia.

The specific objectives of this thesis are to:

- develop a mathematical model and analyze the effect of vaccination and treatment in controlling the spread of TB disease in Ethiopia.
- propose a modified mathematical model and study the dynamics of DS-TB with a saturated incidence rate.
- propose efficient TB control strategies in Ethiopia.
- determine the most cost-effective strategy in combating multi-drug-resistant tuberculosis in Ethiopia.
- formulate and analyze a modified mathematical model for the dynamics of TB in the prison system.

# Chapter 2

# Introduction to Epidemic Modeling

## 2.1 Mathematical Modeling in Epidemiology

Epidemiology is the study of the incidence and spread of diseases. An epidemic is a widespread disease outbreak over a relatively short period. On the other hand, a disease is considered endemic when it persists within a specific population. The spread of infectious diseases is influenced not only by disease-related factors like the contagious agent, mode of transmission, latent period, infectious period, susceptibility, and resistance but also by various social, cultural, demographic, economic, and geographic factors.

Mathematical modeling uses mathematics to represent complex phenomena, such as physical objects, processes, and systems. It involves the application of mathematical principles and techniques to real-world problems to create mathematical equations that describe the system's behavior. Mathematical models can be used to predict the behavior of systems, analyze the effects of interventions, and optimize system performance. Some examples of mathematical modeling include financial modeling, epidemiological modeling, and climate modeling [41].

Epidemiological models are used to understand how infectious diseases spread within a population and to estimate how many people will get infected over time. The following steps are generally involved in modeling and developing epidemiolog-

ical systems [42]:

1. Based on the biological knowledge about the disease's pathogenesis and epidemiology, assumptions can be made about the disease transmission process. These assumptions involve considering factors such as the mode of transmission, infection stage, and various environmental factors.

2. Draw the transfer diagram and derive the mathematical equations based on these assumptions.

3. Perform mathematical analysis on the model to understand all possible qualitatively distinct model outcomes. This involves applying mathematical theories on stability and bifurcations.

4. Interpreting the mathematical findings within the modeling context allows us to gain insights into the disease transmission process based on the assumptions made in Step (1). These interpretations contribute to our understanding of how the disease spreads and provide valuable information about the implications of the assumptions made during the modeling process.

5. Gather disease data from public health agencies and research publications and verify the model's accuracy using the collected data.

6. Improve the model by adjusting the initial assumptions made in Step (1) to obtain a more precise comprehension of the disease progression.

Epidemic models can be classified as deterministic or stochastic systems. Deterministic models attempt to explain common occurrences within a population, making them suitable for large populations. The population is divided into compartments or classes in deterministic models, representing different epidemic stages. These models describe average population dynamics and are typically formulated as systems of differential equations (in continuous time) or difference equations (in discrete time).

Stochastic models, encompass environmental variations and treat disease infection as a random process. These perturbed models are particularly useful when analyzing small population groups with many infectious contacts [43].

## 2.2 Compartmental Models in Epidemiology

This section describes the procedure for constructing a mathematical model to depict the transmission process of an infectious disease using a compartmental approach. Our first step involves dividing the host population into mutually exclusive compartments based on the natural history of the disease. For example, for a simple infectious disease, possible compartments may be:

- ***Susceptible***: consists of individuals who are currently healthy but can potentially acquire the infection. The size of this class is represented by the variable $S$.
- ***Infected:*** individuals who have acquired the infection and are manifesting its symptoms. The numerical representation for the size of this category is denoted by the variable $I$.
- ***Removed***: individuals who have successfully recovered from the disease and are now immune, unable to contract it again. Typically, this category is represented by the variable $R$.

The fundamental purpose of epidemiological modeling is to illustrate how the number of individuals changes within each of the three classes at a specific time, $t$. To describe this dynamic process mathematically, we consider a short time interval, $[t, t+\delta t]$, and extract the transitions between the classes using Figure 2.1.

During this time interval, we assume that the overall change in each class is determined by the number of individuals entering the class minus the number leaving the same class. By applying the same logic to each class, we obtain the following equations:

$$\begin{cases} \Delta S\,(t) = \text{new susceptibles} - \text{new infections} - \text{removal from } S \\ \Delta I\,(t) = \text{new infections} - \text{transfer into } R - \text{removal from } I \\ \Delta R\,(t) = \text{transfer from } I - \text{removal from } R \end{cases} \tag{2.1}$$

We divide the two sides of these three equations by $\delta t$ and let $\delta t \to 0$, then the left-hand side will be the derivatives $S'(t), I'(t)$ and $R'(t)$ since we obtain the

following differential equations:

$$\begin{cases} S'(t) = \text{influx of new susceptibles} - \text{incidence rate} - \text{removal rate from } S \\ I'(t) = \text{incidence rate} - \text{transfer rate into } R - \text{removalrate from } I \\ R'(t) = \text{transfer rate from } I - \text{removal rate from } R \end{cases} \tag{2.2}$$

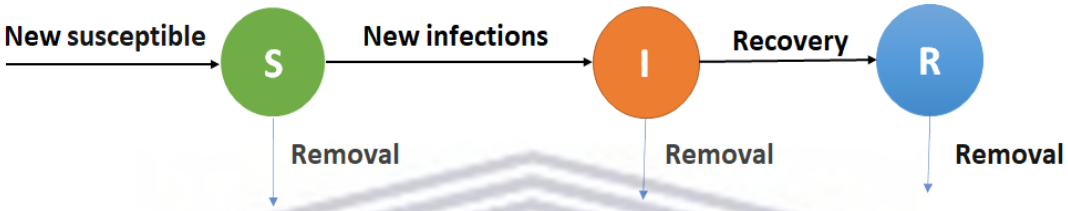


Figure 2.1: Transfer diagram for a simple compartment epidemic model

To develop a deterministic model in the form of an ordinary differential equation (ODE) system, we establish a set of assumptions based on the unique characteristics of the epidemic. Subsequently, we express the transfer rates on the right side of the equations as functions dependent on the variables $S(t)$, $I(t)$, and $R(t)$. The following section introduces a simple model that captures the dynamics of susceptible, infectious, and removed individuals to provide an illustrative example.

### 2.2.1 An example: The SIR model without demography

In order to illustrate the dependence of the rates in Equation (2.2) on $S(t), I(t)$, and $R(t)$, we make the following assumptions regarding the transmission mechanism of an epidemic.

- Only horizontal transmission, including airborne infections, food poisoning, and sexually transmitted diseases, is considered.
- Mixing in the population to be homogeneous, meaning that contact between two individuals in a population happens randomly with an equal probability of infection.
- Upon infection, infected individuals become infectious immediately without any latency period.

- Immunity is permanent in this scenario, and reinfection is not possible.
- No new susceptible individuals are entering the population, and no individuals are being removed from any compartments.
- The total host population remains constant.

A susceptible person becomes infected through contact with an infectious individual. The rate of individuals who become infected per unit of time is called the incidence rate, and the rate of change of the susceptible compartment is given by

$$S'(t) = -\text{incidence rate}.$$

To calculate the incidence rate, we consider two important factors:

- The probability that contact with a susceptible individual causes infection is denoted by $p$.
- The per capita contact rate is denoted as $c$.

We define the function $F(t) = \beta I(t)$ as the force of infection, where $\beta = pc$ represents the transmission rate. $F(t)S$ then gives the number of people who become infected per unit of time. This quantity is called the "mass action incidence," representing the simplest form of the various incidence expressions. Using this incidence rate approach, we can derive the following differential equation for susceptible individuals:

$$S'(t) = -\beta S(t)I(t).$$

The infected individuals class is denoted as $I(t)$. Additionally, individuals in the infected class recover at a constant rate $\gamma$. As a result, the differential equation for infected individuals takes the form:

$$I'(t) = \beta S(t)I(t) - \gamma I(t).$$

Individuals who recovered from the infected class and moved to the removed

class resulted in the differential equation:

$$R'(t) = \gamma I(t).$$

Finally, the entire model is shown in Figure 2.2 along with the associated system of differential equations:

$$\begin{cases} S'(t) = -\beta S(t) I(t) \\ I'(t) = \beta S(t) I(t) - \gamma I(t) \\ R'(t) = \gamma I(t) \end{cases} \tag{2.3}$$

with the initial values $S(0) = S_0 > 0, I(0) = I_0 \geq 0$, and $R(0) = R_0 \geq 0$.


Figure 2.2: Transfer diagram for an SIR epidemic model without demography.

By examining the first equation in the model (2.3), we observe that $S'(t) \leq 0$. As a result, $S(t)$ decreases, and its value remains less than or equal to $S_0$. Moving on to the second equation in the model (2.3), it can be deduced that $I'(t) = (\beta S(t) - \gamma)I(t)$. Then, we can establish the following two cases:

1. If $S_0 < \frac{\gamma}{\beta}$, we have $S(t) < S_0 < \frac{\gamma}{\beta}$, then $I'(t) < 0$ for all $t \geq 0$. Consequently, $I(t)$ strictly decreases, and then no pandemic can happen in this state.

2. If $S_0 > \frac{\gamma}{\beta}$, we have $S(t) > \frac{\gamma}{\beta}$ for $t \in [0, t^*)$ where $t^* > 0$. Consequently, $I(t)$ strictly increases for $t \in [0, t^*)$ and the pandemic occurs.

This shows the threshold definition, which is the value to be exceeded for an epidemic. In the same context, we consider the following expression $\beta \times S_0 \times \frac{1}{\gamma}$, which can be explained as:

Within the field of epidemiology, this crucial concept is referred to as the basic reproduction number, denoted as $R_0$. The reproduction number will be discussed in detail in chapter 3.

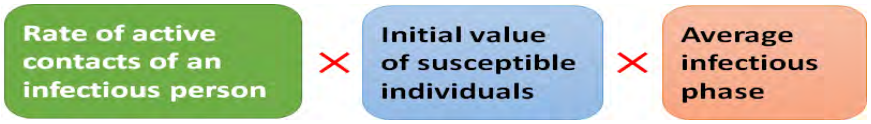


Comparing with the threshold phenomena mentioned above, we have the following conclusions:

- if $R_0 > 1$, then the disease dies out.
- if $R_0 < 1$, then the disease persists in the population.

The model (2.3) is based on the assumption that there are no changes in human demographics and that the population remains closed, excluding any births, deaths, or migration to and from the host population. This assumption appears so restricted and unrealistic. Demographics are one of the most significant factors that must be included in mathematical modeling. The following section will examine an improved model version, considering the population's demographic aspects.

### 2.2.2 An Example: The SIR model with demography

Epidemiological systems that do not consider the births and deaths that occur in the population are called epidemiological systems without demography. This system is essential for modeling diseases on a short time scale, especially for studying the transmission of childhood illnesses. However, there are several long-standing epidemics, like tuberculosis, AIDS, and hepatitis C, where the population undergoes significant changes over extended periods. In such cases, considering the population's demography becomes indispensable and cannot be disregarded.

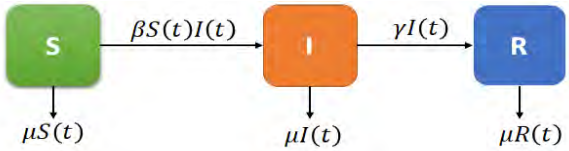


Figure 2.3: Transfer diagram for an SIR epidemic model with demography.

To include the demographics in the SIR epidemic model, we assume that all individuals are born as susceptible. Individuals in each class die at a per capita

mortality rate of $\mu$. The following system of ordinary differential equations gives the epidemic model with demography:

$$\begin{cases} S'(t) = \Lambda - \beta S(t) I(t) - \mu S(t) \\ I'(t) = \beta S(t) I(t) - \gamma I(t) - \mu I(t) \\ R'(t) = \gamma I(t) - \mu R(t) \end{cases} \tag{2.4}$$

The change of the total population is $N'(t) = \Lambda - \mu N(t)$, where $N(t) = S(t) + I(t) + R(t)$. The population size is not constant, but it is asymptotically constant since $N(t) \to \frac{\Lambda}{\mu}$ as $t \to \infty$.

Since $\lim_{t\to\infty} N(t) = \Lambda/\mu$, implies that the total number of species stabilizes at $\Lambda/\mu$. Hence, without loss of generality one can consider $\Lambda = \mu N$ so that system (2.4) can be written as follows:

$$\begin{aligned} S'(t) &= \mu N - \beta S(t) I(t) - \mu S(t) \\ I'(t) &= \beta S(t) I(t) - (\mu + \gamma) I(t) \\ R(t) &= \gamma I(t) - \mu R(t) \end{aligned} \tag{2.5}$$

with $R_0 = \frac{\beta N}{(\mu+\gamma)} = \frac{\Lambda\beta}{\mu(\gamma+\mu)}$.

Let

$$x(\tau) = \frac{S(t)}{N}, \quad y(\tau) = \frac{I(t)}{N}, \quad z(\tau) = \frac{R(t)}{N}, \quad \tau = (\mu+\gamma)t$$

It follows that

$$\begin{aligned} \frac{dx}{d\tau} &= \frac{dx}{dS}\frac{dS}{dt}\frac{dt}{d\tau}, \\ &= \frac{1}{N}[\mu N - \beta S(t) I(t) - \mu S(t)] \frac{1}{\mu+\gamma}, \\ &= \frac{1}{N}[\mu N - \beta (xN)(yN) - \mu (xN)] \frac{1}{\mu+\gamma}, \\ &= \frac{\mu}{(\mu+\gamma)N}(\mu N - \mu x N) - \frac{\beta N^2 xy}{(\mu+\gamma)N}, \\ &= \frac{\mu}{\mu+\gamma}(1-x) - \frac{\beta N}{(\mu+\gamma)} xy, \\ &= \rho(1-x) - R_0 xy. \end{aligned} \tag{2.6}$$

$$
\begin{aligned}
\frac{dy}{d\tau} &= \frac{dy}{dI}\frac{dI}{dt}\frac{dt}{d\tau}, \\
&= \frac{1}{N}[\beta S(t)I(t) - (\mu+\gamma)I(t)]\frac{1}{\mu+\gamma}, \\
&= \frac{1}{N}[\beta(xN)(yN) - (\mu+\gamma)(yN)]\frac{1}{\mu+\gamma}, \\
&= \left(\frac{\beta N}{(\mu+\gamma)}x - 1\right)y, \\
&= (R_0 x - 1)\, y.
\end{aligned} \tag{2.7}
$$

$$
\begin{aligned}
\frac{dz}{d\tau} &= \frac{dz}{dR}\frac{dR}{dt}\frac{dt}{d\tau}, \\
&= \frac{1}{N}[\gamma I - \mu R]\frac{1}{\mu+\gamma}, \\
&= \frac{1}{N}[\gamma(yN) - \mu(zN)]\frac{1}{\mu+\gamma}, \\
&= \frac{\gamma}{\mu+\gamma}y - \frac{\mu}{\mu+\gamma}z, \\
&= ay - bz.
\end{aligned} \tag{2.8}
$$

Thus

$$
\begin{aligned}
x'(\tau) &= \rho(1-x) - R_0 xy, \\
y'(\tau) &= (R_0 x - 1)\, y, \\
z'(\tau) &= ay - bz.
\end{aligned} \tag{2.9}
$$



Since the firs two equations of system (2.5) are independent of the variable $z$, it follows that $z(\tau) = 1 - x(\tau) - y(\tau)$. Therefore it suffices to study the following reduced system:

$$
\begin{aligned}
x'(\tau) &= \rho(1-x) - R_0 xy, \\
y'(\tau) &= (R_0 x - 1)\, y.
\end{aligned} \tag{2.10}
$$

The symbol $R_0$ represents the reproduction number. It is important to note that by employing this approach, we have effectively reduced the number of parameters involved from five to two. The dimensional form of the SIR model with demography is equivalent to its original counterpart, as both systems exhibit identical long-term behavior in terms of their solutions.

The long-term behavior of the model mainly depends on the equilibrium point.

The equilibrium point is the solution of the Equation (2.10) such that $x' = 0$ and $y' = 0$. Solving this simple system (2.10) found two possible equilibrium points:

- The disease-free equilibrium point $E_0 = (1, 0)$ is a state where no disease occurs. The disease-free equilibrium is also **boundary equilibrium** since it lies on the boundary of the feasible region $x \geq 0,\ y \geq 0$.
- Endemic equilibrium point $E_1 = (x^*, y^*)$, where $x^* = \frac{1}{R_0}$, and $y^* = \rho\left(1 - \frac{1}{R_0}\right)$. In this case, the epidemic cannot be stopped but remains in a population. The endemic equilibrium exists only in the case $R_0 > 1$. This equilibrium is also called an **interior equilibrium**.

# Chapter 3

# Mathematical Preliminaries

## 3.1 Well-posedness for ordinary differential equations

**Definition 3.1.1.** An initial-value problem is a first-order ordinary differential equation whose solution satisfies an initial constraint:

$$\frac{dx}{dt} = f\left(t, x(t)\right), x\left(t_0\right) = x_0, \tag{3.1}$$

where $t_0$ and $x_0$ are real numbers. An initial value problem is said to be well-posed when

- a solution exists,
- the solution is unique,
- the solution continously depends on its initial values.

The following theorem shows that the differential Equation (3.1) defines a well-defined initial value problem if $f(t, x)$ satisfies the Lipschitz condition.

**Definition 3.1.2** (Lipschitz condition [44])**.** Let $D$ denote the rectangular region in the $tx$-plane defined by

$$D : a \leq t \leq b, c \leq x \leq d, \tag{3.2}$$

where

$$-\infty < a < b < +\infty,$$

and

$$-\infty < c < d < +\infty.$$

We say that the function $f(t, x)$ is Lipschitz continuous in $x$ over $D$ if there exists a constant $k$, $0 < k < \infty$, such that

$$|f(t, x_1) - f(t, x_2)| \leq k |x_1 - x_2|, \tag{3.3}$$

whenever $(t, x_1)$ and $(t, x_2)$ belong to $D$. The constant $k$ is called a *Lipschitz constant.*

**Theorem 3.1.1.** ***(Picard-Lipschitz Theorem [44].)***

*Given the initial value problem, if $f(t, x)$ is continuous in $t$ and Lipschitz in $x$ in a neighbourhood of the initial point $t \in (t_0 - h, t_0 + h), x \in (x_0 - l, x_0 + l)$, then the ordinary differential equation has a unique solution on some (smaller) interval, $t \in (t_0 - r, t_0 + r)$, which depends continuously on $x_0$.*

## 3.2 Basic and Effective reproduction Number

A basic reproduction number, $R_0$, is crucial for assessing the transmissibility of infectious diseases. Theoretically, $R_0$ is defined as the average number of secondary cases generated by an individual primary case within a fully susceptible population during its entire infectious period [45, 46]. If $R_0$ is greater than 1, the outbreak continues as the infected person is expected to infect at least one other person on average. However, if $R_0$ is less than 1, the outbreak ends because the infected person is less likely to spread the infection.

The basic reproduction number is affected by several factors:

1. The rate of contacts in the host population
2. The probability of infection being transmitted during contact
3. The duration of infectiousness.

A population is rarely totally susceptible to infection in the real world. Some contacts will be immune, for example, if they have previously been infected and gained lifelong immunity or if they have previously been immunised. Consequently, not all contacts will become infected, so the average number of secondary cases per infectious case will be less than the basic reproductive number. This is measured by the effective reproductive rate ($R$). The effective reproductive number is the average number of secondary cases per infectious case in a population made up of both susceptible and non-susceptible hosts. In contrast to the basic reproductive number, the effective reproductive number reflects the actual immunity level in the population. Thus, $R$ can vary over time as immunity changes in the population. R will increase if susceptibles are introduced into the population and decrease if the proportion of susceptibles decreases through vaccination or subsequent immunity.

If the value of $R$ is less than 1, the disease will not persist in its transmission, as each infected individual will, on average, pass the infection to one or fewer people over time. Conversely, when R exceeds one, transmission escalates, leading to the spread of the epidemic until R drops below one, typically as the proportion of immune individuals rises [47].

In simple models, if there is only one infected compartment, the value of $R_0$ is the product of the infection rate and the duration of infection. In cases where there are one or more classes of infectives involved, the next-generation matrix method, as introduced by van den Driessche et al. [48] and Diekmann et al. [49], provides a comprehensive approach for determining the basic reproduction number ($R_0$). Consider the following scenario: $n$ compartments representing disease and $m$ compartments representing non-disease factors. Let $x \in \mathbb{R}^n$ denote the sizes of the disease compartments, and $y \in \mathbb{R}^m$ represent the sizes of the non-disease compartments. Additionally, we use $F_i$ to denote the appearance rate of new infections in compartment $i$. On the other hand, $V_i$ represents the transfer rate of individuals into or out-of-compartment $i$ by all other means. Then, the compartmental model can be written in the form:

$$\begin{cases} \frac{dx_i}{dt} = F_i(x,y) - V_i(x,y), & i = 1,2,3\ldots,n, \\ \frac{dy_i}{dt} = g_j(x,y), & j = 1,2,3,\ldots,m. \end{cases} \tag{3.4}$$

The calculation of the basic reproduction number is based on the linearization of the ordinary differential equations model about a disease-free equilibrium. At the same time, the following assumptions ensure the existence and well-posedness of a model.

1. Assume $F_i(0,y) = 0$ and $V_i(0,y) = 0$ for all $y \geq 0$ and $i = 1,2,3,...,n$. All new infections are secondary, arising from infected hosts.

2. $F_i(0,y) \geq 0$ for all non-negative $x$ and $y$ and $i = 1,2,3...,n$. The function $F$ represents the occurrence of new infections and should always have a non-negative value.

3. $V_i(0,y) \leq 0$ whenever $x_i = 0, i = 1,2,3,...,n$. Each component, $V_i$, represents a net outflow from compartment $i$ and must be negative (inflow only) whenever the compartment is non-empty.

4. Assume $\sum_{i=1}^{n} V_i(x,y) \geq 0$ for all non-negative $x$ and $y$. The sum represents the total outflow from all infected compartments. Terms in the model that contribute to an increase in $\sum_{i=1}^{n} x_i$ are assumed to signify secondary infections and, as a result, should be included in the function $F$.

5. Assume the disease-free system $\frac{dy}{dt} = g(0,y)$ has a unique equilibrium that is asymptotically stable. That is all solutions with initial conditions of the form $(0,y)$ approach a point $(0,y_0)$ as $t \to \infty$. This point is referred to as the disease-free equilibrium.

Assuming that $F_i$ and $V_i$ meet the above conditions, we can form the next generation matrix (operator) $FV^{-1}$ from matrices of partial derivatives of $F_i$ and $V_i$ particularly

$$F = \left[\frac{\partial F_i(x_0)}{\partial x_j}\right] \text{ and } V = \left[\frac{\partial V_i(x_0)}{\partial x_j}\right], \tag{3.5}$$

where $i, j = 1, 2, 3..., m$ and where $x_0$ is the disease-free equilibrium. The $R_0$ is given by the spectral radius (dominant eigenvalue) of the matrix $FV^{-1}$.

## 3.3 Stability analysis

Finding a general solution to the model may be challenging. However, numerical simulations are capable of providing approximate solutions with fixed parameters. In such scenarios, stability analysis emerges as a valuable tool for understanding the long-term behavior of the solution.

Local and global stability are the two common types of stability analysis. Local stability examines the behavior of the model's solution close to an equilibrium point, whereas global stability characterizes solution behavior across the entire domain. To define stability analysis more precisely, we provide a few definitions and related theorems below, which will be used in the subsequent chapters.

**Definition 3.3.1** (Equilibrium and stability [50])**.**

A point $x^*$ is an equilibrium solution of Equation (3.1) if $f(t, x^*) = 0$. We say an equilibrium point is

1. locally stable, if for every $R > 0$ there exists $r > 0$, such that

$$\|x(0) - x^*\| < r \Longrightarrow \|x\,(t) - x^*\| < R, t \geq 0.$$

2. locally asymptotically stable, if locally stable and

$$\lim_{x \to \infty} x\,(t) \; = x^*.$$

3. globally asymptotically stable, asymptotically stable for all $x(0) \in \mathbb{R}^n$.

### 3.3.1 Linearization and local stability criterion

This section presents a criterion for confirming the locally asymptotically stability of an equilibrium point, $x^*$, to a n-dimensional first-order system of differential

equations.

$$\dot{x} = f(x). \tag{3.6}$$

Before stating the stability criterion for system (3.6), it is essential to linearize the system about the equilibrium point. It is assumed that $f(x)$ has continuous second-order partial derivatives in a neighbourhood of $x^*$. Then, applying a Taylor series expansion about the equilibrium yields

$$f(x) = f(x^*) + Df(x^*)(x - x^*) + R(\overline{x}) = Df(x^*)(x - x^*) + R(\overline{x}), \tag{3.7}$$

where $Df(x^*)$ is the matrix of first-order partial derivatives of $f(x)$ evaluated at $x^*$. If $f = (f_1,\ f_2,\ \ldots,\ f_n)$ and $x = (x_1,\ x_2,\ \ldots,\ x_n)$, then the matrix is given by

$$Df(x) = \begin{bmatrix} \frac{\partial f_1}{\partial x_1} & \frac{\partial f_1}{\partial x_2} & \cdots & \frac{\partial f_1}{\partial x_n} \\ \frac{\partial f_2}{\partial x_1} & \frac{\partial f_2}{\partial x_2} & \cdots & \frac{\partial f_2}{\partial x_n} \\ \vdots & \vdots & \ddots & \vdots \\ \frac{\partial f_n}{\partial x_1} & \frac{\partial f_n}{\partial x_2} & \cdots & \frac{\partial f_n}{\partial x_n} \end{bmatrix}.$$

The remainder is $R(\overline{x})$ where $\overline{x}$ is some value dependent on $x$ and $x^*$ and includes the second and higher-order terms of the original function. The linearized system is

$$\dot{x} = Df(x^*)(x - x^*),$$

but we can make the change of variables $y = x - x^*$ and consider instead

$$\dot{y} = Ay, \tag{3.8}$$

where $A = Df(x^*)$.

The stability of the linear system (3.8) can be determined by the eigenvalues of the matrix $A$ which are the roots to the polynomial $p(\lambda) = \det(A - \lambda I) = 0$ where $I$ is the identity matrix. An eigenvector $v$ corresponding to an eigenvalue $\lambda$ is a nonzero vector for which $Av = \lambda v$. The eigenvalues can be real or complex-valued. If $\lambda = \alpha + \ell\beta$ is an eigenvalue, written as a complex number, the real part of $\lambda$ is

the real number $\alpha$.

**Stability of the Linear System**

1. The system (3.8) is stable at $x^*$ if all the eigenvalues of $A$ have negative real part.

2. The system (3.8) is unstable at $x^*$ if at least one eigenvalue of $A$ has positive real part.

3. Suppose that the eigenvalues of $A$ all have real parts that are zero or negative. List those eigenvalues with zero real part as $\lambda_j = \ell\beta_j$ for $1 \leq j \leq \ell$. Let the multiplicity of $\lambda_j$ be $m_j$ ; that is, $p(\lambda) = (\lambda - \lambda_j)^{m_j} q(\lambda)$ where $q(\lambda_j) \neq 0$. Every solution is stable if $A$ has $m_j$ linearly independent eigenvectors for each $\lambda_j$. Otherwise, every solution is unstable.

**Theorem 3.3.1.** ***(Linearization Theorem [51]).*** *Assume a nonlinear system (3.6) has a simple fixed point at $x^*$. Then, in a neighbourhood of the origin, the phase portraits of the system and its linearization are qualitatively equivalent, provided the linearized system is not at the centre.*

### 3.3.2 Routh–Hurwitz stability criterion

The Routh Hurwitz stability criterion [52] is essential for determining the stability of a system using a characteristic polynomial, with the help of some criteria that use only the coefficients of this polynomial. This criterion is a necessary and sufficient condition for all roots of the characteristic polynomial. Consider the characteristic polynomial

$$\lambda^n + a_1\lambda^{n-1} + \cdots + a_{n-1}\lambda + a_n = 0, \tag{3.9}$$

determining the $n$ eigenvalues $\lambda$ of a real $n \times n$ square matrix $A$. Then the eigenvalues $\lambda$ all have negative real parts if

$$H_1 > 0,\ H_2 > 0,\ H_3 > 0,\ \ldots H_n > 0,$$

where $H_i$ are the following determinants:

$$H_1 = |a_1|,$$

$$H_2 = \begin{vmatrix} a_1 & 1 \\ a_3 & a_2 \end{vmatrix},$$

$$H_3 = \begin{vmatrix} a_1 & 1 & 0 \\ a_3 & a_2 & a_1 \\ a_5 & a_4 & a_3 \end{vmatrix},$$

$$H_n = \begin{vmatrix} a_1 & 1 & \cdots & 0 \\ a_3 & a_2 & \cdots & 0 \\ \vdots & \vdots & \ddots & \vdots \\ a_{2n-1} & a_{2n-2} & \cdots & a_n \end{vmatrix}.$$

### 3.3.3 Global Stability via Lyapunov Functions

For higher-dimensional systems, several techniques can establish the global stability of the equilibrium points. The most commonly used is the Lyapunov function [53]. The global stability of equilibrium points may be proved using the scalar function known as the Lyapunov function.



**Lyapunov–Kasovskii–LaSalle Stability Theorems**

Let $x^*$ be an equilibrium point of the system $\dot{x} = f(x)$, where $f : \mathbb{R}^n \to \mathbb{R}^n$.

**Definition 3.3.2.** A scalar function $V(x)$ such that $V : \mathbb{R}^n \to \mathbb{R}$ is called *radially unbounded* if

$$V(x) \to \infty \quad \text{if} \quad ||x|| \to \infty.$$

One significant property of Lyapunov functions is that they are positive definite in the entire space.

**Definition 3.3.3.** Let $V$ be a continuous scalar function, that is,

$$V : \mathbb{R}^n \to \mathbb{R}.$$

The function $V$ is called *positive definite* on the entire space if

- $V(x^*) = 0$,
- $V(x) > 0$ for $x \neq x^*$,

where $x^*$ is an equilibrium of the autonomous system $\dot{x} = f(x)$. We define the derivative of $V(x)$ along the solutions of the system of differential equations as

$$\dot{V}(x) = \frac{d}{dt}V(x(t)) = \frac{\partial V}{\partial x}\frac{dx}{dt}.$$

Now, we can state Lyapunov's theorem for global stability of the equilibrium $x^*$. For proof of Lyapunov's theorem (see [54]).

**Theorem 3.3.2.** ***(Lyapunov's Stability Theorem),*** *If the function $V(x)$ is globally positive definite and radially unbounded, and its time derivative is globally negative, then the equilibrium $x^*$ is globally stable.*

**Definition 3.3.4.** If there exists a function $V(x)$ satisfying the theorem 3.3.2, then this function is called a *Lyapunov function.*

There are no set rules for finding Lyapunov functions, and they are often tricky and computationally expensive to find. However, once a Lyapunov function is identified, it is possible to determine the equilibrium point's global stability.

According to the Lyapunov theorem, the Lyapunov function's derivative with respect to $t$ must be negative definite. But often, we can only show non-positivity. In this case, the extension of the Lyapunov theorem was given by LaSalle [55] and Krasovskii [56].

**Theorem 3.3.3.** *(Krasovkii–LaSalle Theorem) Consider the autonomous system $\dot{x} = f(x)$, where $x^*$ is an equilibrium, that is, $f(x^*) = 0$. Suppose there exists a*

*continuously differentiable function* $V : \mathbb{R}^n \to \mathbb{R}$ *and that this function is positive-definite on the entire space and radially unbounded and that it satisfies* $\dot{\mathrm{V}}\,(\mathrm{x}) \leq 0$ *for all* $t$ *and all* $x \in \mathbb{R}^n$.

*Define the invariant set*

$$\mathcal{L} = \left\{ x \in \mathbb{R}^n \,\middle|\, \dot{V}\,(x) = 0 \right\}.$$

*If* $\mathcal{L}$ *contains only the equilibrium* $x^*$*, then the equilibrium* $x^*$ *is globally stable.*

## 3.4 Sensitivity analysis

A sensitivity analysis (SA) measures the uncertainties in a complex model. It aims to identify the critical inputs of a model (parameters and initial conditions) and quantify how the uncertainty of the inputs affects the model results. SA helps in allocating resources for follow-up experiments and field studies, isolating the primary sources of parametric uncertainty, identifying parameters that can be omitted to create a simple model, clarifying the plausible range of system results for predictive purposes when data are not available, and assessing the robustness of the qualitative conclusions drawn from a modeling study [57–60]. SA techniques have been broadly applied in systems biology [61, 62], environmental modeling [63, 64], and infectious disease modeling [65–67].

Many sensitivity analytical techniques are available: scatterplots, the Morris method, Latin hypercube sampling or partial rank correlation coefficient (PRCC), Sobol's method, and the sensitivity heat map method.

### 3.4.1 Scatter plots

Scatter plots are used to visually inspect the relationship between a model output variable and parameters. A model output variable sensitive to the selected parameter will produce a clear relationship pattern in the scatter plot. Typically, a Monte Carlo algorithm is used to sample the parameter space, and multiple scatter plots are used to illustrate the relationship between each parameter and each output variable of interest [57].

### 3.4.2 The Morris method

The Morris method, sometimes called the elementary effects method, is based on the ratio of the change in an output variable to the change in an input parameter [68]. Given the general relationship between a model's output Y and input parameters $X$, $Y = f(X)$, the elementary effect of $x_i$ can be expressed as

$$EE_i(X) = \frac{y_j\left(x_1, x_2, \ldots, x_i+\Delta, x_{i+1}, \ldots, x_k\right) - y_j(X)}{\Delta}$$

where $X \in [0,1]^k$ is a scaled vector of $k$ input parameters, $y_j$ is the state variable of interest, $\Delta$ is a value in the set $\left\{\frac{1}{p-1}, \ldots, 1-\frac{1}{p-1}\right\}$ and $p$ is the number of levels into which each dimension of the parameter space is divided. The distribution of $EE_i(X)$, denoted $F_i$, is obtained by repeated random sampling of $X$ from its $k$-dimensional, $p$-level parameter space.

An output variable's sensitivity measures include its mean of $|F_i|$ (denoted $\mu^*$ ), and its standard deviation $F_i$ (denoted $\sigma$ ). A large $\mu$ indicates that the parameter strongly influences the output. By contrast, if $\sigma$ is large, the correlation between the parameter and result is either nonlinear or interacts with other parameters [69, 70]. It is important to note that elementary effects may cancel each other out when the distribution of $F_i$ contains both positive and negative values. However, the parameter can still be influential when elementary effects are canceled out. Therefore, it is recommended that the absolute elementary effect be used to remedy the problem. The elementary effect of $x_i$, as estimated by the Morris method, is closer to $\frac{\Delta y_i}{\Delta x_i}\big|_\chi$ than $\frac{\Delta y_i}{\Delta x_i}\big|_\chi$ [68]. The Morris index is more accurate depending on the smoothness of $y$ over the parameter domain.

Models are run by the Morris method using $r(k+1)$, where $r$ is the number of trajectory points (a sampling path where each successive point varies only one randomly selected parameter while keeping all others constant at their last values) through the input parameter space, where $EE\left(x_i\right)$ is calculated at $k+1$ points along each trajectory [68]. Even though the Morris method is easy to understand (does not rely on assumptions about the model e.g., monotonicity), and is computationally

inexpensive, it cannot quantify the contribution of a parameter to the output's variability [65].

### 3.4.3 Latin hypercube sampling-partial rank correlation coefficient (PRCC)

A PRCC is a sampling-based SA method that measures the monotonicity between model parameters and output after eliminating the linear effects of all parameters except the parameter of interest [62]. It measures nonlinear but monotonic relationships between two variables. For two variables, $x$ and $y$, a standard correlation coefficient, $\rho$, is calculated as follows:

$$\rho = \frac{\sum_i (x_i - \hat{x})(y_i - \hat{y})}{\sqrt{\sum_i (x_i - \hat{x})^2 \sum_i (y_i - \hat{y})^2}},$$

where $\{(x_i, y_i) \,|x_i \in x, y_i \in y\}$ is the set of paired, sampled data, $\hat{x}$ is the sample mean of $x$, and $\hat{y}$ is the sample mean of $y$. When all other parameter values are held constant, the PRCC calculates the sensitivity of an output state variable to an input parameter as the linear correlation, $\rho$, between the residuals, $\left(X_j - \hat{X}_j\right)$ and $(Y - \hat{Y})$ where $X_j$ is the rank-transformed, $j$ is the input parameter and $Y$ is the rank-transformed output state variable [68, 71]. $\hat{X}_j$ and $\hat{Y}$ are determined for $k$ samples by the linear regression models

$$\hat{X}_j = c_o + \sum_{\substack{p=1 \\ p \neq j}}^{k} c_p X_p$$

and

$$\hat{Y} = b_o + \sum_{\substack{p=1 \\ p \neq j}}^{k} b_p X_p$$

The LHS method uses a stratified Monte Carlo sampling method in which the parameter range is divided into N equal intervals, and samples are randomly drawn from each interval [62,72]. The method explores the entire range of each parameter, and each parameter interval is sampled only once [62,67]. LHS is more efficient with fewer simulations than a conventional Monte Carlo sampling strategy because of its dense stratification across the input parameter space and the fast convergence of the sample mean to the real population mean as the number of samples grows [73]. The combined LHS-PRCC procedure involves generating a Latin hypercube sample of the parameter space, obtaining model output for each set of sampled parameters, ranking parameters and output values, and calculating the PRCC for each input parameter [62,67].

### 3.4.4 Sobol's method

The Sobol method is a variance-based sensitivity analysis technique that can be used to estimate the influence of individual parameters, or groups of parameters, on the output variables of a nonlinear model. The method is based on variance decomposition, which decomposes the total variance of the output variables into contributions from individual parameters and groups of parameters. The Sobol method is a powerful tool for understanding the sensitivity of nonlinear models and can be used to identify the most important parameters for further study or optimization [74].

Given a model of the relationship between output variables and parameters,

$$Y = f(X) = f(x_1, x_2, \ldots, x_k)$$

that is square integrable over its unit hypercube parameter space, the model function for a single state variable, $y=f(X)$, can be decomposed into summands of increasing dimensionality, known as the high-dimensional model representation:

$$y = f(X) = f_0 + \sum_{i=1}^{k} f_i(x_i) + \sum_{j>i}^{k} f_{ij}(x_i, x_j) + \cdots + f_{1,2,\ldots,k}(x_1, x_2, \ldots, x_k)$$

where $f_0$ is the constant term.

Sobol demonstrated that if each term in the expansion of the model function into summands of increasing dimensionality has a zero mean, then the total variance of an output variable can be decomposed into the HDMR ANOVA, represented as

$$\begin{aligned} V(y) &= \int f(X)^2 \, \mathrm{d}X - f_0 \\ &= \sum_{i=1}^{k} V_i + \sum_{i}^{k} \sum_{j>i}^{k} V_{ij} + \sum_{i}^{k} \sum_{j>i}^{k} \sum_{h>j}^{k} V_{ijh} + \cdots + V_{1,2,\ldots,k} \end{aligned}$$

where $V(y)$ is the variance of the model output $y, k$ is the number of parameters and

$$V_{i_1,i_2,\ldots,i_s} = \int f^2_{i_1,i_2,\ldots,i_s} \, \mathrm{d}x_{i_1} \mathrm{d}x_{i_2}, \ldots, \mathrm{d}x_{i_s}$$

for a given set of indices, $i_1, \ldots, i_s$. Sobol's sensitivity indices are the ratios of the partial variance given an individual parameter or the interactions of a parameter subset to the total variance.

$$S_i = \frac{V\left[E\left(y|x_i\right)\right]}{V(y)}$$

and

$$S_{T_i} = 1 - \frac{V\left[E\left(y|X_{\sim i}\right)\right]}{V(y)}$$

where $X_{\sim i}$ denotes all elements of $X$ except $x_i$. These indices have the property that $S_i \leq S_{T_i} \leq 1$ and when $S_i = S_{T_i} = 0$, it can be concluded that $f(X)$ does not depend on $x_i$, while $S_i = S_{T_i} = 1$ indicates that $f(X)$ depends solely on $x_i$ [70].

The Sobol method is independent of model structure (e.g., linearity and monotonicity) and captures the effects of individual parameters and their interactions. The method also provides quantitative information on the contribution of each parameter to model sensitivity.

A major disadvantage of the Sobol method is its high computational cost. Given a model with k parameters and n samples from each parameter, the model must run at least $k(n+2)$ times to generate sufficient output to calculate partial variances for individual parameters. This can be a significant burden for models with a large number of parameters or a large number of samples.

Despite its high computational cost, the Sobol method is a powerful tool for

understanding the sensitivity of nonlinear models. It can be used to identify the most important parameters for further study or optimization, and it can help to improve the accuracy and reliability of model predictions.

### 3.4.5 Sensitivity heat map method

There are two graphical methods to examine the sensitivity of complex models: the sensitivity heat map (SHM) and the parameter sensitivity spectrum (PSS). The SHM illustrates how sensitive each output variable is to all (or a subset of) model parameters, while the PSS displays the sensitivity of all (or a subset of) output variables to each parameter [61].

Given a set of $n$ ODEs:

$$\frac{\mathrm{d}X}{\mathrm{d}t}=f(t,X,K)$$

where $X=(x_1,\ldots,x_n)$ is the vector of state variables, $t$ is time and $K=(k_1,\ldots,k_s)$ is a vector of parameters, there is a solution or set of solutions $X=g(t,K)$ for $0\leq t\leq T$. When the parameter $\delta K$ is changed, the solution $\delta g$ also changes so that $\delta g(t)=M\delta K+\mathcal{O}\left(\|\delta K\|^2\right)$, where $M$ is the linear map (as described in [75]) from parameter space $\mathbb{R}^s$ to a Hilbert space $H$.

Applying Rand's notation [61], we subject a time-interval normalized (that is, by $\sqrt{(t_{m+1}-t_m)/t_N)}$) matrix $M_1$, to singular value decomposition. This matrix is made up of the partial derivatives $\partial g_j/\partial k_i$ at all simulation time points $t=\{t_1,\ldots,t_N\}$. The values for $U, W$ and $\{\sigma_i\}$, as defined below, quantify the sensitivity of output variables to parameters. Rand demonstrates that there is a unique set of positive numbers $\sigma_1\geq\ldots\geq\sigma_s$, a unique set of orthonormal vectors $\{V_i\}$ in $\mathbb{R}^s$, and a unique n-dimensional orthogonal time-series basis set $\{U_1(t),\ldots,U_n(t)\}$ in $\mathcal{H}$, such that $\delta g(t)=\sum_i \sigma_i\left[\sum_j W_{ij}\delta k_j\right]+\mathcal{O}\left(\|\delta K\|^2\right)$ , where $W_{ij}$ are the elements of $W=V^{-1}$, and $V=[V_1,\ldots,V_n]$ [61].

The SHM for the state variable $g_i(t)$ is therefore represented as $\sigma_i\left(\max_j\ |W_{ij}|\right)U_i(t)$, and the influence of a single parameter on the system. The PSS is stated as $\partial g(t)/\partial k_j=\sum_i \sigma_i W_{ij}U_i(t)$. Compared to previous SA approaches, this very computationally efficient methodology enables the modeler to see the sensitivity charac-

teristics of the set of all output variables instead of just one output variable.

## 3.5 Optimal control theory applied to epidemiological models

Optimal control theory is a mathematical optimization approach to formulate control strategies. It deals with the problem of finding a control law for a given system that satisfies a certain optimality criterion. The optimal control problem typically describes the control system (the process to be controlled) using ordinary differential equations (ODEs), control objectives, physical constraints, and a performance index. Given the following ODEs-system

$$\begin{cases} \frac{dx}{dt} = y(x(t), t) \\ x(0) = x_0, \end{cases} \tag{3.10}$$

where the unknown vector $x : \mathbb{R}^+ \to \mathbb{R}^n$ is considered to be piecewise differentiable and continuous with given initial conditions $x_0 \in \mathbb{R}^n$ and $y : \mathbb{R}^n \to \mathbb{R}^n$.

Let us generalize the system in Equation (3.10) by adding a new time-dependent function $u(t)$ to the right-hand side, such that $u$: $\mathbb{R}^+ \to D$, where $u$ is from a set, $D \subset \mathbb{R}^m$.

$$\begin{cases} \frac{dx}{dt} = y(x(t), u(t), t) \\ x(0) = x_0 \end{cases} \tag{3.11}$$

The variable $u(t)$ is called "control," and the new system described by the Equation (3.11) is called "control system." The vectors $x, u$, and function $y$ can be generalized as:

$$x(t) = \begin{bmatrix} x_1(t) \\ x_2(t) \\ . \\ . \\ . \\ x_n(t) \end{bmatrix},$$

$$u(t) = \begin{bmatrix} u_1(t) \\ u_2(t) \\ . \\ . \\ . \\ u_m(t) \end{bmatrix},$$

and

$$y(x(t), u(t), t) = \begin{bmatrix} y_1(x_1(t), x_2(t) \dots x_n(t), u_1(t), u_2(t) \dots u_m(t)) \\ y_2(x_1(t), x_2(t) \dots x_n(t), u_1(t), u_2(t) \dots u_m(t)) \\ . \\ . \\ . \\ y_n(x_1(t), x_2(t) \dots x_n(t), u_1(t), u_2(t) \dots u_m(t)) \end{bmatrix}.$$

After developing the controlled system, the control objective is defined using a suitable performance index. Regarding epidemic control models, the aim is to obtain a cost of control inputs that will minimize the prevalence and the cost of controlling the disease. More explicitly, the objective function is given by:

$$J[u] = \int_0^T L(x(t), u(t))\, dt, \tag{3.12}$$

where $x(t)$ solves (3.12) for specified control $u(t)$. The *Lagrangian* function $L$ is continuous and differentiable, representing the running payoff, such that $L : \mathbb{R}^n \times D \to \mathbb{R}$. Both the final time $T$ and the function $L$ are given. Thus the optimal control problem is to determine the control $u^*$ that minimizes the objective functional (3.13) subject to the system state (3.12) over the closed interval $[0, T]$, that is,

$$J[u^*] = \min_{u \in \Pi} J[u]. \tag{3.13}$$

Here $\Pi$ is the set of admissible controls defined by

$$\Pi = \left\{ u(t) \in L^1(0, t_f) \,|\, u(t) \in D \right\}.$$

If it exists, the control $u^*(t)$ is called the optimal control. The next step is to check the existence of the optimal control pair $(u^*, x^*)$. This can be achieved by using Theorem 4.1 from [76]:

**Theorem 3.5.1.** *Suppose that,*

*i* $y$ *is of class* $C^1$ *and there exist a constant* $\varepsilon$ *exists such that*

$$|y(t,0,0)| \leq \varepsilon,$$

$$|y_x(t,x,u)| \leq \varepsilon(1+|u|), \text{ and}$$

$$|y_u(t,x,u)| \leq \varepsilon;$$

*ii The admissible set of solutions to system (3.12) along with initial conditions and associated control in* $\Pi$ *is nonempty;*

*iii* $y(t,x,u) = a(t,x) + b(t,x)u$;

*iv The optimal control set* $U$ *is closed, compact, and convex;*

*v The objective functional integrand* $L(x(t), u(t))$ *is convex in* $U$.

Then there exists an optimal control $u^*$ and the corresponding optimal solution $x^*$ to the problem (3.12). Now that the existence of the optimal control has been proved, the optimal control solution is provided by Pontryagin's maximum principle [77]. Let's introduce a time-varying Lagrange multiplier vector $\lambda(t)$ and define a new function $H$ (called Hamiltonian function) for all time $t \in [0, t_f]$ as

$$H(x(t), u(t), \lambda(t), t) = L(x(t), u(t)) + \sum_{j=1}^{n} \lambda_j(t)\, y_j(x(t), u(t), t). \tag{3.14}$$

**Theorem 3.5.2.** *(Pontryagin's Maximum Principle). For the optimality of control $u^*(t)$ and associated optimal trajectory, $x^*(t)$, there must exist a nonzero co-state vector $\lambda^*(t)$ that is a solution to the co-state system*

$$\frac{d\lambda}{dt} = -\frac{\partial H\left(x\left(t\right), u\left(t\right), \lambda\left(t\right), t\right)}{\partial t}. \tag{3.15}$$

*Such that*

$$H\left(x\left(t\right), u\left(t\right), \lambda\left(t\right), t\right) = \min_{u \in \Pi} H\left(x^*\left(t\right), u\left(t\right), \lambda^*\left(t\right)\right).$$

*Consequently, the necessary conditions for optimizing the Hamiltonian are [78]:*

1. *Optimality condition*

$$\frac{dH}{dt} = 0.$$

2. *The co-state system*

$$\frac{d\lambda_j\left(t\right)}{dt} = -\frac{\partial H\left(x\left(t\right), u\left(t\right), \lambda\left(t\right), t\right)}{\partial x_i}.$$

3. *Transversality condition*

$$\lambda_j(t_f) = 0.$$

*For minimization, we must also have $\frac{\partial^2 H}{\partial u^2} \geq 0$ at $u^*$.*

# Chapter 4

# Modeling the effects of vaccination and treatment on tuberculosis transmission dynamics

In this chapter, we develop and analyze the deterministic mathematical tuberculosis transmission dynamics model. The model in this chapter modifies the models in [17, 19] by including newborn TB vaccination. The model includes vaccination for newborns and treatment for high-risk latent and active TB patients.

## 4.1 Introduction

Mathematical models and computer simulations are inexpensive, easy to manage, relatively fast, and productive experimental tools. They have been widely used to examine, explain, and predict infectious disease transmission dynamics. Different mathematical models for tuberculosis transmission dynamics have been formulated, analyzed, and utilized, starting from the first mathematical model for TB by Waaler et al. [22]. Those models have been applied to different populations, such as a city or country, a school, a prison, or a refugee camp, for instance, [79, 80]. Other mathematical models are developed that consider progression rate, treatment, vaccination, immigration, and other factors see [35, 81, 82].

For many years, mathematical models have been used to study the transmission dynamics of TB in different countries by using real data. For example, Zhao et

al. [25] investigated age's role in TB transmission in Mainland China and found that the BCG vaccine is valid only for younger people. They also showed that the DOTS program is more critical for the senior-aged group.

Choi et al. [17] introduced three control mechanisms: distancing, case finding, and case holding into the SEIL model in South Korea. They showed that distancing control is the most effective prevention mechanism of all.

On the other hand, Moualeu et al. [21] developed a model for the transmission dynamics of TB and applied it to the data for Cameroon. They identified that the combined effort of education and chemoprophylaxis might lead to a reduction of 80% in the number of infected people in 10 years.

Finally, Kim et al. [19] developed a mathematical model for TB and fitted it to the Philippine data. Their result showed that applying a combination of distancing and case-finding control strategies has significant potential for curtailing the spread of TB in the Philippines.

As we have seen above, various researchers have studied the transmission dynamics of TB in different countries using mathematical models. However, such studies are rare in Ethiopia. Therefore, in this chapter, we have examined the effect of the BCG vaccine and TB treatment in preventing the spread of TB disease in Ethiopia.



## 4.2 Model Formulation

The homogeneously mixing total population at time $t$, of size $N(t)$, is divided into five subclasses: Susceptible $S(t)$, Vaccinated $V(t)$, high-risk latently infected $E(t)$, Infectious (or active TB) $I(t)$, and low-risk latent $L(t)$.
We make the following assumptions in the formulation of the model:

- We assume that the recruitment rate into the population is $\Lambda$ and some portion of it, $(\varepsilon\Lambda)$, will receive a vaccination at birth where $(0 \leq \varepsilon \leq 1)$.
- The natural death rate (any death which is not due to TB) is assumed to be the same for each class and denoted by $\mu$.
- The mortality due to the TB disease will happen only in the $I$-class with a

rate $\delta$.

- The efficiency of the BCG vaccine is not complete [83]. Hence, it is assumed that vaccinated individuals develop temporary immunity that lasts for a duration $1-\theta$, after which they become susceptible to infection.
- Susceptible individuals can be infected with TB through the transmission coefficient $\beta$.
- The treatment rate for the $E-$ class is denoted by $\alpha$.
- It is assumed that the untreated portion of the $E$-class will develop active TB at the rate $k$.
- If treatment is administered for the $I$-class with a rate $r$, then some of them will complete their treatment correctly at a rate $(1-p)r$ for $(0 \leq p \leq 1)$. The recovered individuals are moved to the $L$-class because treatment cannot completely remove the TB bacteria from the body of the patients. Hence, recovered and low-risk latently infected individuals are classified into a single class of low-risk latent individuals.
- It is assumed that there is no permanent immunity to tuberculosis; hence, recovered (low-risk latent) individuals may lose their immunity and become high-risk latently infected with the relapse rate $\sigma$.
- We further assume that all parameters to be used in this model are non-negative.

Given these assumptions, the following flow diagram 4.1 describes the interaction between classes.

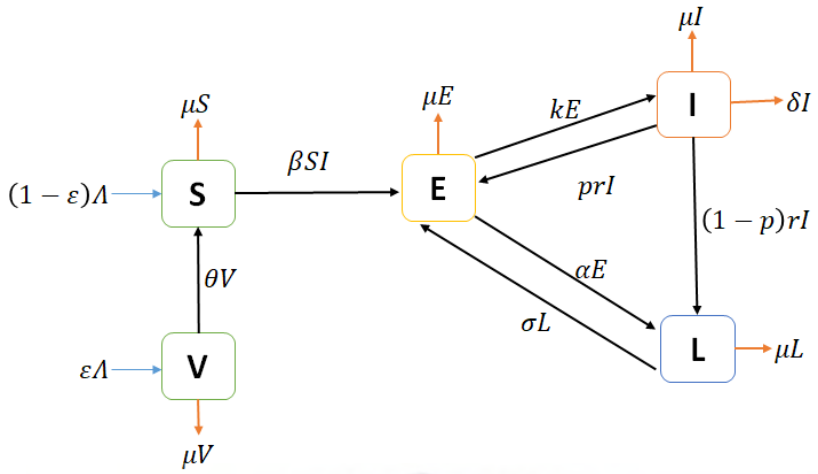


Figure 4.1: Flow diagram of the TB transmission model

Based on our definitions, assumptions, and interrelations between the variables, the system of ODE that describes the dynamics of TB is formulated as follows,

$$\begin{cases} \frac{dS}{dt} = (1-\varepsilon)\,\Lambda + \theta V - \beta SI - \mu S \\ \frac{dV}{dt} = \varepsilon\Lambda - (\theta+\mu)\,V \\ \frac{dE}{dt} = \beta SI + prI + \sigma L - (k+\alpha+\mu)\,E \\ \frac{dI}{dt} = kE - (\mu+r+\delta)\,I \\ \frac{dL}{dt} = (1-p)\,rI + \alpha E - (\mu+\sigma)\,L \\ N(t) = S(t) + V(t) + E(t) + I(t) + L(t). \end{cases} \tag{4.1}$$



## 4.3 Model Analysis

### 4.3.1 Positivity of the solutions

**Theorem 4.3.1.** *Let the initial data $S_0, V_0, E_0, I_0$ and $L_0$ be non-negative. Then the solution set $\Omega = \{S(t), V(t), E(t), I(t), L(t)\}$ is non-negative for all $t > 0$.*

***Proof:*** Take the second equation of the model (4.1)

$$\frac{dV(t)}{dt} = \varepsilon\Lambda - (\theta+\mu)\,V(t).$$

For simplicity let us write

$$\theta + \mu = \varphi,$$

and

$$\varepsilon\Lambda = \lambda.$$

Then,

$$\frac{dV(t)}{dt} + \varphi V(t) = \lambda. \tag{4.2}$$

Multiplying both sides of Equation (4.2) by $\exp(\varphi t)$ gives

$$\frac{dV(t)}{dt}\exp(\varphi t) + \varphi V(t)\exp(\varphi t) = \lambda\exp(\varphi t). \tag{4.3}$$

By the product rule of the derivative we have

$$\frac{dV(t)}{dt}\exp(\varphi t) + \varphi V(t)\exp(\varphi t) = \frac{d}{dt}\left[V(t)\exp(\varphi t)\right]. \tag{4.4}$$

Hence from Equation (4.3), we have

$$\frac{d}{dt}\left[V(t)\exp(\varphi t)\right] = \lambda\exp(\varphi t). \tag{4.5}$$

Integrating both sides of Equation (4.5) gives

$$V(t) = V(0)\exp(-\varphi t) + \frac{\lambda}{\varphi}(1 - \exp(-\varphi t)) \geq 0. \tag{4.6}$$

***Remark***: Note that, in particular, from Equation (4.6), it follows that

$$\lim_{t\to\infty} V(t) = \frac{\varepsilon\Lambda}{\theta + \mu}. \tag{4.7}$$

Similarly taking the first equation of the model (4.1) gives

$$\frac{dS(t)}{dt} = (1 - \varepsilon)\Lambda + \theta V(t) - (\beta I(t) - \mu) S(t).$$

By letting

$$(1-\varepsilon)\,\Lambda = \phi,$$

and

$$(\beta I\,(t) - \mu) = H(t),$$

we have

$$\frac{dS(t)}{dt} + H\,(t)\,S(t) = \phi + \theta V(t). \tag{4.8}$$

Multiply both sides of Equation (4.8) by $\exp\left\{\int_0^t H\,(\tau)\,d\tau\right\}$ gives

$$\frac{dS\,(t)}{dt}\exp\left\{\int_0^t H\,(\tau)\,d\tau\right\} + H\,(t)\,S\,(t)\exp\left\{\int_0^t H\,(\tau)\,d\tau\right\}$$

$$= \phi\exp\left\{\int_0^t H\,(\tau)\,d\tau\right\} + \theta V\,(t)\exp\left\{\int_0^t H\,(\tau)\,d\tau\right\},$$

By the product rule of the derivative, we have

$$\frac{dS(t)}{dt}\exp\left\{\int_0^t H\,(\tau)\,d\tau\right\} + H\,(t)\,S\,(t)\exp\left\{\int_0^t H\,(\tau)\,d\tau\right\} = \frac{d}{dt}\left[S\,(t)\exp\left\{\int_0^t H\,(\tau)\,d\tau\right\}\right].$$

Hence,

$$\frac{d}{dt}\left[S\,(t)\exp\left\{\int_0^t H\,(\tau)\,d\tau\right\}\right] = \phi\exp\left\{\int_0^t H\,(\tau)\,d\tau\right\} + \theta V(t)\exp\left\{\int_0^t H\,(\tau)\,d\tau\right\}. \tag{4.9}$$

Integrating both sides of Equation (4.9) gives

$$S\,(t)\exp\left\{\int_0^t H\,(\tau)\,d\tau\right\} - S_0 = \phi\int_0^t \exp\left\{\int_0^\tau H\,(u)\,du\right\} + \int_0^t \theta V(u)\exp\left\{\int_0^\tau H\,(u)\,du\right\}.$$

Then,

$$S\,(t) = S_0\exp\left\{-\int_0^t H\,(\tau)\,d\tau\right\} + \left[\phi\int_0^t \exp\left\{\int_0^\tau H\,(u)\,du\right\}\right]\left[\exp\left\{-\int_0^t H\,(\tau)\,d\tau\right\}\right]$$
$$+ \left[\int_0^t \theta V\,(u)\exp\left\{\int_0^\tau H\,(u)\,du\right\}\right]\left[\int_0^t \theta V\,(u)\exp\left\{\int_0^\tau H\,(u)\,du\right\}\right] \geq 0.$$

Similarly, we can show that $E\,(t)\,, I\,(t)\,,$ and $L\,(t)$ are non-negative.

### 4.3.2 Invariant regions

**Theorem 4.3.2.** *With the non-negative initial conditions, the feasible region of the model is defined by*

$$\Omega = \left\{ (S(t), V(t), E(t), I(t), L(t)) \in \mathbb{R}_+{}^5 \;\middle|\; S(t) + V(t) + E(t) + I(t) + L(t) \leq \frac{\Lambda}{\mu} \right\}.$$

**Proof:** The change of total population size is

$$\begin{aligned} \frac{dN(t)}{dt} &= \frac{dS(t)}{dt} + \frac{dV(t)}{dt} + \frac{dE(t)}{dt} + \frac{dI(t)}{dt} + \frac{dL(t)}{dt} \\ &= \Lambda - \mu N(t) - \delta I(t) \end{aligned} \tag{4.10}$$

The inequality (4.10) implies

$$e^{\mu t}\frac{dN(t)}{dt} + \mu e^{\mu t} N(t) \leq \Lambda e^{\mu t},$$

$$\frac{d}{dt}\left(N(t)\, e^{\mu t}\right) \leq \Lambda e^{\mu t}, \tag{4.11}$$

where $e^{\mu t}$ is the integration factor.

Integrating both sides gives of Equation (4.11)

$$N(t)\, e^{\mu t} \leq \frac{\Lambda}{\mu} e^{\mu t} + C,$$

where $C$ is a constant. It follows that when $t = 0$, we have $N_0 - \frac{\Lambda}{\mu} \leq C$. Substituting and simplifying leads to:

$$N(t) \leq \frac{\Lambda}{\mu} + \left(N_0 - \frac{\Lambda}{\mu}\right) e^{-\mu t}.$$

Thus for every $t > 0$, as $t \to \infty$, $N(t) \leq \frac{\Lambda}{\mu}$.

Hence an invariant region for this model is

$$\Omega = \left\{ (S(t), V(t), E(t), I(t), L(t)) \in \mathbb{R}_+{}^5 \;\middle|\; S(t) + V(t) + E(t) + I(t) + L(t) \leq \frac{\Lambda}{\mu} \right\} \blacksquare \tag{4.12}$$

### 4.3.3 Disease-free equilibrium point and the basic reproduction number

In the absence of the disease ($E = I = L = 0$), the model (4.1) has a disease-free

equilibrium point(DFE), obtained by setting the right-hand sides of the equations in the model to zero, given by:

$$P_0^* = (S_0^*, V_0^*, 0, 0, 0),$$

where

$$S_0^* = \frac{\Lambda}{\mu}\frac{\theta + \mu(1-\varepsilon)}{(\theta+\mu)},$$

and

$$V_0^* = \frac{\varepsilon\Lambda}{\theta+\mu}.$$

We obtained basic reproduction number $\mathcal{R}_0$ by using the next-generation matrix method given in [84]. This amounts to calculating the two matrices $M$ and $F$, where $M$ is the transfer rate of individuals into and out of the infected classes and $F$ is the rate of new infections in the compartment. Hence, by the equations we obtain,

$$F = \begin{pmatrix} \beta SI \\ 0 \\ 0 \end{pmatrix},$$

$$\mathrm{M} = \begin{pmatrix} -\sigma L - prI + (k+\alpha+\mu)E \\ -kE + (r+\mu+\delta)I \\ -(1-p)rI - \alpha E + (\mu+\sigma)L \end{pmatrix}.$$

Then the linearization of the system (4.1) at disease free equilibrium is given by

$$\mathcal{F} = \begin{pmatrix} 0 & \beta\Lambda\left(\frac{1}{\mu} - \frac{\varepsilon}{\theta+\mu}\right) & 0 \\ 0 & 0 & 0 \\ 0 & 0 & 0 \end{pmatrix},$$

and

$$\mathcal{M} = \begin{pmatrix} k+\alpha+\mu & -pr & -\sigma \\ -k & r+\delta+\mu & 0 \\ -\alpha & -(1-p)r & \mu+\sigma \end{pmatrix}.$$

Then $\mathcal{R}_0$ is the dominant eigenvalue of the matrix $\mathcal{F}\mathcal{M}^{-1}$.

Thus we have

$$\mathcal{R}_0 = \frac{k\beta\Lambda\left[\theta+\mu\left(1-\varepsilon\right)\right]\left(\mu+\sigma\right)}{\mu\left(\theta+\mu\right)\left[\mu\left(r+\delta+\mu\right)\left(\alpha+\mu+\sigma\right)+k\left\{r\mu\left(1-p\right)+\left(\delta+\mu\right)\left(\mu+\sigma\right)\right\}\right]}\ .$$

The following number, $\mathcal{R}_{\mathrm{g}}$ , serves as an indicator for global stability of the disease-free equilibrium point:

$$\mathcal{R}_{\mathrm{g}} = \frac{k\beta\Lambda\left[\theta+\mu\left(1-\varepsilon\right)+\eta\right]}{\mu\left(\theta+\mu\right)\left[\mu_1\mu_2-kpr\right]}, \tag{4.13}$$

with

$$\mu_1 = \alpha+\mu+k,$$

$$\mu_2 = r+\delta+\mu,$$

and

$$\eta = \frac{\mu\sigma}{k\beta\Lambda}\left[\alpha\mu_1+\left(1-p\right)rk\right].$$

Note that since $p \leq 1$ and $\mu > 0$, we are guaranteed that $\mu_1\mu_2 - kpr > 0$.

**Theorem 4.3.3.** *For the model (4.1), the disease-free equilibrium point $P_0^*$ is globally asymptotically stable if $\mathcal{R}_{\mathrm{g}} < 1$.*

**Proof:** We follow a methodology similarly as in the stability analysis of [85, 86].
For $\mathcal{R}_{\mathrm{g}} < 1$ we have

$$\frac{k\beta\Lambda\left[\theta+\mu\left(1-\varepsilon\right)+\eta\right]}{\mu\left(\theta+\mu\right)} - \left[\mu_1\mu_2-kpr\right] < 0. \tag{4.14}$$

This can be written as

$$\frac{k\beta\Lambda\left[\theta+\mu\left(1-\varepsilon\right)\right]}{\mu\left(\theta+\mu\right)} + \frac{k\beta\Lambda\eta}{\mu\left(\theta+\mu\right)} - \left[\mu_1\mu_2-kpr\right] < 0. \tag{4.15}$$

By the Archimedean property of $\mathbb{R}$, there exists $\gamma_0 > 0$, for which

$$\frac{k\beta\Lambda\left[\theta+\mu\left(1-\varepsilon\right)\right]}{\mu\left(\theta+\mu\right)} + \gamma_0 k\beta + \frac{k\beta\Lambda\eta}{\mu\left(\theta+\mu\right)} - \left[\mu_1\mu_2-kpr\right] < 0. \tag{4.16}$$

Also, we can find a number $\gamma_1$, with $0 < \gamma_1 < \mu$, and such that

$$\frac{k\beta\Lambda\left[\theta+\mu\left(1-\varepsilon\right)\right]}{\mu\left(\theta+\mu\right)} + \gamma_0 k\beta + \frac{k\beta\Lambda\eta}{\mu\left(\theta+\mu\right)}\frac{\sigma+\gamma_1}{\gamma_1} - \left[\mu_1\mu_2-kpr\right] < 0. \tag{4.17}$$

We require an upper bound for $S(t)$. From Remark (4.7) it follows that there exists $t_0$ such that

$$\left|V(t) - \frac{\varepsilon\Lambda}{\theta+\mu}\right| < \gamma_0,$$

whenever $t > t_0$ . Without loss of generality, we can assume that

$$\left|V(t) - \frac{\varepsilon\Lambda}{\theta+\mu}\right| < \gamma_0,$$

whenever $t > 0$.

The latter inequality implies that

$$\frac{\varepsilon\Lambda}{\theta+\mu} - \gamma_0 < V(t),$$

and consequently, that

$$-V(t) < -\frac{\varepsilon\Lambda}{\theta+\mu} + \gamma_0.$$

Also, we have

$$N(t) \leq \frac{\Lambda}{\mu}.$$

Thus for every $t > 0$,

$$\begin{aligned} S(t) &\leq N(t) - V(t) \\ &< \frac{\Lambda}{\mu} - \frac{\varepsilon\Lambda}{\theta+\mu} + \gamma_0 \\ &= \frac{\Lambda}{\mu}\frac{\theta+\mu(1-\varepsilon)}{(\theta+\mu)} + \gamma_0. \end{aligned} \tag{4.18}$$

Now taking $\gamma_2 = \frac{\gamma_1}{2}$, we introduce two constants $C_0$ and $C_1$ as follows:

$$\begin{aligned} C_0 &= \frac{\mu_2}{k} - \frac{\alpha(\sigma+\gamma_1)}{k(\mu+\sigma)}, \\ C_1 &= \frac{\sigma+\gamma_2}{\mu+\sigma}. \end{aligned}$$

In particular then, $C_0 > 0$.

Now we define a function:

$$Q(t) = E(t) + C_0 I(t) + C_1 L(t). \tag{4.19}$$

We prove now that $\dot{Q}(t)$ is negative-definite. Note that we can write

$$\dot{Q}(t) = C_2 E + C_3 I + C_4 L$$

where

$$C_2 = C_0 k - \mu_2 + C_1 \alpha,$$
$$C_3 = \beta S + pr - C_0 \mu_1 + (1-p) r C_1,$$

and

$$C_4 = \sigma - C_1 (\mu + \sigma).$$

Then

$$C_4 = -\gamma_2 < 0.$$
$$C_2 = -\frac{\alpha(\sigma+\gamma_1)}{(\mu+\sigma)} + \frac{\alpha(\sigma+\gamma_2)}{(\mu+\sigma)}$$
$$= \frac{\alpha(\gamma_2-\gamma_1)}{(\mu+\sigma)}$$

Since $\gamma_2 < \gamma_1$, it follows that $C_2 < 0$.

We can write $kC_3$ as:

$$kC_3 = k(\beta S + pr) - \mu_1\mu_2 + C_5,$$

where

$$C_5 = \frac{\mu_1\alpha(\sigma+\gamma_1) + rk(1-p)(\sigma+\gamma_2)}{\mu+\sigma}$$
$$\leq \frac{\sigma+\gamma_1}{\mu+\sigma}[\mu_1\alpha + rk(1-p)]$$
$$= \frac{(\sigma+\gamma_1)k\beta\Lambda}{\sigma\mu(\mu+\sigma)}\eta.$$

Noting also the upper bound for $S(t)$, we obtain the following inequality

$$kC_3 \leq k\left\{\frac{\Lambda\beta}{\mu\left(\theta+\mu\right)}\left[\theta+\mu\left(1-\varepsilon\right)\right]+\gamma_0\beta+pr\right\}-\mu_1\mu_2+\frac{k\Lambda\beta}{\mu\left(\theta+\mu\right)}\frac{\sigma+\gamma_1}{\sigma}\eta.$$

Therefore by the inequality (4.17), it follows that $kC_3 < 0$. This proves that $\dot{Q}\left(t\right)$ is negative-definite. Hence, $Q(t)$ is a Lyapunov function on $\Omega$. Therefore, by LaSalle's invariance principle [87], every solution of model (4.1), with any initial conditions in $\Omega$, approaches $P_0^*$ as $t \to \infty$, whenever $\mathcal{R}_0 < 1$. ■

The results in Theorem 4.3.3 imply that for any initial size of the subpopulation of the model, TB can be eliminated from the population when $\mathcal{R}_0 < 1$.

### 4.3.4 Existence of the endemic equilibrium point

In this section, we show the existence of an endemic equilibrium point of the model (4.1). The endemic equilibrium point is the steady state where the disease remains alive in the population when at least one of the infected classes of the model is non-zero.

**Theorem 4.3.4.** *If $\mathcal{R}_0 > 1$, then the model (4.1) has a unique positive endemic equilibrium $P^* = (S^*, V^*, E, I^*, L^*)$. With:*

$$\begin{aligned}
S^* &= \frac{\Lambda\left[\theta+\mu\left(1-\varepsilon\right)\right]}{\mathcal{R}_0\left(\theta+\mu\right)},\\
V^* &= \frac{\varepsilon\Lambda}{\theta+\mu},\\
E^* &= \frac{\left(r+\delta+\mu\right)\mu}{k\beta}\left(\mathcal{R}_0-1\right),\\
I^* &= \frac{\mu}{\beta}\left(\mathcal{R}_0-1\right),
\end{aligned}$$

and

$$L^* = \frac{\mu\left(kr\left(1-p\right)+\alpha\left(r+\delta+\mu\right)\right)\left(\mathcal{R}_0-1\right)}{k\beta\left(\mu+\sigma\right)}.$$

## 4.4 Numerical analysis of the model

### 4.4.1 Estimation of the model parameters

In this subsection, we estimate the values of the model's parameters of the system (4.1)

based on the existing literature and the epidemiological data of Ethiopia between 2003 and 2017. The values of the parameters are summarised in Table 4.1, and the detailed estimation process of the parameter values is as follows.

1. According to the World Bank report, [88], the average life expectancy of Ethiopia in the years between 2003 and 2017 is 60.93 years. The natural death rate can be calculated as the inverse of life expectancy [20, 79]. Hence, we estimate $\mu = 0.016$.

2. The upper limit of the total population in the absence of the disease is $\frac{\Lambda}{\mu}$. Hence, $\Lambda$ can be taken as a product of $\mu$ and the average population size over 2003-2017. Using this formula and the WHO report [89], the average yearly recruitment rate to the population of Ethiopia is $1.4 \times 10^6$.

3. The WHO report [89] also indicates that the average tuberculosis-related mortality rate is about $\delta = 0.17$.

4. The WHO reported that from 2003 to 2017, Ethiopia's average BCG vaccination coverage was 71.5 % [90]. So $\varepsilon = 0.715$.

5. According to WHO [91], the tuberculosis treatment success rate in Ethiopia is 83.2%. So we estimate $1 - p = 0.832$.

6. On average, the BCG vaccine significantly reduces the risk of TB by 50% [83]. So $\theta = 0.5$.

7. The transmission coefficient, progression rate from $E$-class to $I$-class, the treatment coverage rate of $I$-class, the relapse rate from $L$-class to $E$-class, and treatment rate of $E$-class are obtained by fitting the yearly TB incidence data obtained from WHO [89] to the model by using fmincon MATLAB routine. Figure 4.2 shows the graph of TB incidence data obtained (■) and the estimated solid curve. The estimated values are $\beta = 1.646 \times 10^{-7}$, $\kappa = 0.023$, $r = 0.546, \sigma = 0.0013$ and $\alpha = 0.153$.

8. We calculate the initial number of vaccinated children as the product of the average number of newborns and the vaccination coverage, which is $V_0 = 1 \times 10^6$. We calculate the initial number of vaccinated children as the product of the average number of newborns and the vaccination coverage, which is $V_0 = 1 \times 10^6$.

9. The initial fraction for the infectious class $I_0 = 3.73 \times 10^5$ is taken from the TB-prevalence in 2003 reported by the WHO [89].

10. We estimate the initial value of the $E$-class and the $L$-class from the data-fitting process. Thus, the amount of $E_0$ and $L_0$ is 16.37% and 30% out of the total population, respectively. This gives $E_0 = 1.19 \times 10^7$and $L_0 = 2.18 \times 10^7$.

11. Finally, the initial number of the susceptible class is found from $S_0 = N_0 - (V_0 + E_0 + I_0 + L_0) = 3.75 \times 10^7$.

12. Therefore, using these estimated parameter values, we calculated the average value of the basic reproduction number $\mathcal{R}_0$ for the year 2003-2017 TB cases in Ethiopia to be $\mathcal{R}_0 = 2.13$.

Table 4.1: The parameter values of the model (4.1)

| Parameters | Description | Value | Source |
|---|---|---|---|
| $N_0$ | Initial total population | $7.25 \times 10^7$ | [89] |
| $S_0$ | The initial number of susceptible individuals | $3.75 \times 10^7$ | Estimated |
| $V_0$ | The initial number of vaccinated individuals | $1 \times 10^6$ | Estimated |
| $E_0$ | The initial number of high-risk latent individuals | $1.19 \times 10^7$ | Fitted |
| $I_0$ | The initial number of infectious individuals | $3.73 \times 10^5$ | [89] |
| $L_0$ | The initial number of low-risk latent individuals | $2.18 \times 10^7$ | Fitted |
| $\Lambda$ | Recruitment rate | $1.4 \times 10^6$ | Estimated |
| $\beta$ | The transmission coefficient | $1.646 \times 10^{-7}$ | Fitted |
| $\varepsilon$ | Vaccination coverage rate | 0.715 | [90] |
| $\theta$ | Lose of protection for vaccination | 0.5 | [83] |
| $\mu$ | The natural death rate | 0.016 | Estimated |
| $k$ | Progression rate from $E$ *to* $I$ | 0.023 | Fitted |
| $r$ | The treatment rate of $I$ | 0.546 | Fitted |
| $1-p$ | Successful treatment rate of $I$ | 0.832 | [91] |
| $\alpha$ | Treatment rate of $E$ | 0.153 | Fitted |
| $\delta$ | TB-induced death rate | 0.17 | [89] |

### 4.4.2 Sensitivity analysis of the basic reproduction number

A sensitivity analysis using the normalized forward sensitivity index determines the relative importance of various parameters involved in disease transmission. In this section,

we use the normalized forward sensitivity index to compute the sensitivity index for the model parameter $\mathcal{R}_0$.

**Definition 4.4.1.** The normalized forward sensitivity index of $\mathcal{R}_0$ which is differentiable with respect to a given parameter $\pi$, is defined by

$$\Gamma_{\tau}^{\mathcal{R}_0} = \frac{\partial \mathcal{R}_0}{\partial \pi} \times \frac{\pi}{\mathcal{R}_0}.$$

Using this formula, we calculate the sensitivity indices of $\mathcal{R}_0$ with respect to $\beta, \alpha, r, \varepsilon$, and $p$. The values of $\Gamma_{\beta}^{\mathcal{R}_0}$ and $\Gamma_{p}^{\mathcal{R}_0}$ are positive. This tells us the total number of infected people can be decreased by reducing the contact rate of active TB-infected individuals and the treatment failure rate. On the other hand, $\Gamma_{\alpha}^{\mathcal{R}_0}$, $\Gamma_{r}^{\mathcal{R}_0}$, and $\Gamma_{\varepsilon}^{\mathcal{R}_0}$ are negative. This means that TB infection can be controlled by increasing active and latent TB-infected individuals' treatment and vaccination coverage rates. The values of the sensitivity indices for $\mathcal{R}_0$ are summarized in Table 4.2.

Table 4.2: Sensitivity indices of $\mathcal{R}_0$.

| Parameters | Description | Sensitivity index of $\mathcal{R}_0$ | Corresponding % changes |
|---|---|---|---|
| $\beta$ | The transmission coefficient | $+1$ | $-1\%$ |
| $\alpha$ | Treatment rate of $E$ | $-0.801543$ | $+1.25\%$ |
| $r$ | The treatment rate of $I$ | $-0.742021$ | $+1.35\%$ |
| $\varepsilon$ | Vaccination coverage rate | $-0.0226732$ | $+44.1\%$ |
| $p$ | Treatment failure rate | $+0.0219702$ | $-45.5\%$ |

The most sensitive parameter for $\mathcal{R}_0$ is the transmission coefficient $\beta$. The next essential parameters are the treatment rates of latent and active TB patients. Table 4.2 shows that to have 1% decrease in the value of $\mathcal{R}_0$, it is necessary to decrease the amount of $\beta$ and $p$ to 1%, and 45.5% respectively. While to have 1% decrease in the value of $\mathcal{R}_0$ it is necessary to increase the amount of $\varepsilon, r$ and $\alpha$ to 44.1%, 1.35%, and 1.25% respectively.

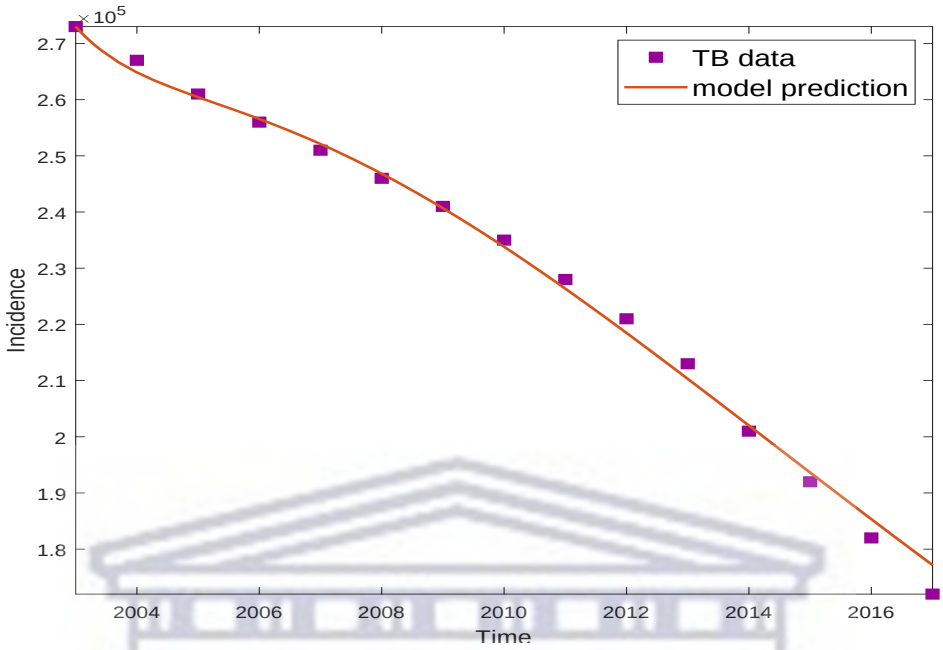


Figure 4.2: The fitted data to the reported cases using model (4.1) for Ethiopia from 2003 to 2017.

### 4.4.3 Simulations

This subsection simulates the model results using ODE 45 solvers code in MATLAB programming language. The effect of epidemiological parameters on the number of active TB patients is simulated, and their impact is determined. The results of numerical simulations are displayed graphically.

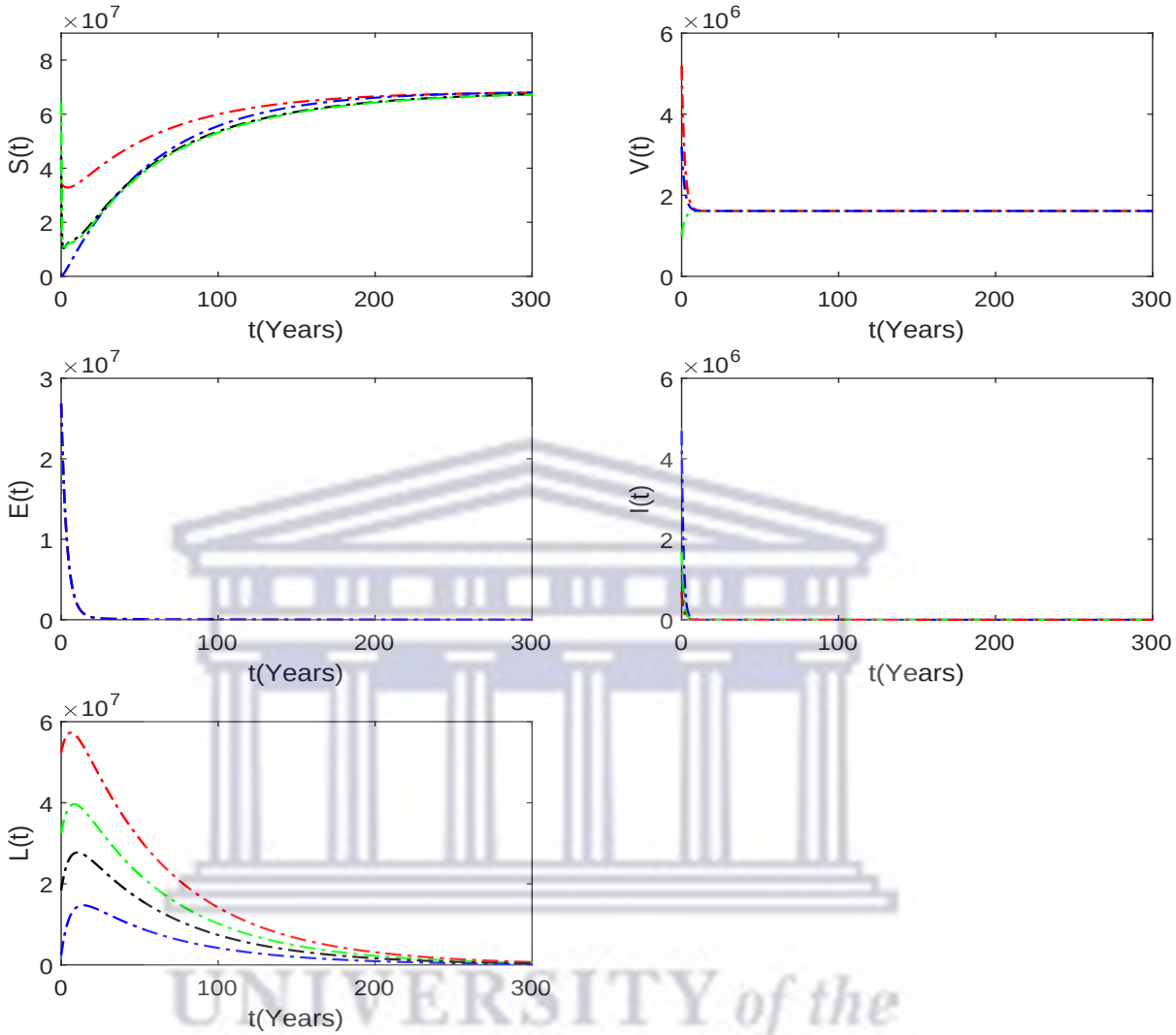


Figure 4.3: The stability of the DFE for the model (4.1) when $\mathcal{R}_g = 0.65$.

As shown in Figure 4.3, for $\mathcal{R}_g < 1$, for different initial conditions, the solution curve of the model converges to the disease-free equilibrium point $P_0^*$, this indicates that $P_0^*$ is globally asymptotically stable for $\mathcal{R}_g < 1$ and this agrees with Theorem 4.3.3.

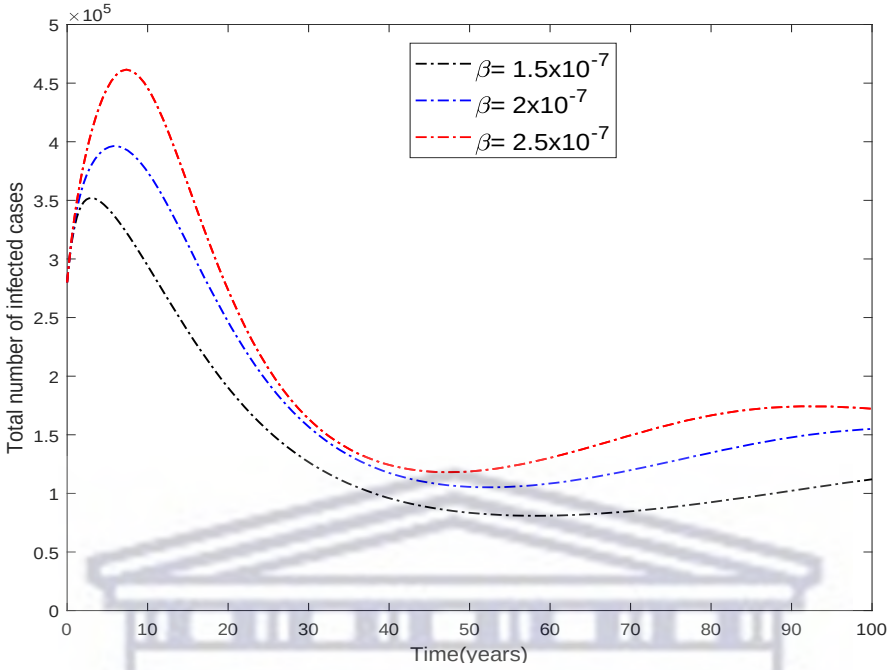


Figure 4.4: The plot shows the effect of transmission coefficient on the total number of infected class.

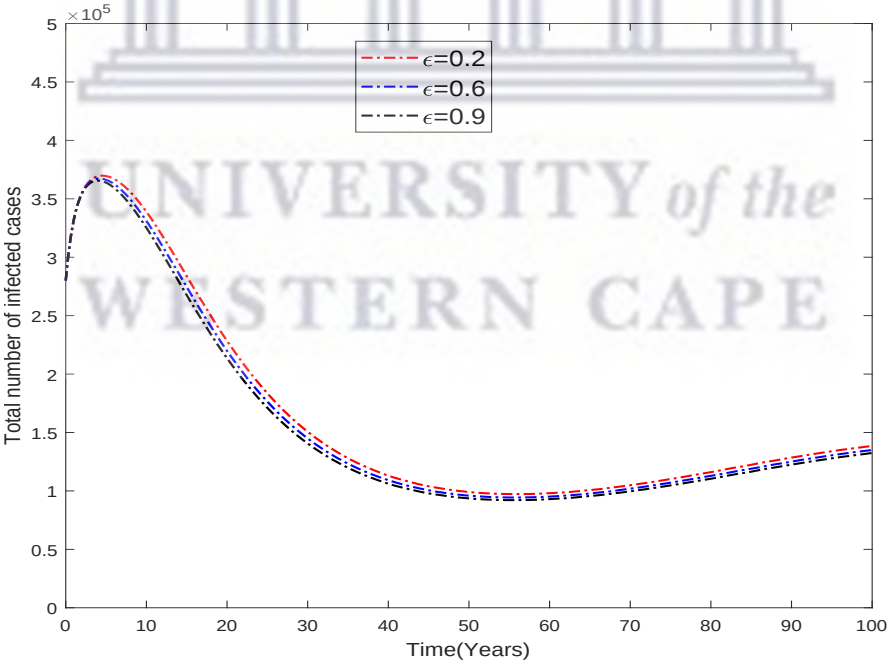


Figure 4.5: The effect of vaccination coverage on the number of infected class.

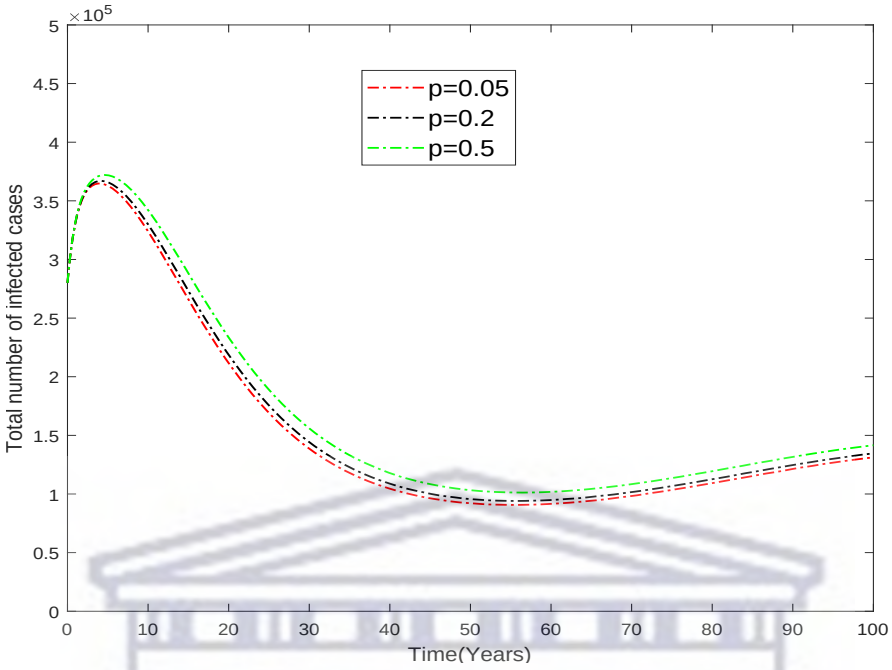


Figure 4.6: The effect of treatment failure rate on the number of infected class.

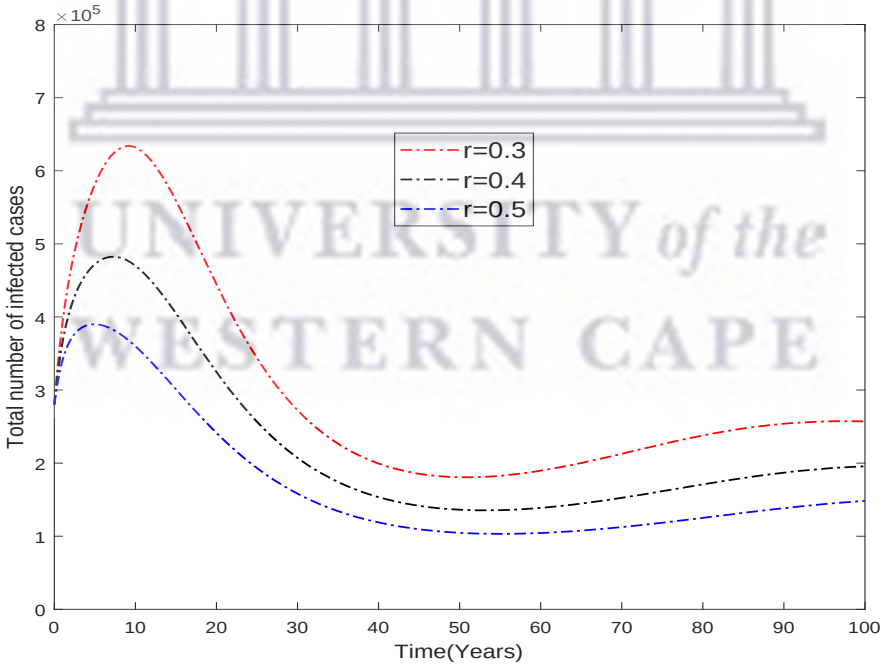


Figure 4.7: The effect of treatment coverage on the number of infected class.

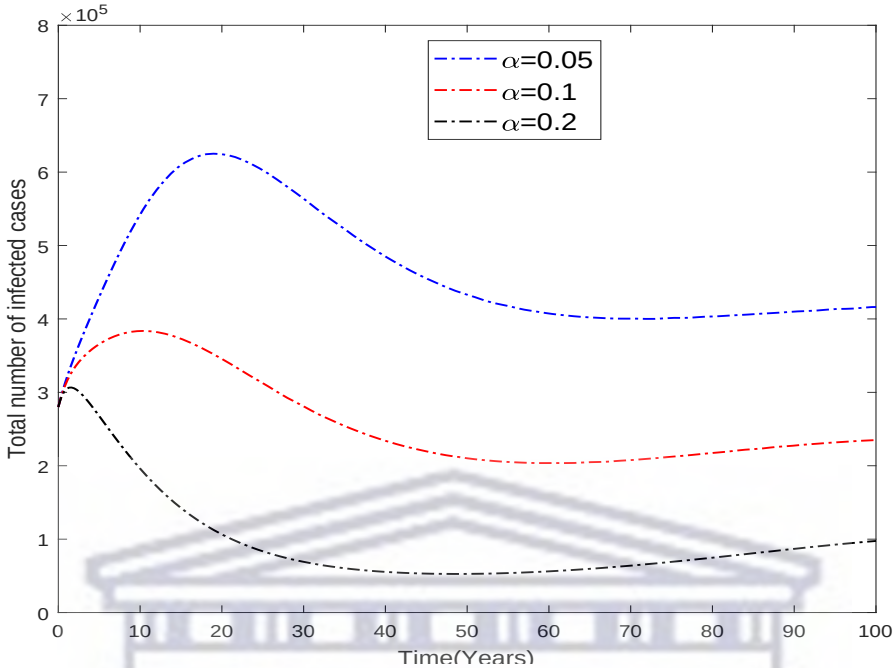


Figure 4.8: The effect of treatment coverage of high-risk latent class on the number of infected class.

Figures 4.5– 4.8 show the effect of different epidemiological parameters on the number of the infected population. It is found that decreasing the transmission coefficient (the contact between susceptible class and active TB patients) and minimizing the treatment failure rate is essential to reduce the number of infected TB patients. Also, increasing the treatment and vaccination coverage is vital to decrease the infected TB patient population.

## 4.5 Conclusion

In this chapter, a mathematical model of the transmission dynamics of TB is developed and analyzed. The reproduction number is calculated, and the equilibrium points are described. We showed that the disease-free equilibrium point $P_0^*$ is globally asymptotically stable when $\mathcal{R}_g < 1$ so that the disease dies out. Finally, we showed that increasing treatment and vaccination coverage gives rise to fewer infected TB patients.

The parameters' values of the model are obtained from the existing literature and by fitting the yearly reported TB incidence cases in Ethiopia. We estimate the basic reproduction number for TB transmission in Ethiopia as $R_0 = 2.13$. The implication is that TB is still endemic in the country, and more emphasis should be given to preventing TB transmission. Using sensitivity analysis, we found that the most influential parameter is the transmission coefficient, followed by the treatment rate of latent TB and active

TB infective individuals. Therefore, we propose that the effective strategy to eliminate TB infection in Ethiopia is reducing the transmission coefficient. This may be achieved through increasing the isolation of infectious people. The second important strategy is expanding the treatment coverage for latent and active TB contagious individuals.

The findings of this chapter suggest that the incidence rate (the rate of new infections) is a crucial factor in the transmission of TB. It is also well-known that the functional form of the incidence rate plays a critical role in modeling epidemic dynamics. As a result, various researchers have considered different incidence function forms, such as the bilinear, standard, and saturation incidence rates. Therefore, in the next chapter, we develop and analyze a model with a saturated incidence rate.

# Chapter 5

# Mathematical analysis of TB model with vaccination and saturated incidence rate

In this chapter, we introduce the saturated incidence on the compartmental model of Chapter 4. We show that if the basic reproduction number is less than unity, the disease-free equilibrium is globally asymptotically stable. Moreover, we prove that if $R_0 > 1$, the endemic equilibrium is locally asymptotically stable. Simulations with parameters calibrated to Ethiopia illustrate our theoretical results.



## 5.1 Introduction

The incidence rate (rate of new infections) plays a vital role in modeling infectious diseases. Some factors, such as population density and lifestyle, may affect the incidence rate directly or indirectly, and incidence function can determine the rise and fall of epidemics [92, 93]. In many epidemic models, the bilinear ($\beta SI$) and the standard ($\frac{\beta SI}{N}$) incidence rates are frequently used. The bilinear incidence rate is based on the law of mass action.

The saturated incidence rate $g(I)S$ was introduced into epidemic models by Capasso and Serio in 1973 [94], where $g(I)$ tends to a saturation level when $I$ gets large. The rate $\beta I$ measures the infection force of the disease, and $g(I) = \frac{1}{1 + aI}$ measures the inhibition effect from the behavioral change of the susceptible individuals when their number increases or from the crowding effect of the infective individuals. The saturation

incidence rate is more reasonable than the bilinear incidence rate when we must include the infective individuals' behavioral change and crowding effect to curb the contact rate [95–97].

This chapter develops and analyzes a basic tuberculosis mathematical model with a saturated incidence rate and BCG vaccine.

## 5.2 Model formulation

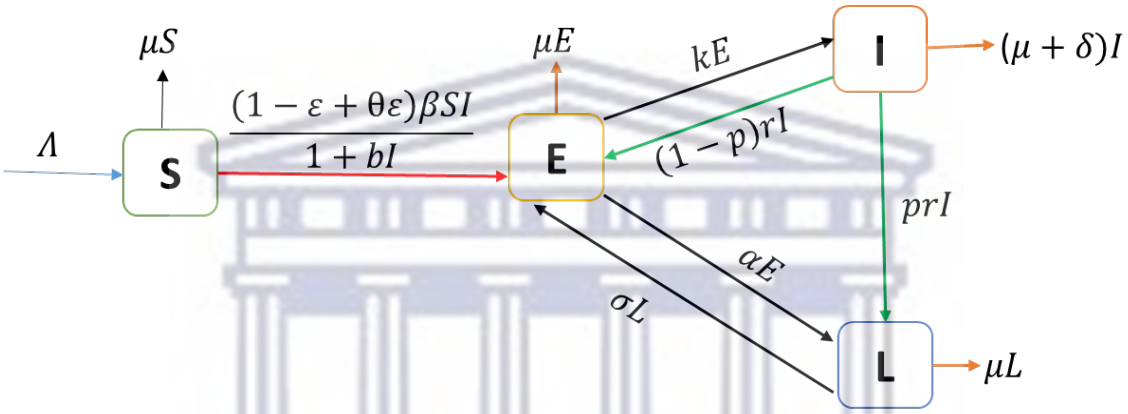


Figure 5.1: A schematic diagram of the TB model (5.1)

Based on the disease status of individuals, we divide the total population $N(t)$ into four subclasses, namely, Susceptible $S(t)$, high-risk latently infected $E(t)$, infectious (or active TB) $I(t)$, and low-risk latent $L(t)$. For the model framework, we consider the following assumptions:

1. The rate at which new individuals enter the susceptible class due to birth is denoted by $\Lambda$.

2. Following [98–100], the disease transmission rate is considered as $\frac{\beta I}{1+bI}$, where $b$ is the saturation constant and $\beta$ is the maximum contact rate between susceptible and infected individual.

3. The BCG vaccine will be given to the susceptible population of a rate $(\varepsilon S)$, where $(0 \leq \varepsilon \leq 1)$. The BCG vaccine efficacy in preventing adults from TB is incomplete, with an average efficacy of 50% [83]. This shows that vaccinated individuals may still be vulnerable to bacteria. Hence, it is reasonable to classify the vaccinated and

non-vaccinated individuals into a single class with a different chance of infection. It is assumed that the chance of being infected by the bacteria for the vaccinated and non-vaccinated population is $\frac{\theta\beta\varepsilon SI}{1+bI}$ and $\frac{\beta S(1-\varepsilon)I}{1+bI}$ respectively. Where $\theta$, with $(0 \leq \theta \leq 1)$, is a vaccinated person's immunity loss.

4. $k$ is the rate at which individuals in the high-risk latent class $E$ become infective.

5. It is assumed that treatment will be administered for both high-risk latent and active TB-infected classes. The $E$-class and $I$-class treatment rates are denoted by $\alpha$ and $r$, respectively.

6. If treatment is administered for the $I$-class with a rate $r$, then some of them will complete their treatment and recover completely at a rate $(0 \leq p \leq 1)$, and move to the $L$-class. Others, $(1-p)\,rI$, will not be cured and will remain vulnerable to the bacteria and move to the $E$ - class.

7. Patients who have completed anti-TB treatment will recover, but these individuals may remain latent because the TB bacteria stay dormant in the host body. Accordingly, we classify these individuals as low-risk latent.

8. After being cured, it is assumed that some recovered (low-risk latent) individuals can be re-infected with the bacteria and become high-risk-latently infected with the rate $\sigma$.

9. We assume that the natural death rate (any death not due to TB) is the same for all classes and is denoted by $\mu$.

10. Death due to the TB disease will happen only to $I$-class, and we denote this mortality rate as $\delta$.

11. We further assume that all parameters used in this model are non-negative.

Based on the above assumptions, we describe the dynamics of TB by the following system

of ordinary differential equations (ODEs) with four compartments.

$$\begin{cases} \frac{dS}{dt} = \Lambda - \frac{(1-\varepsilon+\theta\varepsilon)\beta SI}{1+bI} - \mu S \\ \frac{dE}{dt} = \frac{(1-\varepsilon+\theta\varepsilon)\beta SI}{1+bI} + (1-p)rI + \sigma L - (k+\alpha+\mu)\,E \\ \frac{dI}{dt} = kE - (\mu + r + \delta)\,I \\ \frac{dL}{dt} = prI + \alpha E - (\mu+\sigma)\,L \\ N(t) = S(t) + E(t) + I(t) + L(t)\,. \end{cases} \tag{5.1}$$

with the initial conditions $S_0, E_0, I_0, L_0 \geq 0$.

The complete transfer flow of the model parameters is shown in Figure 5.1. The time unit "$t$" has been considered in "years".

## 5.3 Basic properties of the model

### 5.3.1 Positivity of the solutions

Since the model system (5.1) involves the human population, it is necessary to prove that all its associated variables and parameters are nonnegative, so we have the following theorem.

**Theorem 5.3.1.** *Let the initial data $S_0, E_0, I_0$ and $L_0$ be non-negative. Then the solution set $\Omega = \{S(t), E(t), I(t), L(t)\}$ is non-negative for all $t \geq 0$.*

***Proof:*** If we let

$$\frac{(1-\varepsilon+\theta\varepsilon)\,\beta I(t)}{1+bI(t)} - \mu = H(t),$$

then it follows from the first equation of the model (5.1) that

$$\frac{dS(t)}{dt} + H(t)\,S(t) = \Lambda. \tag{5.2}$$

Multiplying both sides of Equation (5.2) by

$$\exp\left\{\int_0^t H(\tau)\,d\tau\right\},$$

gives

$$\frac{dS(t)}{dt}\exp\left\{\int_0^t H(\tau)\,d\tau\right\} + H(t)\,S(t)\exp\left\{\int_0^t H(\tau)\,d\tau\right\} = \Lambda\exp\left\{\int_0^t H(\tau)\,d\tau\right\}.$$

By the product rule of the derivative, we have

$$\frac{dS(t)}{dt}\exp\left\{\int_0^t H(\tau)\,d\tau\right\}+H(t)\,S(t)\exp\left\{\int_0^t H(\tau)\,d\tau\right\}=\frac{d}{dt}\left[S(t)\exp\left\{\int_0^t H(\tau)\,d\tau\right\}\right].$$

Hence

$$\frac{d}{dt}\left[S(t)\exp\left\{\int_0^t H(\tau)\,d\tau\right\}\right]=\Lambda\exp\left\{\int_0^t H(\tau)\,d\tau\right\}. \tag{5.3}$$

Integrating both sides of Equation (5.3) gives

$$S(t)\exp\left\{\int_0^t H(\tau)\,d\tau\right\}-S_0=\Lambda\int_0^t\exp\left\{\int_0^\tau H(u)\,du\right\}.$$

Then,

$$S(t)=S_0\exp\left\{-\int_0^t H(\tau)\,d\tau\right\}+\left[\Lambda\int_0^t\exp\left\{\int_0^\tau H(u)\,du\right\}\right]\left[\exp\left\{-\int_0^t H(\tau)\,d\tau\right\}\right]\geq 0.$$

Similarly, it can be shown that $E(t)$, $I(t)$, and $L(t)$ are non-negative for all time $t\geq 0$. This completes the proof.

### 5.3.2 Invariant region

The TB model (5.1) will be studied in a biologically feasible region as given below.

$$\Omega=\left\{(S(t),E(t),I(t),L(t))\in{\mathbb{R}_+}^4\;\middle|\;0\leq S(t)+E(t)+I(t)+L(t)\leq\frac{\Lambda}{\mu}\right\}.$$

**Lemma 5.3.2.** *The region $\Omega\subset{\mathbb{R}_+}^4$, is positively invariant for the model (5.1) with non-negativeinitial conditions in ${\mathbb{R}_+}^4$.*

***Proof***: For this model, the total population is given by:

$$N(t)=S(t)+E(t)+I(t)+L(t).$$

Then

$$\frac{dN(t)}{dt}=\frac{dS(t)}{dt}+\frac{dE(t)}{dt}+\frac{dI(t)}{dt}+\frac{dL(t)}{dt}.$$

Substituting the values from the model (5.1) we get

$$\frac{dN(t)}{dt}=\Lambda-\mu N(t)-\delta I(t)\leq\Lambda-\mu N(t).$$

Thus, integrating both sides and taking as $t \to \infty$ we get $0 \leq N(t) \leq \frac{\Lambda}{\mu}$.
Therefore the feasible solution set for the model given by

$$\Omega = \left\{ (S(t), E(t), I(t), L(t)) \in \mathbb{R}_+{}^4 \;\middle|\; 0 \leq S(t) + E(t) + I(t) + L(t) \leq \frac{\Lambda}{\mu} \right\}.$$

### 5.3.3 Disease-free equilibrium point and the basic reproduction number

The long-term behavior of a model is quite essential. When left for a long time with no external interference, we want to know whether there will eventually be a stable state to which the system converges. The system converges to a *disease-free equilibrium* if the disease consistently vanishes. It is also possible that the disease persists, and the class sizes tend to converge to a single stable point, an endemic equilibrium point.

We obtained the basic reproduction number , $R_0$, using the next-generation matrix method given in [84].
Let $X = (E,\ I, L)^T$, then it follows from the system (5.1) that

$$\frac{dX}{dt} = \mathcal{F} - \mathcal{M},$$

where

$$\mathcal{F} = \begin{pmatrix} \frac{(1-\varepsilon+\theta\varepsilon)\beta SI}{1+bI} \\ 0 \\ 0 \end{pmatrix},$$

and

$$\mathcal{M} = \begin{pmatrix} -(1-p)rI - \sigma L + (k+\alpha+\mu)E \\ -kE + (\mu + r + \delta)I \\ -prI - \alpha E + (\mu+\sigma)L \end{pmatrix}.$$

Evaluating the derivatives of $\mathcal{F}$ and $\mathcal{M}$ at DFE leads to the following matrices $F$ and:

$$F = \begin{pmatrix} 0 & \frac{\beta\Lambda(1-\varepsilon+\theta\varepsilon)}{\mu} & 0 \\ 0 & 0 & 0 \\ 0 & 0 & 0 \end{pmatrix}$$

and

$$M = \begin{pmatrix} k+\alpha+\mu & (-1+p)\,r & -\sigma \\ -k & r+\delta+\mu & 0 \\ -\alpha & -pr & \mu+\sigma \end{pmatrix}.$$

Then $R_0$ is the dominant eigenvalue of the matrix $FM^{-1}$.

Thus we have

$$R_0 = \frac{k\beta\Lambda\,(1-\varepsilon+\theta\varepsilon)\,(\mu+\sigma)}{\mu\,(\mu\,(r+\delta+\mu)\,(\alpha+\mu+\sigma)+k\,(pr\mu+(\delta+\mu)\,(\mu+\sigma)))}\,. \tag{5.4}$$

### 5.3.4 Global stability of the DFE

Global asymptotic stability of an equilibrium point means that, given any initial state, the system converges to that equilibrium point.

**Theorem 5.3.3.** *For the model (5.1), the disease-free equilibrium point $P_0^*$ is globally asymptotically stable if $R_0 \leq 1$.*

***Proof***: To establish the global stability of the disease-free equilibrium, we construct the following function:

$$T = (\mu+\sigma)\,E + \frac{k(\mu+\sigma)+\mu(\alpha+\mu+\sigma)}{k} I + \sigma L. \tag{5.5}$$

Note that $T$ is nonnegative and $T\,(P_0^*) = 0$. Differentiating with respect to $t$ and using Equation (5.1) gives

$$\begin{aligned} \dot{T} &= (\mu+\sigma)\,\dot{E} + \frac{k(\mu+\sigma)+\mu(\alpha+\mu+\sigma)}{k}\dot{I} + \sigma\dot{L}, \\ &= (\mu+\sigma)\left\{\frac{(1-\varepsilon+\theta\varepsilon)\,\beta SI}{1+bI} + (1-p)rI + \sigma L - (k+\alpha+\mu)\,E\right\} \\ &+ \frac{k\,(\mu+\sigma)+\mu\,(\alpha+\mu+\sigma)}{k}\left\{kE-(\mu+r+\delta)\,I\right\} + \sigma\left\{prI+\alpha E-(\mu+\sigma)\,L\right\}. \end{aligned}$$

Since

$$\frac{\beta SI}{1+bI} \leq \beta SI,$$

we have

$$\dot{T} \leq (\mu+\sigma)\left\{(1-\varepsilon+\theta\varepsilon)\,\beta SI+(1-p)rI+\sigma L-(k+\alpha+\mu)\,E\right\}$$
$$+\frac{k\,(\mu+\sigma)+\mu\,(\alpha+\mu+\sigma)}{k}\left\{kE-(\mu+r+\delta)\,I\right\}+\sigma\left\{prI+\alpha E-(\mu+\sigma)\,L\right\}.$$

Using $S(t) \leq \frac{\Lambda}{\mu}$ and after simplification, we have

$$\dot{T} \leq \left\{\frac{\beta\Lambda\,(\mu+\sigma)\,(1-\varepsilon+\theta\varepsilon)}{\mu}+(\mu+\sigma)\,(1-p)\,r-\frac{k(\mu+\sigma)+\mu(\alpha+\mu+\sigma)}{k}\,(\mu+r+\delta)+\sigma pr\right\}I.$$

Finally, with some rearrangement, we showed:

$$\dot{T} \leq \frac{\mu\,(r+\delta+\mu)\,(\alpha+\mu+\sigma)+k\,(pr\mu+(\delta+\mu)\,(\mu+\sigma))}{k}\left\{R_0-1\right\}I.$$

Since all model parameters are nonnegative, it follows that $\dot{T} \leq 0$ for $R_0 \leq 1$ and $\dot{T}=0$ only if $I=0$. Hence, $T$ is a Lyapunov function on $\Omega$ and the largest compact invariant subset of $\{(S(t),E(t),I(t),L(t)) \in \Omega\colon\ \dot{T}=0\}$ is the singleton $P_0^*$. LaSalle's invariant principle [87] implies that $P_0^*$ is globally asymptotically stable in $\Omega$.

### 5.3.5 The Endemic Equilibrium point (EEP)

**Lemma 5.3.4.** *If $R_0>1$, then the model (5.1) has a unique positive endemic equilibrium point.*

***Proof:*** The EEP of the model (5.1) at $P^*=(S^*,\ E,I^*,L^*)$ is obtained by setting the right-hand side ofthe system (5.1) equal to zero, we get:

$$S^*=\frac{\mu(r+\delta+\mu)(\alpha+\mu+\sigma)+kpr\mu+k\,(\delta+b\Lambda+\mu)\,(\mu+\sigma)}{k\beta\,(1-\varepsilon+\theta\varepsilon)\,(\mu+\sigma)+kb\mu(\mu+\sigma)},$$
$$E^*=\frac{\mu\,(r+\delta+\mu)}{k\,(\beta\,(1-\varepsilon+\theta\varepsilon)+b\mu)}\,(R_0-1),$$
$$I^*=\frac{\mu}{\beta\,(1-\varepsilon+\theta\varepsilon)+b\mu}\,(R_0-1),$$

and

$$L^*=\frac{\mu\,(krp+\alpha\,(r+\delta+\mu))}{k\,(\beta\,(1-\varepsilon+\theta\varepsilon)+b\mu)\,(\mu+\sigma)}\,(R_0-1).$$

Clearly, from the above, we can conclude that a unique positive EEP exists whenever $R_0>1$.

**Theorem 5.3.5.** *(Local stability at EEP): If $R_0 > 1$ and $\sigma = 0$ then the system (5.1) is locally asymptotically stable about the endemic equilibrium point $P^*$.*

***Proof*:** For $\sigma = 0$ the variable $L$ will only appear in the fourth equation of the model (5.1), hence the system can be reduced to the three-dimensional system:

$$\begin{cases} \frac{dS}{dt} = \Lambda - \frac{(1-\varepsilon+\theta\varepsilon)\beta SI}{1+bI} - \mu S \\ \frac{dE}{dt} = \frac{(1-\varepsilon+\theta\varepsilon)\beta SI}{1+bI} + (1-p)rI - (k+\alpha+\mu)\,E \\ \frac{dI}{dt} = kE - (\mu+r+\delta)\,I \end{cases} \tag{5.6}$$

By applying the Routh-Hurwitz criterion of stability [52] and by denoting $\psi = (1-\varepsilon+\theta\varepsilon)\beta$ for the system (5.6) we have the following Jacobian matrix at $P^*$:

$$J^* = \begin{pmatrix} -\mu - \frac{\beta\psi I^*}{1+bI^*} & 0 & -\frac{\beta\psi S^*}{(1+bI^*)^2} \\ \frac{\beta\psi I^*}{1+bI^*} & -k-\alpha-\mu & r - pr + \frac{\beta\psi S^*}{(1+bI^*)^2} \\ 0 & k & -r-\delta-\mu \end{pmatrix}.$$

The associated characteristic equation of $J^*$ is given by:

$$\lambda^3 + a_1\lambda^2 + a_2\lambda + a_3 = 0.$$

where

$$\begin{aligned} a_1 &= k + r + \alpha + \delta + 3\mu + \frac{\beta\psi I^*}{1+bI^*}, \\ a_2 &= \frac{k\beta^2\Lambda\,(k+r+\alpha+\delta+2\mu)\,\psi^2 + b\left[\mu((\alpha+\mu)\,(r+\delta+\mu) + k\,(pr+\delta+\mu))^2\,[\mathcal{R}_0-1]\right]}{\beta\,((\alpha+\mu)\,(r+\delta+\mu) + k\,(pr+\delta+b\Lambda+\mu))\,\psi} \\ &\quad + \frac{k\beta^2\Lambda\,(k+r+\alpha+\delta+2\mu)\,\psi^2 + b\left[k\beta\Lambda\psi\,(k+r+\alpha+\delta)\,\mu + 2\mu^2\psi\right]}{\beta\,((\alpha+\mu)\,(r+\delta+\mu) + k\,(pr+\delta+b\Lambda+\mu))\,\psi}, \\ a_3 &= \frac{\mu\,(b\mu+\beta\psi)\left\{((\alpha+\mu)\,(r+\delta+\mu) + k\,(pr+\delta+\mu))^2\right\}[R_0-1]}{\beta((\alpha+\mu)(r+\delta+\mu) + k(pr+\delta+b\Lambda+\mu))\psi}, \\ a_1a_2 - a_3 &= \frac{[R_0-1]\,\mu((\alpha+\mu)\,(r+\delta+\mu) + k\,(pr+\delta+\mu))^2\,((\alpha+\mu)\,(r+\delta+\mu))\,(b\mu+\beta\psi)}{\beta((\alpha+\mu)\,(r+\delta+\mu) + k\,(pr+\delta+b\Lambda+\mu))^2\psi} \\ &\quad + \frac{[R_0-1]\,\mu((\alpha+\mu)\,(r+\delta+\mu) + k\,(pr+\delta+\mu))^2\,(k\,(pr+\delta+b\Lambda+\mu))\,(b\mu+\beta\psi)}{\beta((\alpha+\mu)\,(r+\delta+\mu) + k\,(pr+\delta+b\Lambda+\mu))^2\psi} \\ &\quad + \frac{A\left(k\beta^2\Lambda\,(k+r+\alpha+\delta+2\mu)\,\psi^2\right) + bA\left([\mathcal{R}_0-1]\,\mu((\alpha+\mu)\,(r+\delta+\mu) + k\,(pr+\delta+\mu))^2\right)}{\beta((\alpha+\mu)\,(r+\delta+\mu) + k\,(pr+\delta+b\Lambda+\mu))^2\psi} \\ &\quad + \frac{bA\left(k\beta\,(k+r+\alpha+\delta)\,\Lambda\psi + 2\mu^2\psi\right)}{\beta((\alpha+\mu)\,(r+\delta+\mu) + k\,(pr+\delta+b\Lambda+\mu))^2\psi}. \end{aligned}$$

where

$$A = k^2\left(pr+\delta+b\Lambda+\mu\right)+\left(\alpha+\mu\right)\left(r+\delta+\mu\right)\left(r+\alpha+\delta+2\mu\right)+k\left(r\left(\alpha+\delta+b\Lambda+2\mu\right)+\beta\Lambda\psi\right)$$
$$+k\left(2\alpha\delta+\delta^2+b\alpha\Lambda+b\delta\Lambda+2\alpha\mu+4\delta\mu+3b\Lambda\mu+3\mu^2+pr\left(r+\alpha+\delta+2\mu\right)\right).$$

Clearly $a_1$, $a_2$, $a_3$ and $a_1a_2-a_3$ are positive whenever $R_0>1$, Thus, the Routh-Hurwitz criterion is satisfied. Therefore, the endemic equilibrium point $P^*$ of the system (5.6) is locally asymptotically stable for $R_0>1$.

This completes the proof.

## 5.4 Sensitivity analysis of $R_0$

This section examines the effects of various model parameters on the basic reproduction number $R_0$. For this purpose, we used the normalized forward sensitivity index, also known as elasticity [71]. Let $R_0$ be a differentiable function with respect to $\pi$, then the normalized forward sensitivity index of $R_0$ with respect to the parameter $\pi$ is given by:

$$\Gamma_{\pi}^{R_0} = \frac{\partial R_0}{\partial \pi}\times\frac{\pi}{R_0}. \tag{5.7}$$

This normalized sensitivity index measures the relative change of $R_0$ with respect to $\pi$.

To study the sensitivity of $R_0$, we choose the parameters $\beta, \alpha, r, \varepsilon$, and $p$. The sensitivity index, however, was not calculated for the other parameters since they are not useful for disease control. For example, when the natural death rate increases, the number of both (the infected and the susceptible) decreases. Furthermore, we are powerless to control the natural death.

Using the above formula (5.7) and taking the parameters' value in Table 5.1, we calculate the sensitivity indices of the basic reproduction number with respect to these parameters.

Table 5.1: Sensitivity indices of $R_0$ with respect to model parameters.

| Parameters | Description | Sensitivity index of $R_0$ |
|---|---|---|
| $\beta$ | The transmission coefficient | $+1$ |
| $\alpha$ | Treatment rate of $E$ | $-0.801497$ |
| $r$ | The treatment rate of $I$ | $-0.74021$ |
| $\varepsilon$ | Vaccination coverage rate | $-0.55642$ |
| $p$ | Successful treatment rate of $I$ | $-0.0747728$ |

The positive (negative) values indicate a positive (negative) correlation with $R_0$, whereas the magnitude determines the importance of parameter [101]. From Table 5.1, we can see that $\beta$ has a positive sensitivity index value, implying that a positive change in this parameter will increase the total infected population $(E + I)$. In contrast, $\alpha\, r, \varepsilon$, and $p$ have negative sensitivity index values; thus, raising these parameters will decrease the number of the total infected population. The effect of the transmission rate $(\beta)$ has the largest influence on $R_0$ while the effect of successful treatment rate for the $I$ class( $p$) has the smallest impact to $R_0$. Further, this implies that increasing the value of $\beta$ by 10% will increase the basic reproduction number by 10%. On the other hand, the parameters $\alpha$ , $r, \varepsilon$, and $p$ have negative influence hence, increasing these parameters by 10% will decrease the basic reproduction number by 8.015%, 7.402%, 5.564%, and 0.748% respectively.

## 5.5 Numerical simulation and discussion

In Chapter 4, we estimated the value of the parameters of the TB model based on Ethiopian data, and in the current Chapter, we used those parameters' values. Additionally, we assume the value of $b$ to be 0.0004

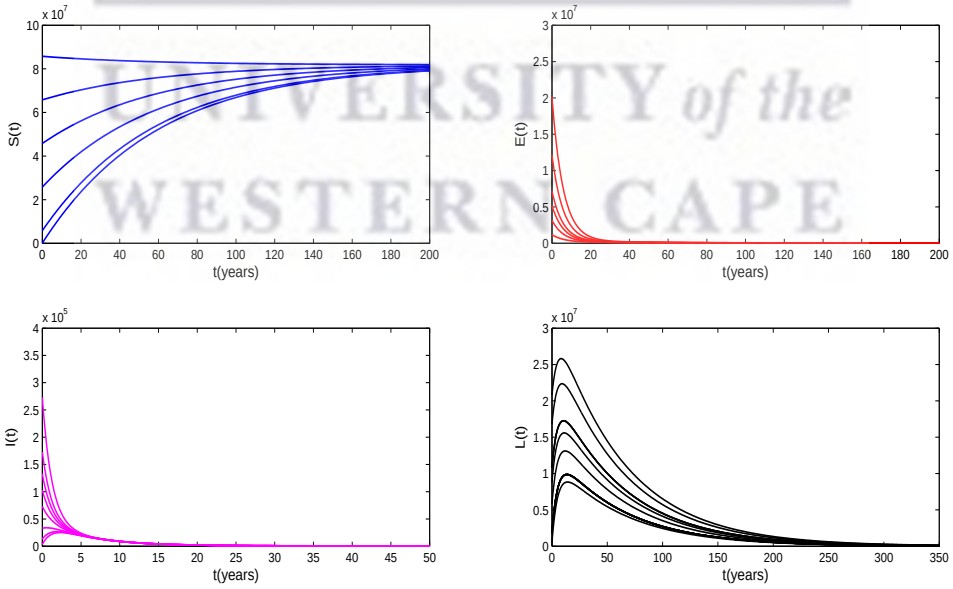


Figure 5.2: The stability of the DFE for the model (5.1) when $\beta = 1.65 \times 10^{-8}$ and $R_0 = 0.164$.

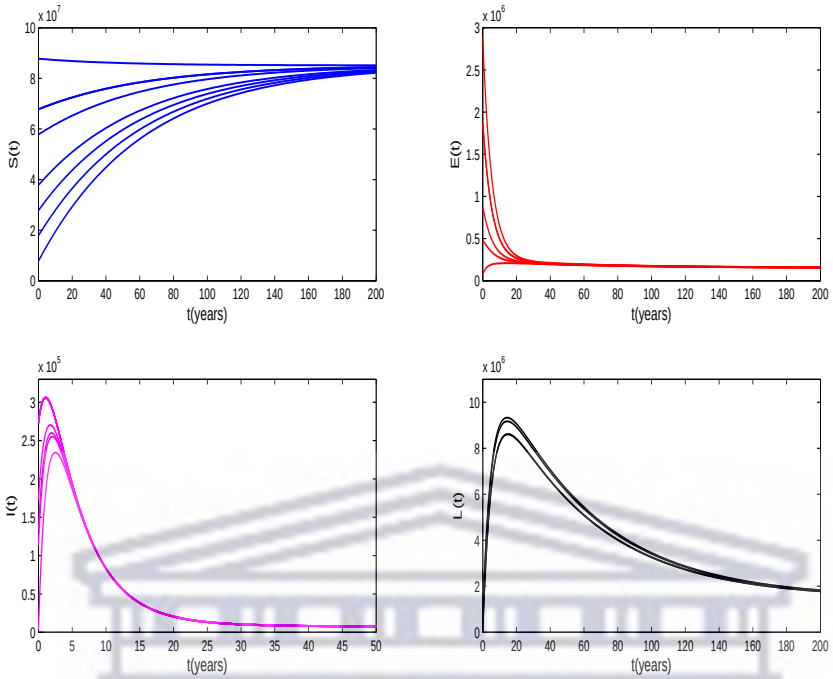


Figure 5.3: The stability of the EEP for the model (5.1) when $\beta = 3.02 \times 10^{-7}$ and $R_0 = 3.0014$.

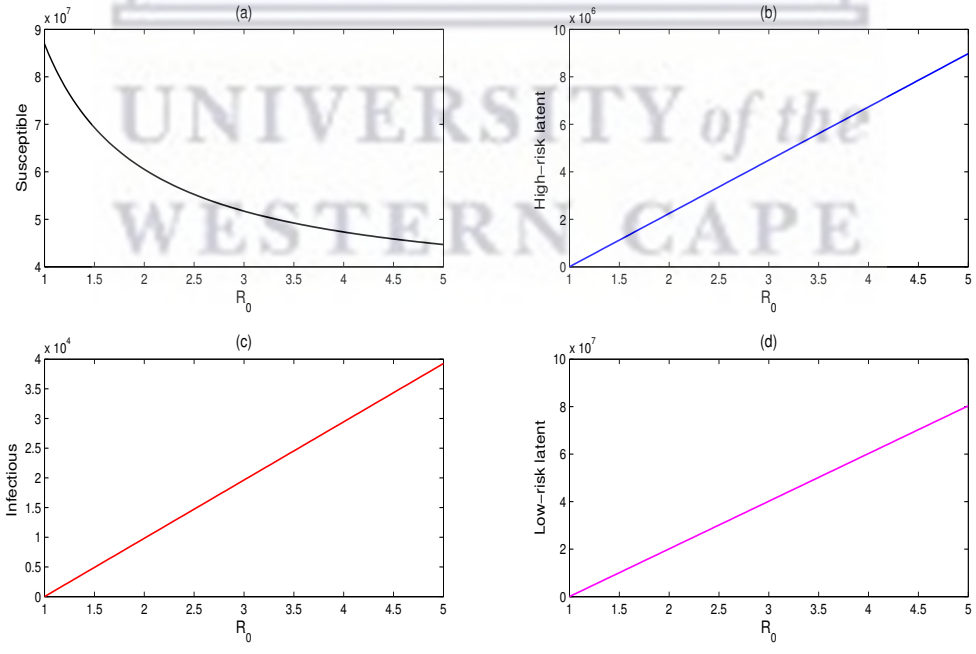


Figure 5.4: Graphs show the behavior of each state variables as the reproduction number gets larger.

Figure 5.2 presents the dynamics of the model for different initial conditions. It shows that only the susceptible population ($S^* = 8.7 \times 10^7$) persists, but the high-risk latent ($E$), infective ($I$), and the low-risk latent ($L$ ) decline to zero. It shows that system (5.1) is globally asymptotically stable at the DFE whenever $R_0 \leq 1$, which supports our analytical results stated in Theorem 5.3.3. Similarly, in Figure 5.3, for $R_0 > 1$, the solution curves of the model are plotted by varying the initial values of the compartments, and it tends to the endemic equilibrium point. This confirms that $P^*$ is locally asymptotically stable, supporting the conclusion of Theorem 5.3.5.

Figure 5.4 is a graphical representation of the components of the endemic equilibrium point, $P^*$. It shows the changes in the susceptible individuals, high-risk latent, infectious, and low-risk latent classes as the reproduction number, $R_0$, varies. In Figure 5.4(a), the susceptible individuals are being depleted rapidly as $R_0$ becomes large. Figure 5.4(b), (c), and (d) show that the number of high-risk latent, infectious, and low-risk latent individuals have linear relationships with the reproduction number, $R_0$.

Generally, Figure 5.2–5.4 shows the role of reproduction number in determining the dynamics of TB. It is shown that if $R_0 < 1$, the system appears disease-free. That is, TB will ultimately be eradicated from the population. On the other hand, when the reproduction number is higher than unity, the system will persist in the endemic state. That is, TB will spread in the population.

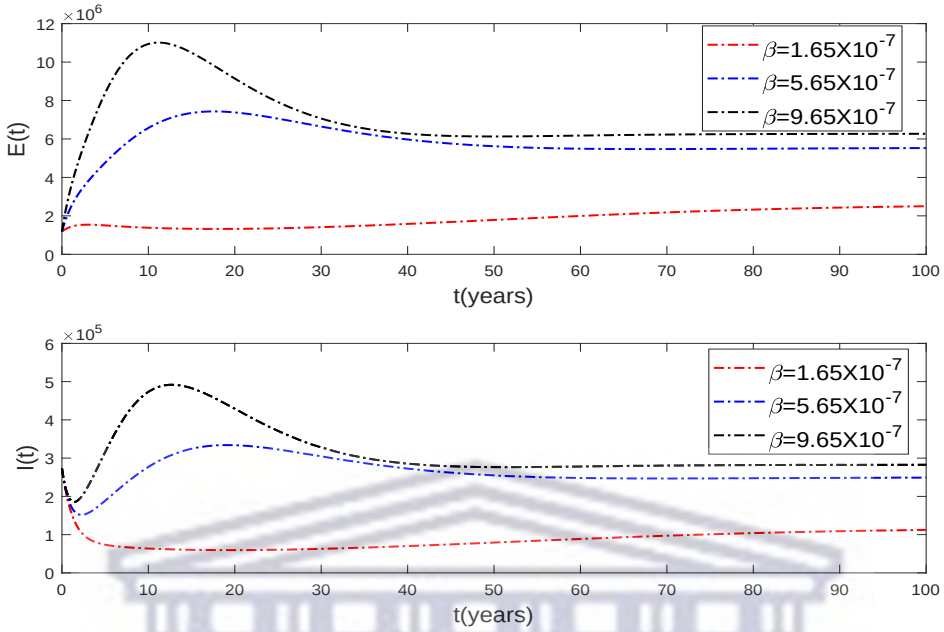


Figure 5.5: Simulation of high-risk exposed and active TB infected population with different values of $\beta$.

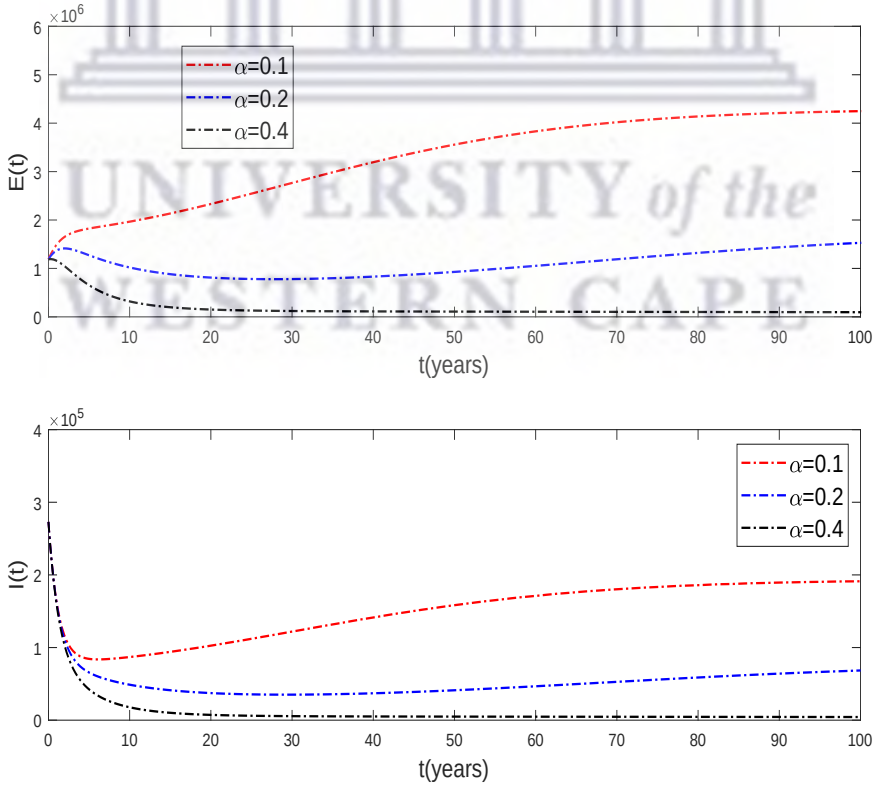


Figure 5.6: Simulation of high-risk exposed and active TB infected population with different values of $\alpha$.

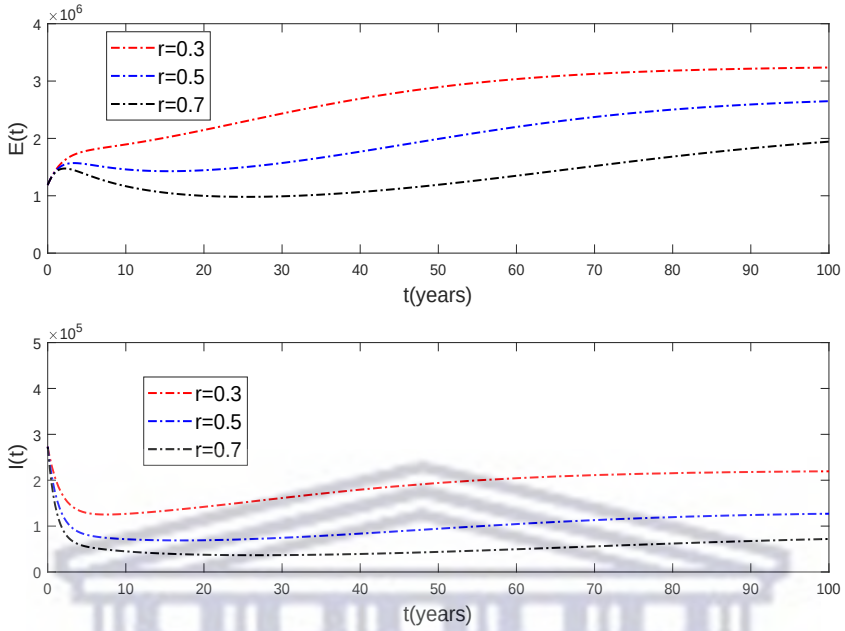


Figure 5.7: Simulation of high-risk exposed and active TB infected population with different values of $r$.

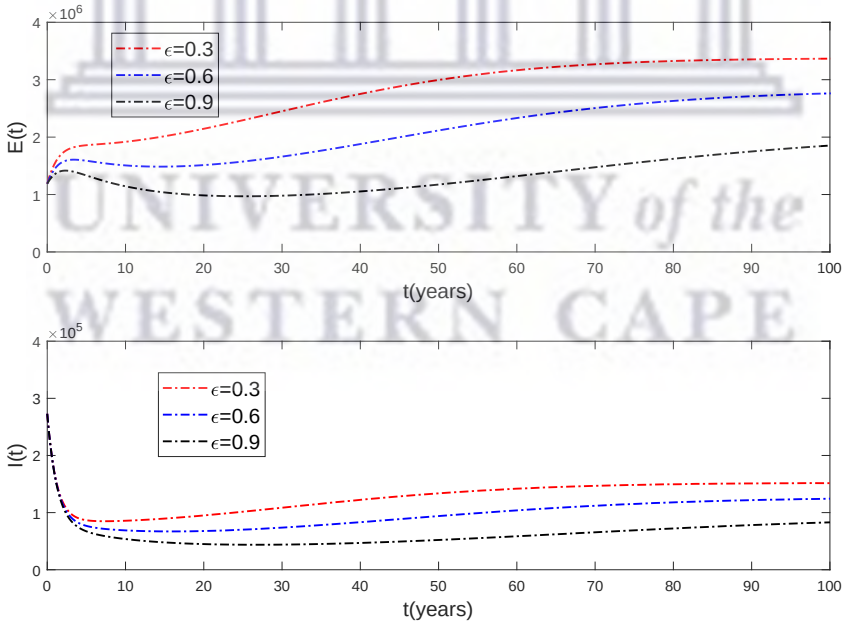


Figure 5.8: Simulation of high-risk exposed and active TB infected population with different values of $\varepsilon$

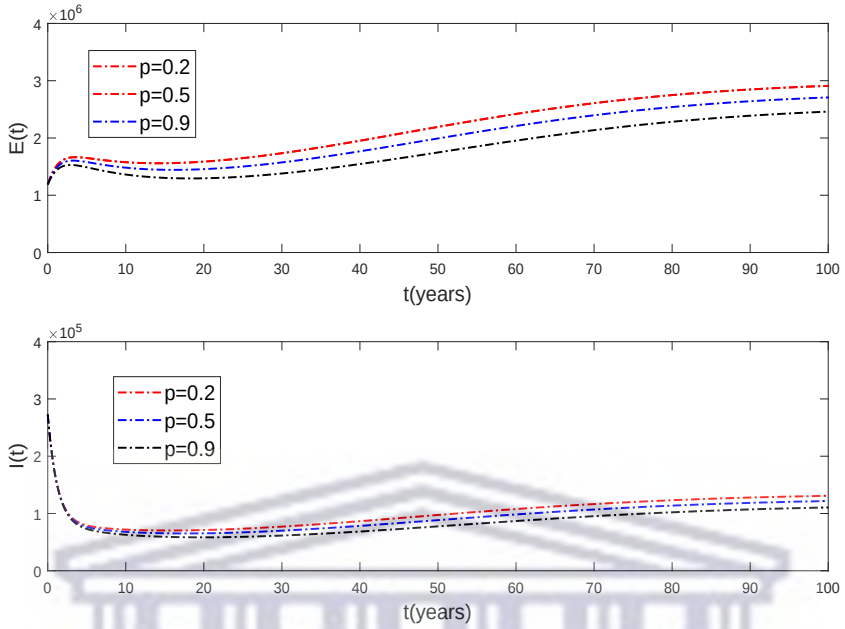


Figure 5.9: Simulation of high-risk exposed and active TB infected population with different values of $p$

Figure 5.5 explains the effect of the transmission coefficient $\beta$ on the number of high-risk exposed and active TB populations. It shows that an increase in the TB transmission rate increases the number of high-risk exposed and active TB populations. Figure 5.6 shows the simulation of active TB and high-risk exposed populations for different values of $\alpha$. Thus, it can be seen that increasing the treatment rate for high-risk latent TB patients helps to reduce the total number of both high-risk exposed and active TB individuals. From Figure 5.7, it is clear that by increasing the treatment rate for active TB patients, the total number of high-risk exposed and active TB individuals decreases.

Similarly, Figure 5.8 shows the simulation of active TB and high-risk exposed populations for different values of $\varepsilon$. As we can see from the figure, increasing the coverage of the BCG vaccine for newborns can reduce the total number of the infected population. Finally, Figure 5.9 shows the effect of successful treatment rate $p$. Again, the number of infected individuals decreases when $p$ increases.

## 5.6 Conclusion

This chapter investigates the tuberculosis disease model with vaccination and a saturated incidence rate. Our model divides the population into four compartments: susceptible, high-risk latent, infective, and low-risk latent population. Two equilibria, the

disease-free and endemic equilibrium, are derived for the proposed model. In addition, we have found the basic reproduction number, which helps us to determine the model's behavior. We obtain that the disease-free equilibrium point of the model (5.1) is globally asymptotically stable when $R_0 < 1$. On the other hand, if $R_0 > 1$, the endemic equilibrium point is locally asymptotically stable.

From the numerical simulations, the number of high-risk exposed class and active TB infected population has a linear relationship with the reproduction number. All become large as $R_0$ becomes large. On the other hand, the basic reproduction number depends on the transmission rate $\beta$, treatment rate of high-risk latent $\alpha$, treatment rate of active TB $r$, vaccination coverage rate $\varepsilon$, and successful treatment rate of active TB $p$. Therefore, it is vital to identify the best strategies to control and eradicate the disease.

Using sensitivity analysis in this study, we found that the first effective way to prevent the spread of tuberculosis in Ethiopia is to minimize contact between TB-infected and susceptible individuals. The second important strategy is to increase access to treatment for latently infected individuals. Therefore, early detection and isolation of infectious people, conducting health campaigns and educating the community, screening high-risk exposed individuals, and treating latent TB are essential strategies to control the spread of TB in Ethiopia. At the same time, the BCG vaccine plays a vital role in preventing the disease.

# Chapter 6

# Tuberculosis in Ethiopia: Optimal Intervention Strategies and Cost-Effectiveness Analysis

In this chapter, we use the mathematical model of tuberculosis disease dynamics developed in Chapter 5 to design optimal strategies to minimize the number of high-risk latent and active TB infectious individuals in Ethiopia.

## 6.1 Introduction

Infectious diseases can exhibit complex nonlinear dynamics, and it is possible to examine, explain, and predict their transmission dynamics using mathematical models (see for example [37, 79, 102–105]). An optimal control problem entails the identification of a feasible scheme, policy, program, strategy, or campaign to achieve the optimal possible outcome of a system [106]. Numerous scholars (for example, [17–19, 107–109]) have applied the optimal control theory to determine the best mitigation strategies for TB disease.

Sunhwa Choi and Eunok Jung [17] developed a mathematical model for the transmission dynamics of TB in South Korea by considering three different control strategies (distancing, case finding, and case holding efforts). Their result showed that isolation of infectious people, early TB patient detection, and educational programs are the most effective interventions to prevent TB transmission in South Korea.

In the paper [19], a mathematical TB model with control was developed and analyzed

based on the Philippines' data. Their study showed that enhancing active case finding instead of the case holding control together with distancing has significant potential for curtailing the spread of TB in the Philippines.

Gao and Huang [107] analyzed a TB model incorporating vaccination, case finding, and case holding controls. Their result revealed that combining the three controls is the most effective and less expensive among different strategies.

The mathematical model developed by Silva et al. [108] for the transmission dynamics of TB in Angola by considering two control strategies (case finding and case holding controls). Their result showed that the combined strategy that involves both controls is preferable.

Kereyu and Seleshi Demie [18] developed and analyzed a TB model for Haramaya district, Ethiopia. They considered three control strategies (distancing, case finding, and treatment efforts). Their result suggested that combining all interventions makes for the best strategy to eradicate TB disease from the district at an optimal level with minimum cost.

All the above studies showed that the strategies we use to control the spread of TB may vary depending on the situation in the country. Therefore, each government must adopt a better, more cost-effective approach based on its realities.

In Ethiopia, tuberculosis is still a major health problem and one of the leading causes of death [13]. Therefore, effective prevention measures are needed to stop the spread of tuberculosis in Ethiopia. This chapter searches for optimal strategies to minimize the number of TB-infectious individuals using actual data from Ethiopia.

## 6.2 TB Model with Controls

The total population size $N(t)$ is partitioned into four subclasses: susceptible ($S$), high-risk latent ($E$), infectious ($I$), and low-risk latent ($L$). We aggregated the two groups, the recovered and the low-risk latent, in a class called low-risk individuals ($L$).

$$\begin{cases} \frac{dS}{dt} = \Lambda - \frac{\beta\psi SI}{1+bI} - \mu S \\ \frac{dE}{dt} = \frac{\beta\psi SI}{1+bI} + (1-p)\, rI + \sigma L - (k+\alpha+\mu)\, E \\ \frac{dI}{dt} = kE - (\mu + r + \delta)\, I \\ \frac{dL}{dt} = prI + \alpha E - (\mu + \sigma)\, L \\ N = S + E + I + L, \end{cases} \tag{6.1}$$

with $\psi = (1-\varepsilon+\theta\varepsilon)$.

The recruitment rate to the susceptible population is assumed to be constant $\Lambda$. We assume that all classes have the same natural death rate $\mu$, with disease-induced mortalities occurring only in the $I$ class at a rate $\delta$. The susceptible individual acquires the TB bacteria through contact with infected individuals with a nonlinear transmission rate $\frac{\beta I}{1+bI}$. It is assumed that the BCG vaccine will be administered to susceptible individuals (at a rate $\varepsilon S$). People who have been vaccinated can become infected because the vaccine is imperfect and does not completely protect against the disease. The vaccinated individuals are infected at a rate $\theta\varepsilon\beta SI$ where $0 \leq \theta \leq 1$ is the loss of vaccine protection. Newly infected individuals (with a latent level) will develop active TB (at a rate of $k$). We assume that patients at the latent stage will move to the $L$-class with a $\alpha E$ rate when treated. Here $r$ is the treatment coverage rate, $p$ represents the successful treatment rate for active TB-infected individuals, and $\sigma$ represents the relapse rate.

We modified the model (6.1) by including three control strategies, $u_i = u_i(t)$, for $i \in \{1, 2, 3\}$. The controls represent the intensities of different public health interventions. The function $u_1(t)$ is a distancing control associated with the effort to reduce susceptible individuals that become infected, and such effort includes an isolation policy, wearing a face mask, or a public educational program. A case finding control ($u_2(t)$) represents the effort of decreasing the number of latently infected individuals that may develop active TB. Such activities include screening and treating latent individuals at high risk of developing active TB. The third strategy is a case holding control, denoted by $u_3(t)$. It refers to efforts to prevent the failure of treatment in infectious individuals (e.g., patient supervision, including activities used to ensure the regularity of drug intake until the last treatment stage is attained).

This leads to the following system of ODEs:

$$\begin{cases} \frac{dS}{dt} = \Lambda - \frac{(1-u_1)\beta\psi SI}{1+bI} - \mu S \\ \frac{dE}{dt} = \frac{(1-u_1)\beta\psi SI}{1+bI} + (1-(1+u_3)\,p)\,rI + \sigma L - (k + (1+u_2)\,\alpha + \mu)\,E \\ \frac{dI}{dt} = kE - (\mu + r + \delta)\,I \\ \frac{dL}{dt} = (1+u_3)\,prI + (1+u_2)\,\alpha E - (\mu+\sigma)\,L \\ N = S + E + I + L, \end{cases} \tag{6.2}$$

with initial conditions $S_0, E_0, I_0, L_0 \geq 0$.

Let $U$=$\{ (u_1,\ u_2,\ u_3\ ) \mid u_1, u_2$ and $u_3$ are Lebesgue integrable functions on the interval $[0,\infty)$, with $0 \leq u_i \leq 1,\ i = 1,\ 2,\ 3\}$.

We searched for an optimal control $(u_1^*, u_2^*, u_3^*) \in U$ that minimizes the objective functional $J(u_1, u_2, u_3)$

where

$$J(u_1, u_2, u_3) = \int_{t_0}^{t_f} \left[ E(t) + I + \frac{1}{2} B_1 u_1^2 + \frac{1}{2} B_2 u_2^2 + \frac{1}{2} B_3 u_3^2 \right] dt. \tag{6.3}$$

In Equation (6.3), the values of $t_0$ and $t_f$ are taken as 0 and 20, respectively, to determine Ethiopia's 20-year (2019–2038) effective TB control strategies. The constants $B_i$, $i = 1, 2, 3$, are positive weight constants, which balance the cost factors associated with the controls $u_1,\ u_2$ and $u_3$, respectively. The functions $\frac{1}{2} B_1 u_1^2$, $\frac{1}{2} B_2 u_2^2$ and $\frac{1}{2} B_3 u_3^2$ are the costs of the controls $u_1,\ u_2$ and $u_3$, respectively. The cost terms are considered nonlinear quadratic functions (as in [109–111]).

***Existence of an Optimal Control***

**Theorem 6.2.1.** *There exists an optimal control $(u_1^*,\ u_2^*,\ u_3^*)$ that minimizes the objective functional $J(u_1,\ u_2,\ u_3)$ subject to the control system (6.2).*

**Proof.** Let us denote the right-hand side of the system (6.2) by $y(t,\ \overrightarrow{x},\ \overrightarrow{u})$. Then following the same procedure as in [107], we prove the existence of an optimal control $(u_1^*,\ u_2^*,\ u_3^*)$. We must first show that the following conditions are met to achieve this.

i $y$ is of class $C^1$ and there exists a constant $c$ such that

$$|y(t,\ 0,\ 0)| \leq c,\ |y_{\overrightarrow{x}}(t,\ \overrightarrow{x},\ \overrightarrow{u})| \leq c(1 + |\overrightarrow{u}\ |), |\ y_{\overrightarrow{u}}(t,\ \overrightarrow{x},\ \overrightarrow{u})\ | \leq c.$$

ii The set of all solutions to the system (6.2) with corresponding control in $U$ is nonempty.

iii There exist functions $a_1$ and $a_2$ such that $y(t,\ \overrightarrow{x},\ \overrightarrow{u}) = a_1(t,\ \overrightarrow{x}\ ) + a_2(t,\ \overrightarrow{x})\overrightarrow{u}$,

iv The control set $U = [0, 1] \times [0, 1] \times [0, 1]$ is closed, convex and compact,

v The integrand of the objective function is convex in $U$.

To verify the first conditions, let us write

$$y\left(t,\ \overrightarrow{x},\ \overrightarrow{u}\right)=\begin{pmatrix}\Lambda-\frac{(1-u_1)\beta\psi SI}{1+bI}-\mu S\\ \frac{(1-u_1)\beta\psi SI}{1+bI}+\left(1-\left(1+u_3\right)p\right)rI+\sigma L-\left(k+\left(1+u_2\right)\alpha+\mu\right)E\\ kE-\left(\mu+r+\delta\right)I\\ \left(1+u_3\right)prI+\left(1+u_2\right)\alpha E-\left(\mu+\sigma\right)L\end{pmatrix}.$$

Then we can easily show that $y\left(t,\ \overrightarrow{x},\ \overrightarrow{u}\right)$ is of class $C^1$ and $|y(t,\ 0,\ 0)|=\Lambda$. Moreover, we will have the following

$$|y_{\overrightarrow{x}}\left(t,\ \overrightarrow{x},\ \overrightarrow{u}\right)|=\left|\begin{pmatrix}-\mu-\frac{(1-u_1)\beta\psi I}{1+bI} & 0 & -\frac{(1-u_1)\beta\psi S}{(1+bI)^2} & 0\\ \frac{(1-u_1)\beta\psi I}{1+bI} & -k-\alpha-\mu-\alpha u_2 & \frac{((1-p)r-pru_3)(1+bI)^2+(1-u_1)\beta\psi S}{(1+bI)^2} & \sigma\\ 0 & k & -\left(r+\delta+\mu\right) & 0\\ 0 & \alpha\left(1+u_2\right) & pr\left(1+u_3\right) & -\left(\mu+\sigma\right)\end{pmatrix}\right|,$$

and

$$|y_{\overrightarrow{u}}\left(t,\ \overrightarrow{x},\ \overrightarrow{u}\right)|=\left|\begin{pmatrix}\frac{\beta\psi SI}{1+bI} & 0 & 0\\ -\frac{\beta\psi SI}{1+bI} & -\alpha E & -prI\\ 0 & 0 & 0\\ 0 & \alpha E & prI\end{pmatrix}\right|.$$

Since $S,\ E,\ I$, and $L$ are bounded, there exists a constant $c$ such that

$$|y\left(t,\ 0,\ 0\right)|\leq c,\ |y_{\overrightarrow{x}}\left(t,\ \overrightarrow{x},\ \overrightarrow{u}\right)|\leq c\left(1+|\overrightarrow{u}\ |\right),\ |y_{\overrightarrow{u}}\left(t,\ \overrightarrow{x},\ \overrightarrow{u}\right)|\leq c.$$

This shows that condition (i) is satisfied.

According to condition (i), there is a unique solution for the constant controls, which will ensure that condition (ii) is met.
Besides,

$$y\left(t,\ \overrightarrow{x},\ \overrightarrow{u}\right)=\begin{pmatrix}\Lambda-S\mu-\frac{\beta\psi SI}{1+bI}\\ -\left(k+\alpha+\mu\right)E+\sigma L+I\left(r-pr+\frac{\beta\psi S}{1+bI}\right)\\ kE-I\left(r+\delta+\mu\right)\\ \alpha E+prI-L\left(\mu+\sigma\right)\end{pmatrix}+\begin{pmatrix}\frac{\beta\psi SI}{1+bI} & 0 & 0\\ -\frac{\beta\psi SI}{1+bI} & -\alpha E & -prI\\ 0 & 0 & 0\\ 0 & \alpha E & prI\end{pmatrix}\times\begin{pmatrix}u_1\\ u_2\\ u_3\end{pmatrix}.$$

This verifies condition (iii). The subset $U$ of $\mathbb{R}^3$ is closed and bounded, and hence compact. Thus, condition (iv) is fulfilled. We proceed with verifying condition (v), the convexity of the integrand of the objective functional. We must prove that for any two

values $\overrightarrow{u}$ and $\overrightarrow{v}$ of the control vector, and a constant $q \in [0,1]$, the following inequality holds:

$$(1-q)\, g\left(t,\ \overrightarrow{x},\ \overrightarrow{u}\right) + qg\left(t,\ \overrightarrow{x},\ \overrightarrow{v}\right) \geq g\left(t,\ \overrightarrow{x},\ (1-q)\,\overrightarrow{u} + q\,\overrightarrow{v}\right),$$

where

$$g\left(t,\ \overrightarrow{x},\ \overrightarrow{u}\right) = E + I + \frac{1}{2}B_1u_1^2 + \frac{1}{2}B_2u_2^2 + \frac{1}{2}B_3u_3^2.$$

Further,

$$(1-q)\, g\left(t,\ \overrightarrow{x},\ \overrightarrow{u}\right) + qg\left(t,\ \overrightarrow{x},\ \overrightarrow{v}\right) = E + I + \frac{1}{2}(1-q)\left[B_1u_1^2 + B_2u_2^2 + B_3u_3^2\ \right] + \frac{1}{2}q\left[B_1v_1^2 + B_2v_2^2 + B_3v_3^2\right],$$

And

$$g\left(t,\ \overrightarrow{x},\ (1-q)\,\overrightarrow{u} + q\,\overrightarrow{v}\right) = E + I + \frac{1}{2}B_1[(1-q)\,u_1 + qv_1]^2 + \frac{1}{2}B_2[(1-q)\,u_2 + qv_2]^2$$

$$+\frac{1}{2}B_3[(1-q)\,u_3 + qv_3]^2,$$

Then,

$$\begin{aligned}
&(1-q)\, g\left(t,\ \overrightarrow{x}\ ,\ \overrightarrow{u}\right) + qg\left(t,\ \overrightarrow{x}\ ,\ \overrightarrow{v}\right) - g\left(t,\ \overrightarrow{x}\ ,\ (1-q)\,\overrightarrow{u} + q\,\overrightarrow{v}\right)\\
&= (1-q)\left[\frac{B_1}{2}u_1^2 + \frac{B_2}{2}u_2^2 + \frac{B_3}{2}u_3^2\ \right] + q\left[\frac{B_1}{2}v_1^2 + \frac{B_2}{2}v_2^2 + \frac{B_3}{2}v_3^2\right]\\
&- \left[\frac{B_1}{2}[(1-q)\,u_1 + qv_1]^2 + \frac{B_2}{2}[(1-q)\,u_2 + qv_2]^2 + \frac{B_3}{2}[(1-q)\,u_3 + qv_3]^2\right],\\
&= \frac{B_1}{2}\left\{(1-q)\,u_1^2 + qv_1^2 - [(1-q)\,u_1 + qv_1]^2\ \right\}\\
&+ \frac{B_2}{2}\left\{(1-q)\,u_2^2 + qv_2^2 - [(1-q)\,u_2 + qv_2]^2\right\}\\
&+ \frac{B_3}{2}\left\{(1-q)\,u_3^2 + qv_3^2 - [(1-q)\,u_3 + qv_3]^2\right\},\\
&= \frac{B_1}{2}\left\{q\,(1-q)\,u_1^2 - 2q\,(1-q)\,u_1v_1 + q\,(1-q)\,v_1^2\right\}\\
&+ \frac{B_2}{2}\left\{q\,(1-q)\,u_2^2 - 2q\,(1-q)\,u_2v_2 + q\,(1-q)\,v_2^2\right\}\\
&+ \frac{B_3}{2}\left\{q\,(1-q)\,u_3^2 - 2q\,(1-q)\,u_3v_3 + q\,(1-q)\,v_3^2\right\},\\
&= \frac{B_1}{2}\left\{q\,(1-q)\,(u_1-v_1)^2\right\} + \frac{B_2}{2}\left\{q\,(1-q)\,(u_2-v_2)^2\right\} + \frac{B_3}{2}\left\{q\,(1-q)\,(u_3-v_3)^2\right\}\\
&\geq 0.
\end{aligned}$$

Consequently, condition (v) is satisfied, and this completes the proof. ■

To find the best cost-effective strategies for reducing the number of high-risk latent ($E$)

and infectious ($I$), we use optimal control theory. In this section, we derive the conditions for optimal control using Pontryagin's Maximum Principle [77, 112]. We formulate the Hamiltonian

$$\begin{aligned}
&H\left(S,E,I,L,u_1,u_2,u_3,\lambda\right)\\
&=E+I+\frac{1}{2}B_1u_1^2+\frac{1}{2}B_2u_2^2+\frac{1}{2}B_3u_3^2\\
&+\lambda_1\left[\Lambda-\frac{\left(1-u_1\right)\beta\psi SI}{1+bI}-\mu S\right]\\
&+\lambda_2\left[\frac{\left(1-u_1\right)\beta\psi SI}{1+bI}+\left(1-\left(1+u_3\right)p\right)rI+\sigma L-\left(k+\left(1+u_2\right)\alpha+\mu\right)E\right]\\
&+\lambda_3\left[kE-\left(\mu+r+\delta\right)I\right]\\
&+\lambda_4\left[\left(1+u_3\right)prI+\left(1+u_2\right)\alpha E-\left(\mu+\sigma\right)L\right].
\end{aligned}\tag{6.4}$$

Here, $\lambda=\left(\lambda_1,\lambda_2,\lambda_3,\lambda_4\right)\in\mathbb{R}^4$ are the adjoint functions.

**Theorem 6.2.2.** *For the optimal control $(u_1^*,\ u_2^*,\ u_3^*)$ and the corresponding solutions to the variables $\overline{S},\ \overline{E},\ \overline{I},\ \overline{L}$, that minimizes the Equation (6.3), there exist adjoint variables $\lambda_1,\ \lambda_2,\lambda_3,$ and $\lambda_4$ satisfying*

$$\begin{cases}
\frac{d\lambda_1}{dt}=\frac{(1-u_1)\beta\psi I}{1+bI}\lambda_1+\mu\lambda_1-\frac{(1-u_1)\beta\psi I}{1+bI}\lambda_2\\
\frac{d\lambda_2}{dt}=\left[k+\mu+\left(1+u_2\right)\alpha\right]\lambda_2-k\lambda_3-\left(1+u_2\right)\alpha\lambda_4-1\\
\frac{d\lambda_3}{dt}=\left(\mu+r+\delta\right)\lambda_3+\left[\frac{(u_1-1)\beta\psi bSI}{(1+bI)^2}+\frac{(1-u_1)\beta\psi S}{1+bI}\right]\lambda_1\\
\qquad+\left[\frac{(1-u_1)\beta\psi bSI}{(1+bI)^2}+\frac{(u_1-1)\beta\psi S}{1+bI}-\left(1-\left(1+u_3\right)p\right)r\right]\lambda_2-\left(1+u_3\right)pr\lambda_4-1\\
\frac{d\lambda_4}{dt}=\left(\mu+\sigma\right)\lambda_4-\sigma\lambda_2
\end{cases}\tag{6.5}$$

with transversality conditions

$$\lambda_1\left(t_f\right)=\lambda_2\left(t_f\right)=\lambda_3\left(t_f\right)=\lambda_4\left(t_f\right)=0.\tag{6.6}$$

Furthermore,

$$\begin{aligned}
u_1^*&=\min\left\{\max\left\{0,\frac{\left(\lambda_2-\lambda_1\right)\beta\psi\overline{SI}}{\left(1+b\overline{I}\right)B_1}\right\},1\right\},\\
u_2^*&=\min\left\{\max\left\{0,\frac{\left(\lambda_2-\lambda_4\right)\alpha\overline{E}}{B_2}\right\},1\right\},\\
u_3^*&=\min\left\{\max\left\{0,\frac{\left(\lambda_2-\lambda_4\right)pr\overline{I}}{B_3}\right\},1\right\}.
\end{aligned}\tag{6.7}$$

**Proof.** By applying Pontryagin's Maximum Principle, we obtain the adjoint system (6.5) as follows:

$$\frac{d\lambda_1}{dt} = -\frac{\partial H}{\partial S}, \frac{d\lambda_2}{dt} = -\frac{\partial H}{\partial E}, \frac{d\lambda_3}{dt} = -\frac{\partial H}{\partial I}, \frac{d\lambda_4}{dt} = -\frac{\partial H}{\partial L}, \tag{6.8}$$

with

$$\lambda_i(t_f) = 0, i = 1, 2, 3, 4. \tag{6.9}$$

Evaluating the optimal control and corresponding state variables, we obtain the adjoint system (6.5) and the transversality conditions (6.6).

Finally, by applying the optimality condition

$$\frac{\partial H}{\partial u_1} = \frac{\partial H}{\partial u_2} = \frac{\partial H}{\partial u_3} = 0,$$

And using the bounds for the controls $u_1, u_2$ and $u_3$, we can derive the optimal control $(u_1^*,\ u_2^*,\ u_3^*)$ as in Equation (6.7). ■

## 6.3 Numerical Results and Discussion

Using Matlab2019b, the optimal control system is solved by applying the forward-backward sweeping technique. According to [102], in the total population of Ethiopia, the classes $E_0$ and $L_0$ comprise 16.37% and 30% of the population, respectively. Based on these percentages, we can deduce values for $E_0$ and $L_0$.

The values of parameters and the initial values of the variables used in our simulations are presented in Table 6.1. The algorithm used for the solution is based on the approach proposed in [112, 113].

Studies show that applying combined strategies rather than single strategies is more effective in curbing the spread of TB [18, 19]. Therefore, we test the following four possible combinations of control strategies and search for an optimal intervention.

*Strategy A*: distancing and case holding controls ($u_1$ and $u_3$), with $u_2(t) = 0$.

*Strategy B*: case finding and case holding controls ($u_2$ and $u_3$), with $u_1(t) = 0$.

*Strategy C*: distancing and case finding controls ($u_1$ and $u_2$), with $u_3(t) = 0$.

*Strategy D*: Using all the control efforts ($u_1$, $u_2$ and $u_3$).

We assume a value for the weight parameters $B_1 = B_2 = 10^5$. Since the case holding control $u_3$ targets active TB patients undergoing treatment, the numbers in these groups

are smaller than the others. Hence it is reasonable to take $B_3$ as being far smaller than $B_1$ and $B_2$, and we assigned a value $B_3 = 10^3$.

The dynamics of the total infected population $(E + I)$ are shown in Figure 6.1. It can be observed that the number of infected individuals can be significantly decreased when the three control inputs $(u_1, u_2,$ and $u_3)$ are used simultaneously. Like Strategy $D$, Strategies $B$ and $C$ significantly reduce the number of high-risk latent individuals. In contrast, Strategy $A$ has the least impact on reducing the number of patients. This shows that using case-finding control in combination with other strategies to prevent the disease is beneficial.

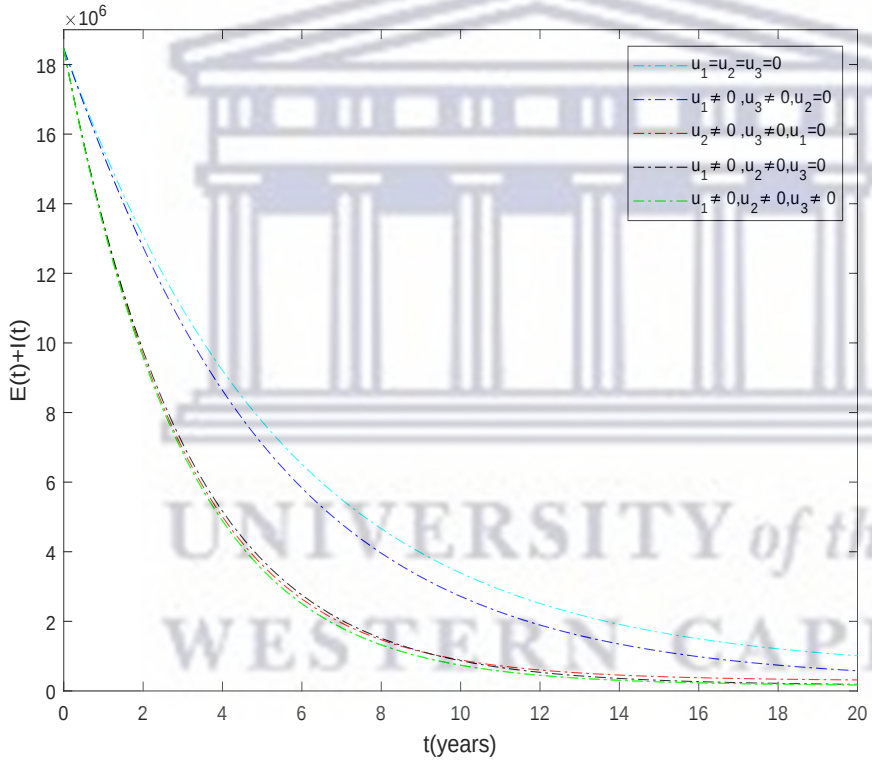


Figure 6.1: The dynamics of the total infected population under different control strategies.

### 6.3.1 Strategy $A$: Use of distancing and case holding controls

In this strategy, the distancing and the case holding controls are used to optimize the objective function $J$ while we set case finding control $(u_2)$ to zero. Figure 6.2 shows that the total number of infected people $(E + I)$ significantly differs compared to control and

without control. Specifically, when this strategy is implemented, $4.32\times10^5$ total infected people are averted. The total cost for the combined effects of these two controls is given in Figure 6.2 b. The simulation results in Figure 6.2 c suggest that this strategy would require distancing and case-holding controls to be at maximum for almost the entire intervention period.

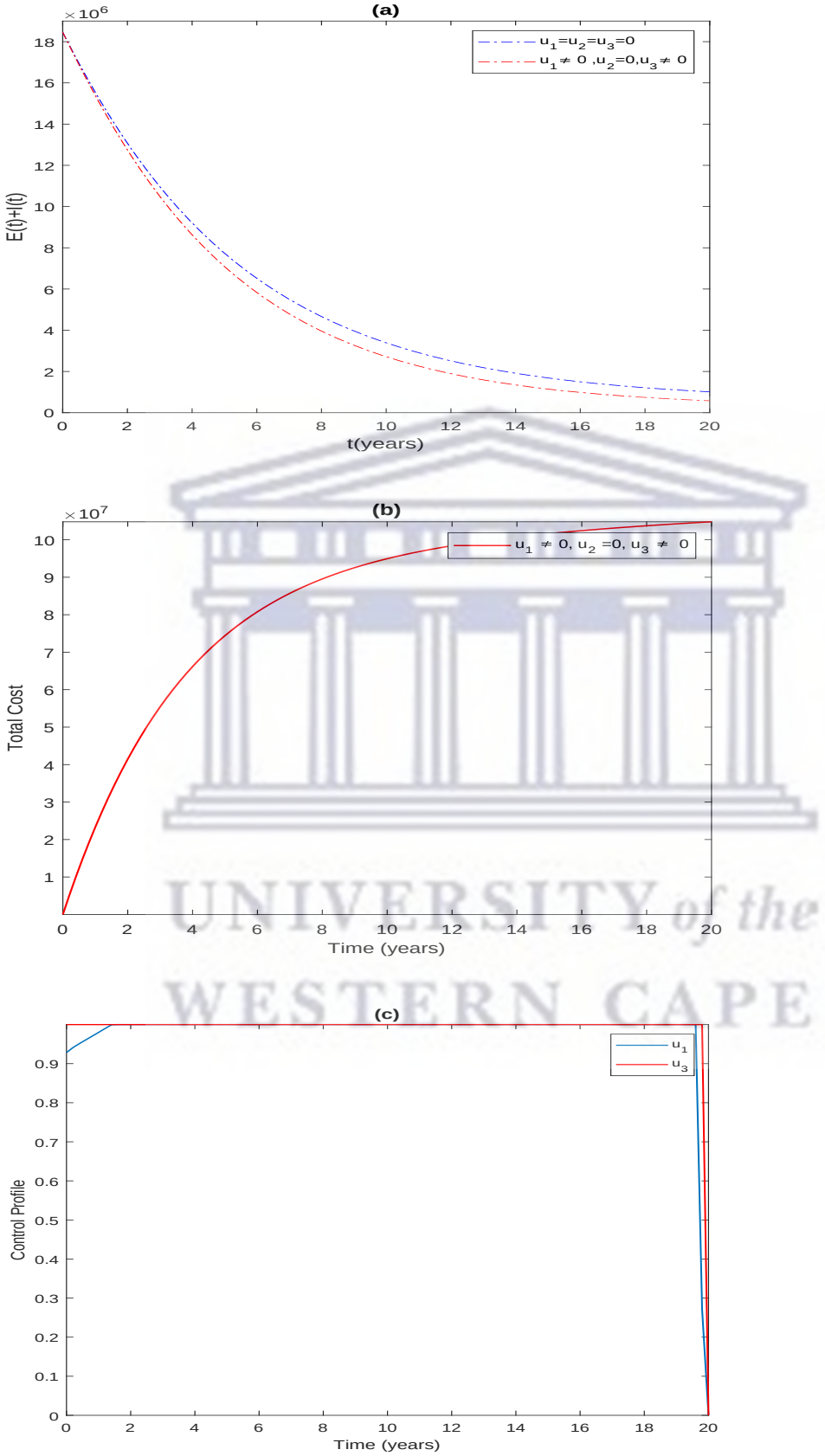


Figure 6.2: The impact of distancing and case holding control on the infected population. (**b**) Cost function. (**c**) Optimal controls profile.

### 6.3.2 Strategy $B$: Control with case finding and case holding

Figure 6.3 a shows the significant difference in the numbers of the total infected population with control and without control. More precisely, the total number of infected people with and without controls at the end of the simulation period is $3.16 \times 10^5$ and $1.011 \times 10^6$, respectively. To achieve this, the control profile $u_2$ and $u_3$ should be implemented at a maximum (Figure 6.3 c). The cost function for this strategy is shown in Figure 6.3 b. The total cost when the strategy is implemented throughout the simulated time horizon is $6.5012 \times 10^7$.

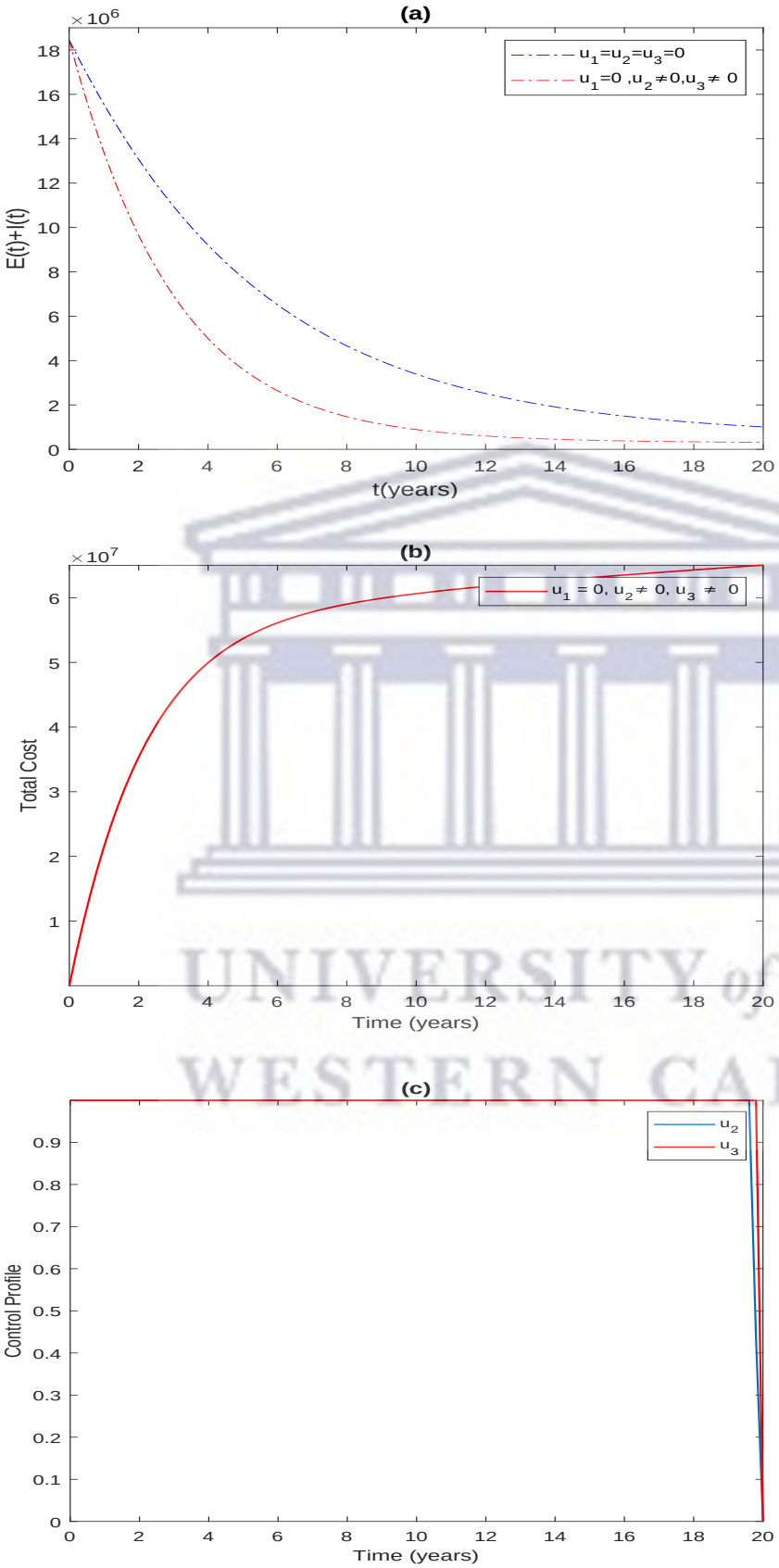


Figure 6.3: (**a**) The impact of case finding and case holding control on the infected population. (**b**) Cost function. (**c**) Optimal controls profile.

### 6.3.3 Strategy $C$: Use of distancing and case finding control

As shown in Figure 6.4 a, there is a significant difference in the number of infected individuals with and without control. By applying this strategy, $8.22 \times 10^5$ infected people are averted. The cost function for this strategy is shown in Figure 6.4 b. The simulation result in Figure 6.4 c shows that this strategy would require that the case finding $u_2$ should be at maximum for almost the entire period of intervention while distancing controls $u_1$ should start at 0.4679 and gradually increase to the maximum.

Table 6.1: Values of variables and parameters

| **Symbols** | **Description** | **Units** | **Value** | **Reference** |
|---|---|---|---|---|
| $N_0$ | Total population | $Humans$ | $1.12\times10^8$ | [114] |
| $S_0$ | Susceptible | $Humans$ | $5.85\times10^7$ | Estimated |
| $E_0$ | High-risk latent | $Humans$ | $1.83\times10^7$ | [102] |
| $I_0$ | Infected | $Humans$ | $1.57\times10^5$ | [114] |
| $L_0$ | Low-risk latent | $Humans$ | $3.36\times10^7$ | [102] |
| $\Lambda$ | Recruitment rate | $Humans/year$ | $1.4\times10^6$ | [102] |
| $\beta$ | Effective contact rate | $1/year$ | $1.646\times10^{-7}$ | [102] |
| $\varepsilon$ | Vaccination rate of new-borns | $dimensionless$ | 0.715 | [90] |
| $\theta$ | Loss of protection for vaccination | $dimensionless$ | 0.5 | [105] |
| $\mu$ | Natural mortality rate | $1/year$ | 0.016 | [102] |
| $k$ | Transfer rate from $E$ to $I$ | $1/year$ | 0.023 | [102] |
| $r$ | Treatment rate of $I$ | $1/year$ | 0.546 | [102] |
| $p$ | Recovery rate of $I$ | $dimensionless$ | 0.832 | [91] |
| $\alpha$ | Treatment rate of $E$ | $1/year$ | 0.153 | [102] |
| $\delta$ | Death rate due to TB | $1/year$ | 0.17 | [14] |
| $\sigma$ | Relapse rate | $1/year$ | 0.0013 | [102] |
| $b$ | Saturation constant | $1/Humans$ | 0.0004 | [105] |
| $u_1$ | Distancing control | $dimensionless$ | $[0, 1]$ | Assumed |
| $u_2$ | Case finding control | $dimensionless$ | $[0, 1]$ | Assumed |
| $u_3$ | Case holding control | $dimensionless$ | $[0, 1]$ | Assumed |

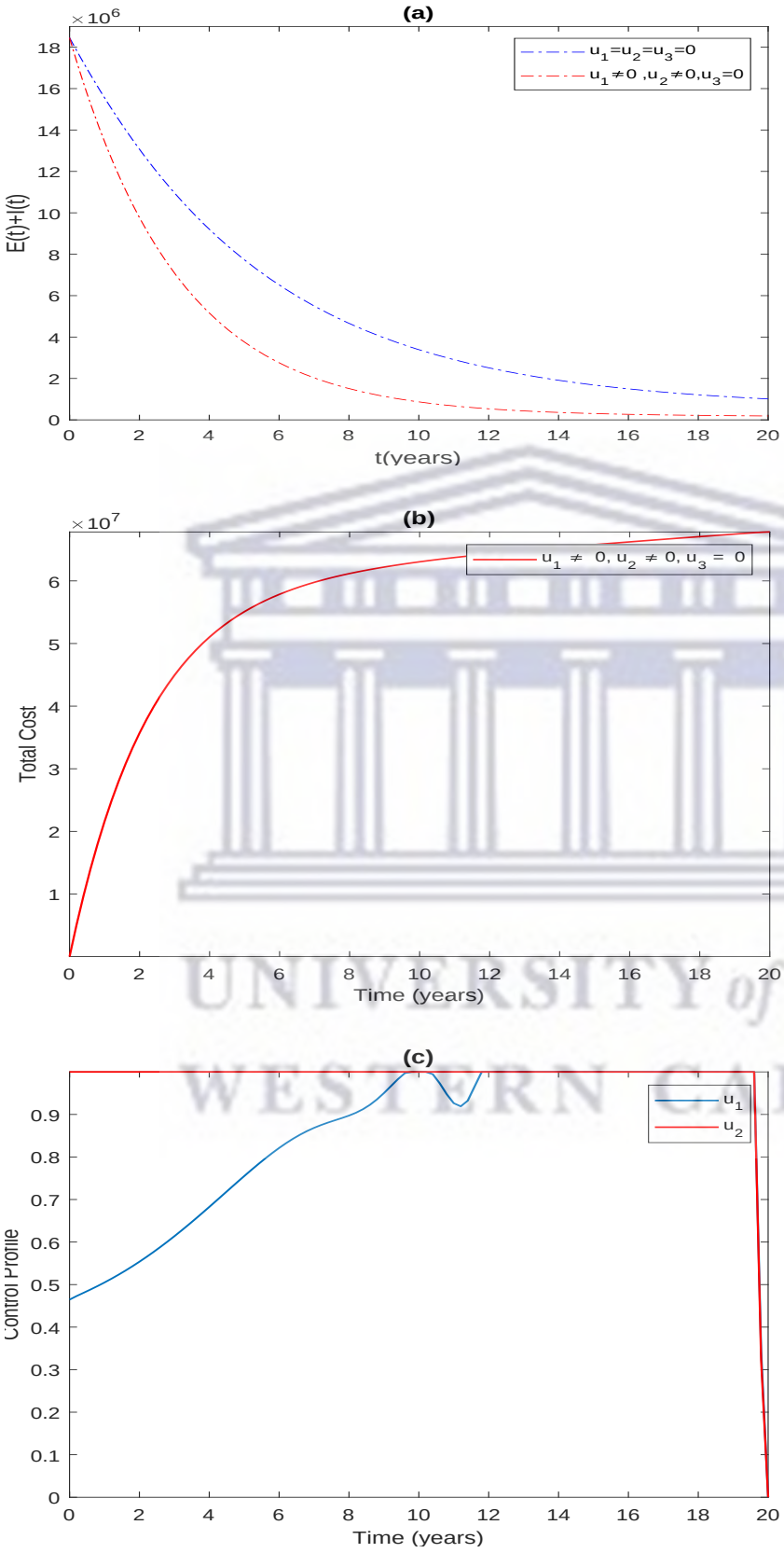


Figure 6.4: (**a**) The impact of distancing and case finding control on the infected population. (**b**) Cost function. (**c**) Optimal controls profile.

### 6.3.4 Strategy $D$: Using All the Controls

In this strategy, we have implemented a combination of all three controls. This method helps us to save more people from disease than any other strategy. As we can see from Figure 6.5 a, it averts about $8.38\times10^5$ infected people. Figure 6.5 b,c displays this strategy's cost and control functions.

Table 6.2: Cost-effectiveness of the control strategies.

| **Strategy** | **Total Infection Averted** | **Total Cost ($)** |
|---|---|---|
| $A$ ($u_1$ and $u_3$) | $4.32\times10^5$ | $1.0479\times10^8$ |
| $B$ ($u_1$ and $u_2$) | $6.95\times10^5$ | $6.5012\times10^7$ |
| $C$ ($u_2$ and $u_3$) | $8.22\times10^5$ | $6.782\times10^7$ |
| $D$ ($u_1, u_2$, and $u_3$) | $8.38\times10^5$ | $6.5122\times10^7$ |

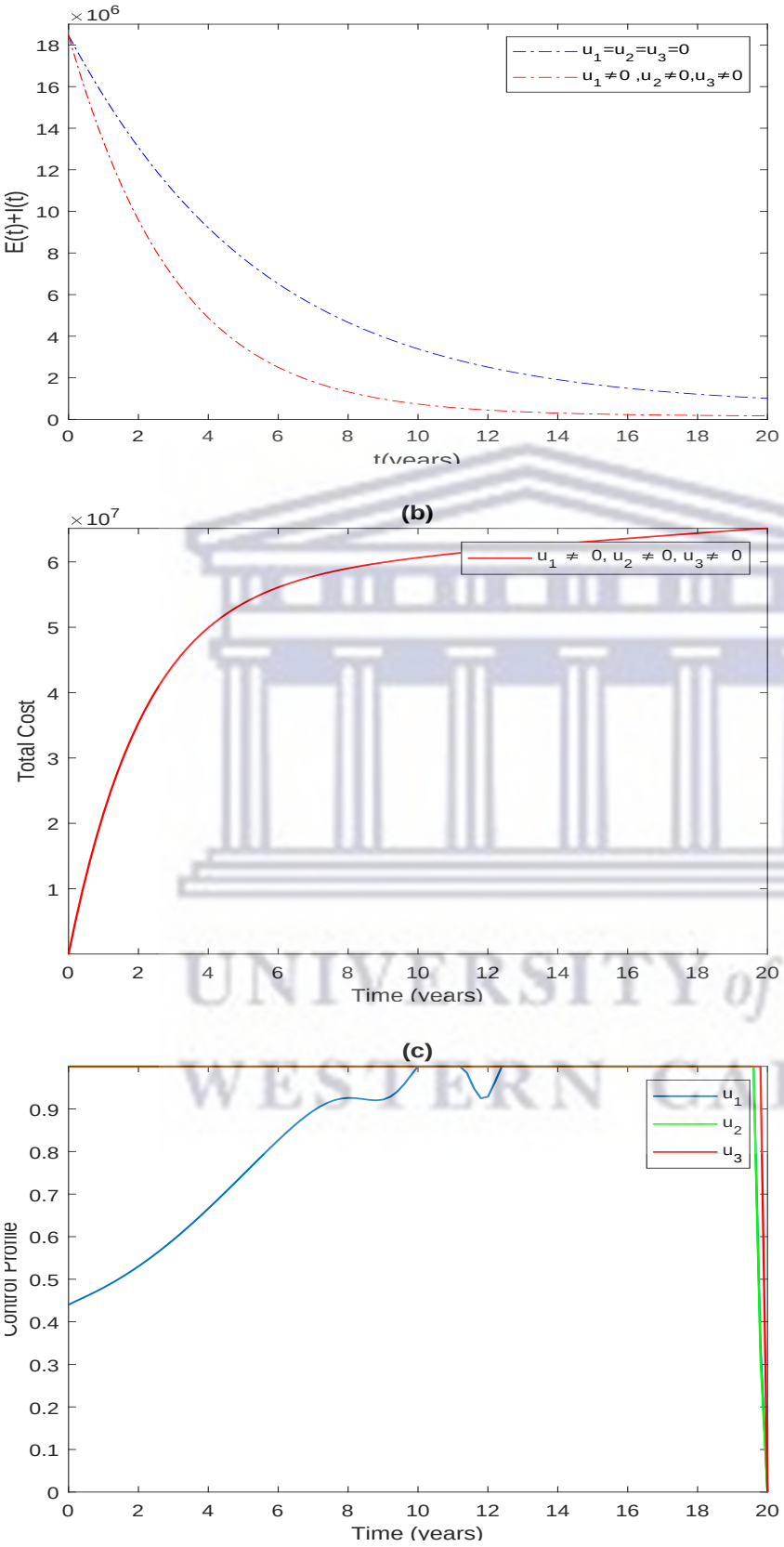


Figure 6.5: (**a**) The impact of the combination of all controls on the infected population. (**b**) Cost function. (**c**) Optimal controls profile.

## 6.4 Cost-Effectiveness Analysis

Controlling and eliminating the spread of infectious diseases in a community requires time and money. Therefore, it is essential to identify and implement cost-effective strategies to prevent the spread of the disease. In addition, community awareness and lifestyle are critical factors determining the spread of disease. As a result, effective methods of controlling the spread of disease may vary from country to country. This Chapter identifies cost-effective ways to prevent the spread of tuberculosis in Ethiopia. The incremental cost-effectiveness ratio ($ICER$) is applied to do this. The $ICER$ is defined as the cost per health outcome, which is given by [115]:

$$ICER = \frac{\text{The difference in costs between strategies}}{\text{Total number of infections averted}}.$$

Table 6.2 calculates the total number of infections averted by each strategy and the total cost of implementing the strategy. We calculated the number of infections averted by subtracting the number of infections with control from those without control. On the other hand, the total cost of each strategy was obtained using the cost function $\frac{B_1}{2}u_1^2(t)$, $\frac{B_2}{2}u_2^2(t)$, and $\frac{B_3}{2}u_3^2(t)$.

To implement the $ICER$ method, we first needed to rank the control strategies based on averted infection, as shown in Table 6.2. Based on this rank, we first compared the $ICER$ of Strategy $A$ and Strategy $B$.

$$ICER(A) = \frac{1.0479 \times 10^8}{4.32 \times 10^5} = 242.57.$$
$$ICER(B) = \frac{6.5012 \times 10^7 - 1.0479 \times 10^8}{6.95 \times 10^5 - 4.32 \times 10^5} = -151.25.$$

This shows that Strategy $B$ is less costly than Strategy $A$. Strategy $A$ was then ignored, and the analysis continued by comparing strategy B with C as:

$$ICER(B) = \frac{6.5012 \times 10^7}{6.95 \times 10^5} = 93.54.$$
$$ICER(C) = \frac{6.782 \times 10^7 - 6.5012 \times 10^7}{8.22 \times 10^5 - 6.95 \times 10^5} = 22.11.$$

This indicates that Strategy $C$ is cheaper and more effective than Strategy $B$ and hence, Strategy B was ignored, and the analysis continued by comparing Strategy $C$ and

Strategy $D$ as follows:

$$ICER\,(C) = \frac{6.782 \times 10^7}{8.22 \times 10^5} = 82.5.$$
$$ICER(D) = \frac{6.5122 \times 10^7 - 6.782 \times 10^7}{8.38 \times 10^5 - 8.22 \times 10^5} = -168.62.$$

Finally, the comparison result revealed that Strategy $D$ is less costly and more effective than Strategy $C$. In conclusion, of the four strategies mentioned, Strategy $D$ (combining the three controls simultaneously) is the most effective way to combat the spread of TB in Ethiopia.

## 6.5 Conclusions

The Ethiopian government is working with partners and the community to stop TB by 2035. Therefore, it is vital to identify and implement effective strategies to eradicate the disease. This chapter has developed a mathematical model by including three control strategies (distancing, case finding, and case holding). After that, using Pontryagin's maximum principle, the conditions for optimal control of the system were analyzed. The optimal solution to the system was then illustrated by numerical simulations using available data from Ethiopia. From the numerical simulation result (Figure 6.1), one can deduce that considering the combination of distancing and case-holding controls (Strategy $A$) does not lead to the best results in decreasing the number of TB-infected individuals. On the other hand, we can understand from this analysis that combining all three controls (Strategy $D$) is an effective way to eradicate tuberculosis from the community.

Finally, we investigated the cost-effectiveness of the control strategies using the ICER technique. Based on the results of these analyses, we concluded that applying the combination of the three controls (distancing, case finding, and case holding) is less costly and more effective than other strategies. This suggested that isolation of infectious people, early TB patient detection, treating high-risk latently infected individuals, educational campaigns, and preventing treatment failure of active TB patients are essential strategies in Ethiopia to control the spread of the disease.

In the previous chapters, we developed mathematical models for the transmission dynamics of drug-susceptible tuberculosis and suggested the best strategies for controlling disease transmission in Ethiopia. In the next chapter, we develop a mathematical model for the dynamics of multi-drug-resistant tuberculosis and identify Ethiopia's most effective

strategy for combating it.

# Chapter 7

# Cost-effectiveness analysis of the optimal control strategies for multi-drug-resistant tuberculosis transmission in Ethiopia

This chapter aims to identify the most effective strategy for combating multi-drug-resistant tuberculosis (MDR-TB) in Ethiopia. We first present a compartmental model of MDR-TB transmission dynamics in Ethiopia. The model is shown to have positive solutions, and the stability of the equilibrium points is analyzed. Then, we extend the model by incorporating time-dependent control variables. These control variables are vaccination, distancing, and treatment for DS-TB and MDR-TB. Finally, the optimality system is numerically simulated by considering different combinations of the strategies and their cost effectiveness is analyzed.

## 7.1 Introduction

Despite the recent progress of global control efforts, tuberculosis remains a significant public health threat worldwide, especially in developing countries, including Ethiopia. Furthermore, the emergence of MDR-TB has further complicated the situation. The treatment of MDR-TB has always been more complicated than the treatment of drug-susceptible tuberculosis (DS-TB). It requires the use of second-line drugs or reserved

drugs for up to two years. The best way to stop the spread of drug-resistant TB is to take all DS-TB drugs as directed by your physician [7].

Mathematical models are essential in understanding the epidemic's trajectory and designing effective control measures under a set of assumptions [116, 117]. In this chapter, a mathematical model is formulated for the transmission dynamics of MDR-TB in Ethiopia with optimal control and cost-effectiveness analysis.

## 7.2 Model formulation and analysis

### 7.2.1 MDR-TB model

This section presents the formulation of the mathematical model for MDR-TB transmission dynamics. This model is comprised of a set of ordinary differential equations. By Considering a homogeneous mixing within the population, the total population $N(t)$ is subdivided into five epidemiological groups: Susceptible individuals $S(t)$, Vaccinated individuals $V(t)$, individuals exposed to drug-susceptible TB $E(t)$, infectious individuals with drug-susceptible TB $I(t)$ and infectious individuals with MDR-TB $J(t)$.

Within the model, the parameter $\Lambda$ represents the rate at which individuals are recruited into the susceptible class. On the other hand, the parameter $\mu$ represents the natural death rate for each class within the system. The vaccination rate for healthy individuals is denoted as $\phi$. We assume the vaccine is imperfect. Therefore, some portion of those who have received vaccinations are expected to be exposed to bacteria at a rate of $\eta$.

Susceptible individuals will be exposed to drug-susceptible TB if they come into effective contact, at a rate $\beta$, with individuals from the $I$-class. Moreover, it is assumed that the susceptible individuals became MDR-TB infected with a rate $\theta$. Some individuals in class $E$ may progress to class $I$ at rate $k$. If treatment is administered for the $I$ -class with a rate $r$, then some will complete their treatment correctly at a rate $\omega r$ for $(0 \leq \ \omega \leq 1\ )$. However, some individuals in the $I$ class may fail to take their treatment correctly and may develop MDR-TB at a rate $(1-\omega)r$. The recovery rate of individuals from infected MDR-TB after treatment is $\alpha$. It is assumed that the recovered individuals from both classes will move to the $S$-class. Individuals who have recently been infected with TB bacteria are at a higher risk of developing active TB disease. In this model, we assume that individuals with drug-resistant TB in the latent stage will progress to the

active stage relatively quickly. Furthermore, infectious individuals in $I$ and $J$ classes will die due to the disease at a rate $\delta$. Figure 7.1 shows the model flow diagram.

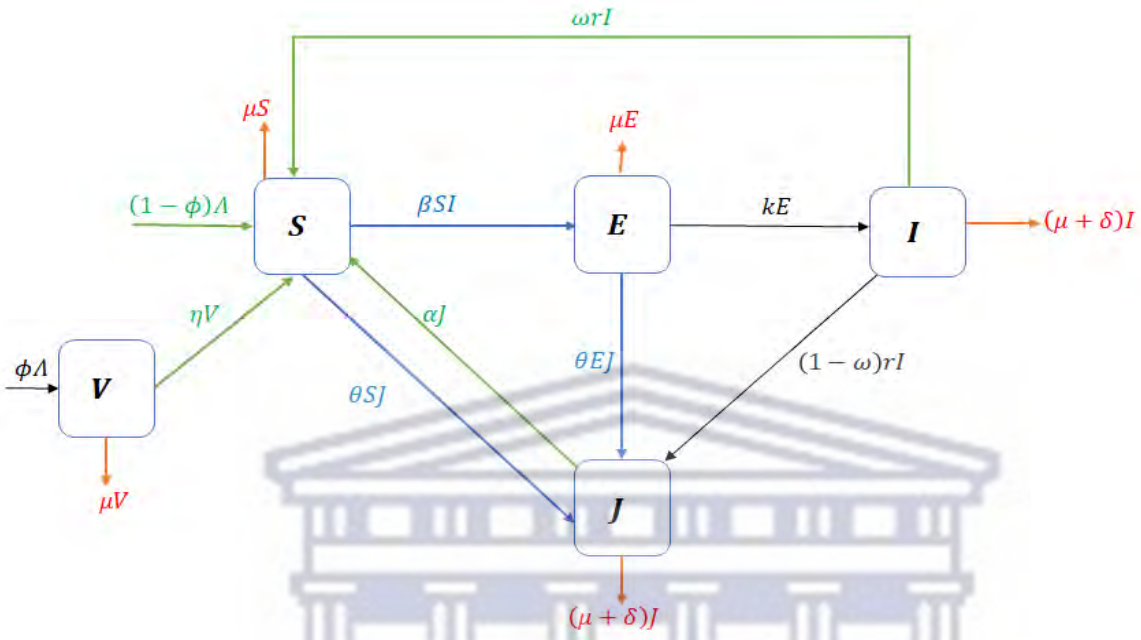


Figure 7.1: Flow diagram of the model.

The following system of differential equations gives the dynamics of DS-TB and MDR-TB.

$$\begin{cases} \frac{dS}{dt} = (1-\phi)\,\Lambda + \eta V + \omega r I + \alpha J - \beta S I - \theta S J - \mu S \\ \frac{dV}{dt} = \phi\Lambda - (\eta + \mu)\,V \\ \frac{dE}{dt} = \beta S I - (k+\mu)E \\ \frac{dI}{dt} = kE - (r + \delta + \mu)I \\ \frac{dJ}{dt} = \theta S J + (1-\omega)\,rI - (\alpha + \mu + \delta)\,J \end{cases} \tag{7.1}$$

## 7.2.2 Model Analysis

### *Positivity of the solution set*

The variables $S(t), V(t), E(t), I(t)$, and $J(t)$ denote the number of people and are assumed to take positive values. From biological and mathematical considerations, it is necessary to prove that starting from positive initial conditions implies that the solution always remains positive.

**Theorem 7.2.1.** *If* $S(0) > 0, V(0) > 0, E(0) > 0, I(0) > 0, J(0) > 0$, *the solution*

$$S(t), V(t), E(t), I(t), J(t)$$

*of system* (7.1) *is positive for all* $t > 0$.

***Proof:*** From the first equation of the model (7.1) we have

$$\frac{dS(t)}{dt} = (1-\phi)\Lambda + \eta V(t) + \omega r I(t) + \alpha J(t) - \beta S(t) I(t) - \theta S(t) J(t) - \mu S(t).$$

By letting

$$(1-\phi)\Lambda = \psi,$$

$$\eta V(t) + \omega r I(t) + \alpha J(t) = R(t),$$

and

$$-[\beta I(t) + \theta J(t) + \mu] = H(t).$$

We have

$$\frac{dS(t)}{dt} + H(t) S(t) = \psi + R(t). \tag{7.2}$$

Then Equation (7.2) can be described as

$$\frac{dS(t)}{dt}\exp\left\{\int_0^t H(\tau)\,d\tau\right\} + H(t) S(t) \exp\left\{\int_0^t H(\tau)\,d\tau\right\} = \frac{d}{dt}\left[S(t)\exp\left\{\int_0^t H(\tau)\,d\tau\right\}\right].$$

So,

$$\frac{d}{dt}\left[S(t)\exp\left\{\int_0^t H(\tau)\,d\tau\right\}\right] = \psi\exp\left\{\int_0^t H(\tau)\,d\tau\right\} + R(t)\exp\left\{\int_0^t H(\tau)\,d\tau\right\}. \tag{7.3}$$

Integrating both sides of Equqtion (7.3) gives

$$S(t) = S_0\exp\left\{-\int_0^t H(\tau)\,d\tau\right\} + \left[\psi\int_0^t \exp\left\{\int_0^\tau H(u)\,du\right\}\right]\left[\exp\left\{-\int_0^t H(\tau)\,d\tau\right\}\right]$$

$$+\left[\left(\int_0^t R(\tau)\exp\left\{\int_0^\tau H(u)\,du\right\}\right)d\tau\right]\left[\exp\left\{-\int_0^t H(\tau)\,d\tau\right\}\right] \geq 0.$$

Similarly, using the second Equation of the model (7.1), we obtain that

$$\frac{dV}{dt} = \phi\Lambda - (\eta+\mu)V. \tag{7.4}$$

Equation (7.4) can be rewritten as

$$\frac{dV(t)}{dt}\exp(\eta+\mu) \; + (\eta+\mu)\,V(t)\exp(\eta+\mu) \; = \phi\Lambda\exp(\eta+\mu)\,. \tag{7.5}$$

Integrating both sides of Equqtion (7.5) gives

$$V(t) = V(0)\exp(-(\eta+\mu)\;t) + \frac{\phi\Lambda}{\eta+\mu}\;[1-\exp(-(\eta+\mu)\;t)] \geq 0. \tag{7.6}$$

Note that from the Equation (7.6), we can show that

$$\lim_{t\to\infty} V(t) = \frac{\phi\Lambda}{\eta+\mu}. \tag{7.7}$$

Similarly, we can show that $E(t), I(t)$ and $J(t)$ are non-negative. So, the solutions

$$\chi = S(t), V(t), E(t), I(t), J(t)$$

of system (7.1) are positive for all $t > 0$. ■

***Invariant region***

The invariant region of the model describes the region in which the solution of the model (7.1) is biologically meaningful.

**Theorem 7.2.2.** *The invariant region* $\Omega$ *defined by*

$$\Omega = \left\{ (S(t), V(t), E(t), I(t), J(t)) \in \mathbb{R}_+^{\,5} \;\middle|\; N(t) \leq \frac{\Lambda}{\mu} \right\}$$

*with non-negative initial conditions is positively invariant for the system* (7.1).

***Proof***: Adding the equations of the system (7.1), we have

$$\frac{dN(t)}{dt} = \Lambda - \mu N(t) - \delta(I(t) + J(t))$$

$$\leq \Lambda - \mu N(t)$$

It follows that

$$0 \leq N(t) = \frac{\Lambda}{\mu} - N(0)\exp(-\mu t) \quad ,$$

where $N(0)$ represents the initial values of the total population.

Therefore, $\lim_{t\to\infty} \sup \mathrm{N}\,(\mathrm{t}) \leq \frac{\Lambda}{\mu}$ . It implies that the region

$$\Omega = \left\{ (S(t), V(t), E(t), I(t), J(t)) \in {\mathbb{R}_+}^5 \;\middle|\; N\,(t) \leq \frac{\Lambda}{\mu} \right\}$$

is a positively invariant region for the system (7.1).■

### *The basic reproduction number*

The model (7.1) has a disease-free equilibrium point (DFE), obtained by setting the right-hand sides of the equations in the system (7.1) as well as the disease classes $(E, I, J)$ to zero, given by

$$P^0 = (S^0, V^0, 0, 0, 0)$$

where

$$S^0 = \Lambda \frac{\eta + \mu(1-\phi)}{\mu(\eta+\mu)},$$

and

$$V^0 = \frac{\Lambda\phi}{\eta+\mu}.$$

Using the next-generation approach [48], the right-hand side of the system (7.1) is written as $\mathcal{F} - \mathcal{M}$, where

$$\mathcal{F} = \begin{pmatrix} \beta SI \\ 0 \\ \theta SJ \end{pmatrix},$$

$$\mathcal{M} = \begin{pmatrix} (k+\mu)E \\ -kE + (r+\delta+\mu)I \\ -(1-\omega)\,rI + (\alpha+\mu+\delta)\,J \end{pmatrix}.$$

The corresponding Jacobian matrices evaluated at the disease-free equilibrium are given by

$$F = \begin{pmatrix} 0 & \beta\Lambda\left(\frac{1}{\mu} - \frac{\phi}{\eta+\mu}\right) & 0 \\ 0 & 0 & 0 \\ 0 & 0 & \theta\Lambda\left(\frac{1}{\mu} - \frac{\phi}{\eta+\mu}\right) \end{pmatrix},$$

and

$$G = \begin{pmatrix} \frac{1}{k+\mu} & 0 & 0 \\ \frac{k}{(k+\mu)(r+\delta+\mu)} & \frac{1}{r+\delta+\mu} & 0 \\ -\frac{kr(-1+\omega)}{(k+\mu)(r+\delta+\mu)(\alpha+\delta+\mu)} & -\frac{r(-1+\omega)}{(r+\delta+\mu)(\alpha+\delta+\mu)} & \frac{1}{\alpha+\delta+\mu} \end{pmatrix}.$$

Therefore,

$$FG^{-1} = \begin{pmatrix} \frac{k\beta\Lambda\left(\frac{1}{\mu}-\frac{\phi}{\eta+\mu}\right)}{(k+\mu)(r+\delta+\mu)} & \frac{\beta\Lambda\left(\frac{1}{\mu}-\frac{\phi}{\eta+\mu}\right)}{r+\delta+\mu} & 0 \\ 0 & 0 & 0 \\ -\frac{kr\theta\Lambda\left(\frac{1}{\mu}-\frac{\phi}{\eta+\mu}\right)(-1+\omega)}{(k+\mu)(r+\delta+\mu)(\alpha+\delta+\mu)} & -\frac{r\theta\Lambda\left(\frac{1}{\mu}-\frac{\phi}{\eta+\mu}\right)(-1+\omega)}{(r+\delta+\mu)(\alpha+\delta+\mu)} & \frac{\theta\Lambda\left(\frac{1}{\mu}-\frac{\phi}{\eta+\mu}\right)}{\alpha+\delta+\mu} \end{pmatrix}.$$

The basic reproduction number is the magnitude of the dominant eigenvalue of $FG^{-1}$. For multi-group disease models or models dealing with more than one strain, the basic reproduction number is expected to emerge as the maximum of a few numbers; see, for instance, [37] and [118]. Since our model has two types of disease, DS-TB and MDR-TB, we have two reproduction numbers. The reproduction number for DS-TB is given by

$$R_1 = k\beta\Lambda\frac{\eta+\mu\left(1-\phi\right)}{\mu\left(\eta+\mu\right)\left(k+\mu\right)\left(r+\delta+\mu\right)} = \frac{k\beta S^0}{\left(\mu+\alpha+\delta\right)\left(k+\mu\right)},$$

and the reproduction number for MDR-TB is

$$R_2 = \theta\Lambda\frac{\eta+\mu\left(1-\phi\right)}{\mu\left(\eta+\mu\right)\left(\alpha+\delta+\mu\right)} = \frac{\theta S^0}{\alpha+\delta+\mu}.$$

Generally the reproduction number for the model (7.1) is $R_0 = \text{Max}\{R_1, R_2\}$.

### *Stability analysis of disease free equilibrium point*

**Theorem 7.2.3.** *The DFE, $P_0$, is locally asymptotically stable (LAS) when the basic reproduction number $R_0 < 1$, and unstable for $R_0 > 1$.*

***Proof:*** We determine the local stability of $P_0$ using the eigenvalues of the Jacobian

matrix at $P_0$, which is given by

$$G(P_0) = \begin{pmatrix} -\mu & \eta & 0 & -\beta\Lambda\left(\frac{\eta+\mu(1-\phi)}{\mu(\eta+\mu)}\right) + r\omega & \alpha - \theta\Lambda\left(\frac{\eta+\mu(1-\phi)}{\mu(\eta+\mu)}\right) \\ 0 & -(\eta+\mu) & 0 & 0 & 0 \\ 0 & 0 & -(k+\mu) & -\beta\Lambda\left(\frac{\eta+\mu(1-\phi)}{\mu(\eta+\mu)}\right) & 0 \\ 0 & 0 & k & -(r+\delta+\mu) & 0 \\ 0 & 0 & 0 & r(1-\omega) & (\alpha+\delta+\mu)(R_2-1) \end{pmatrix}.$$

If $R_2 < 1$, then then the eigenvalues

$$\lambda_1 = -\mu,\ \lambda_2 = -(\eta+\mu)\ ,$$

and

$$\lambda_3 = (\alpha+\delta+\mu)(R_2-1)\,,$$

containing negative real parts. The remaining eigenvalues of $G(P_0)$ can be determined from the following sub matrix

$$Q = \begin{pmatrix} -(k+\mu) & -\beta\Lambda\left(\frac{\eta+\mu(1-\phi)}{\mu(\eta+\mu)}\right) \\ k & -(r+\delta+\mu) \end{pmatrix}.$$

The characteristic polynomial of the matrix $Q$ is given by

$$P(X) = X^2 + a_1 X + a_2 = 0.$$

Where

$$a_1 = k + r + \delta + 2\mu,$$
$$a_2 = (k+\mu)(r+\delta+\mu)(1-R_1)\,.$$

Applying the Routh–Hurwitz stability criterion [118], it can be shown that the eigenvalues of the submatrix $Q$ have negative real parts for $R_1 < 1$. Hence, the disease-free equilibrium point of the system (7.1) is locally asymptotically stable if $R_0 < 1$ and unstable if $R_0 > 1$. Hence, both DS-TB and MDR-TB will die out from the population if $R_0 < 1$, while at least one of the diseases will invade and persist in the population if $R_0 > 1$.

***Existence of the endemic equilibrium point (EEP)***

The endemic equilibrium point of the model (7.1) is the steady state at which disease persists in the population when at least one of the model's infectious compartments is non-zero. It is obtained as follows:

$$P_1 = \left(S^*, V^*, E^*, I^*, J^*\right),$$

where

$$\begin{aligned}
S^* &= \frac{1}{R_1}\Lambda\left(\frac{\eta+\mu\left(1-\phi\right)}{\mu\left(\eta+\mu\right)}\right),\\
V^* &= \frac{\Lambda\phi}{\eta+\mu},\\
E^* &= -\frac{\left(r+\delta+\mu\right)\left[x_1\left\{R_1-R_2\right\}\right]\left[\mu k\left(r+\delta+\mu\right)\left(\eta+\mu\right)\left(\mu+k\left\{1-R_1\right\}\right)\right]}{k\beta\left(\eta+\mu\right)\left[-\theta\mu^2(r+\delta+\mu)^2+x_2\left\{R_1-R_2-\theta\left(\delta+\mu\right)\right\}+x_3\left\{R_1-R_2-r\beta\left(1-\omega\right)\right\}\right]},\\
I^* &= -\frac{\left[x_1\left\{R_1-R_2\right\}\right]\left[\mu k\left(r+\delta+\mu\right)\left(\eta+\mu\right)\left(\mu+k\left\{1-R_1\right\}\right)\right]}{\beta\left(\eta+\mu\right)\left[-\theta\mu^2(r+\delta+\mu)^2+x_2\left\{R_1-R_2-\theta\left(\delta+\mu\right)\right\}+x_3\left\{R_1-R_2-r\beta\left(1-\omega\right)\right\}\right]},\\
J^* &= \frac{kr\left(\eta+\mu\right)\mu\left(r+\delta+\mu\right)\left[\mu+k\left\{1-R_1\right\}\right]\left(1-\omega\right)}{-\left(\eta+\mu\right)\left[-\theta\mu^2(r+\delta+\mu)^2+x_2\left\{R_1-R_2-\theta\left(\delta+\mu\right)\right\}+x_3\left\{R_1-R_2-r\beta\left(1-\omega\right)\right\}\right]}.
\end{aligned}$$

with

$$\begin{aligned}
x_1 &= \left(r+\delta+\mu\right)\left(k+\mu\right)\left(\alpha+\delta+\mu\right)\left(\frac{\mu\left(\eta+\mu\right)}{\Lambda\left(\eta+\mu\left(1-\phi\right)\right)}\right),\\
x_2 &= k\mu\left(r+\delta+\mu\right)\frac{\eta+\mu\left(1-\phi\right)}{\mu\left(\eta+\mu\right)},\\
x_3 &= \frac{k^2\left(\delta+\mu\right)\left(\alpha+\delta+\mu\right)\left(r+\delta+\mu\right)\mu\left(\eta+\mu\right)}{\eta+\mu\left(1-\phi\right)}.
\end{aligned}$$

It is evident from the above that model (7.1) has positive EEP if and only if one of the following conditions hold:

1. $1 < R_1 < 1+\frac{\mu}{k}$ and $0 < R_1-R_2 < \frac{1}{x_2+x_3}\left[\theta\mu^2(r+\delta+\mu)^2+x_2\theta\left(\delta+\mu\right)+x_3r\beta\left(1-\omega\right)\right]$,

2. $R_1 > 1+\frac{\mu}{k}$ and $0 < R_1-R_2 > \frac{1}{x_2+x_3}\left[\theta\mu^2(r+\delta+\mu)^2+x_2\theta\left(\delta+\mu\right)+x_3r\beta\left(1-\omega\right)\right]$.

### *Analysis of the MDR-TB-only model*

The sub-model with MDR-TB-only (obtained by setting $E = 0,\ I = 0$ in the model (7.1) is given by

$$\begin{cases} \frac{dS}{dt} = (1-\phi)\,\Lambda + \eta V + \alpha J - \theta S J - \mu S \\ \frac{dV}{dt} = \phi\Lambda - (\eta+\mu)\,V \\ \frac{dJ}{dt} = \theta S J - (\mu+\delta)\,J - \alpha J \end{cases} \tag{7.8}$$

For this model, it can be shown that the region,

$$\Omega_1 = \left\{ (S(t), V(t), J(t)) \in \mathbb{R}^3_+ : N(t) \leq \frac{\Lambda}{\mu} \right\} \tag{7.9}$$

is a positively invariant region for the model(7.8).

**Theorem 7.2.4.** *The model (7.8) at DFE, $M_0 = \left(\Lambda\frac{\eta+\mu(1-\phi)}{\mu(\eta+\mu)}, \frac{\Lambda\phi}{\eta+\mu}, 0\right)$, is globally asymptotically stable (GAS) for $R_2 < 1$.*

***Proof:*** We follow a methodology similar to the stability analysis of [20, 85, 86, 102, 119]. We observe that

$$S(t) + V(t) \leq \frac{\Lambda}{\mu}.$$

Let's assume $R_2 < 1$. Then there exists $a_0 > 0$ such that $(1+a_0)\,R_0 < 1$. Now we observe that the one-dimensional ODE system

$$\frac{dV(t)}{dt} = \phi\Lambda - (\eta+\mu)\,V(t),\ 0 \leq V(t) \leq \frac{\Lambda}{\mu}$$

is globally asymptotically stable.

So, in particular, there exists $t_1 > 0$ such that, given any $0 \leq V(0) < \frac{\Lambda}{\mu}$, we have $\left|V(t) - V^0\right| < a_0 S^0$ for all $t \geq t_1$.

This implies that given any

$S_0 \in \left[0, \frac{\Lambda}{\mu}\right]$, then $S(t) \leq S^0(1+a_0)$ for all $t \geq t_1$.

Thus in order to prove this theorem, it can be assumed that $S(t) < S^0(1+a_0)$.

Let us define a function

$$F(J) = J(t).$$

We prove now that $\dot{F}(t)$ is negative-definite.

$$\begin{aligned}\dot{F}(t) &= \theta SJ - (\alpha+\mu+\delta)J,\\ &\leq \left[\theta S^0(1+a_0) - (\alpha+\mu+\delta)\right]J,\\ &= (\alpha+\mu+\delta)\left[R_2(a_0+1)-1\right]J.\end{aligned}$$

This proves that $\dot{F}(t) < 0$, whenever $R_2 < 1$. Hence, $F(t)$ is a Lyapunov function on $\Omega_1$. Therefore, by LaSalle's invariance principle [87], every solution of the model (7.8), with any initial conditions in $\Omega_1$, approaches $M_0$ as $t \to \infty$, whenever $R_2 < 1$. Thus, $M_0$ is GAS in the region $\Omega_1$.■

**Theorem 7.2.5.** *If $R_2 > 1$, then the model (7.8) has a unique positive endemic equilibrium $M_1 = (S^*, V^*, J^*)$. With:*

$$\begin{aligned}S^* &= \frac{\alpha+\delta+\mu}{\theta},\\ V^* &= \frac{\Lambda\phi}{\eta+\mu},\\ J^* &= \frac{\mu(\alpha+\delta+\mu)}{\theta(\delta+\mu)}(R_2-1).\end{aligned}$$

***Proof:*** It follows logically from the above that whenever $R_2 > 1$, a unique positive MDR-TB-only endemic equilibrium point exists. ■

## 7.3 Extension of the model to optimal control

This section expands model (7.1) by incorporating the following four control interventions.

- ***Vaccination control*** ($u_1$): Represents using the Bacillus of Calmette and Guerin (BCG) vaccine.
- ***Distancing control*** ($u_2$): It represents an effort to protect susceptible individuals from exposure to tuberculosis by effectively reducing contact between vulnerable and infectious individuals. These include, for example, isolation of infected persons, social distancing, wearing face masks, diagnostic campaigns, and public health awareness programs.
- ***Treatment for DS-TB*** ($u_3$): Represents the effort to reduce treatment failure in

DS-TB infectious individuals, such as taking care of patients until they complete the treatment.

- ***Treatment for MDR-TB*** ($u_4$): Represents the effort of treating and curing MDR-TB-infected individuals.

After incorporating the control variables $u_1$, $u_2$, $u_3$ and $u_4$ into the model (7.1), it takes the following form:

$$\begin{cases} \frac{dS}{dt} = (1-u_1)\,\Lambda + \eta V + u_3 rI + (1+u_4)\,\alpha J - \beta SI - (1-u_2)\,\theta SJ - \mu S \\ \frac{dV}{dt} = u_1\Lambda - (\eta+\mu)\,V \\ \frac{dE}{dt} = \beta SI - (k+\mu)E \\ \frac{dI}{dt} = kE - (r+\delta+\mu)I \\ \frac{dJ}{dt} = (1-u_2)\,\theta SJ + (1-u_3)\,rI - ((1+u_4)\alpha + \mu + \delta)\,J \end{cases} \tag{7.10}$$

In this optimal control problem, our main objective is to reduce the number of MDR-TB-infected individuals in the population while reducing the overall cost of controlling the disease.

Let us consider the following objective functional:

$$Y(u_1, u_2, u_3) = \int_{t_0}^{t_f} \left[ J(t) + \frac{1}{2}B_1 u_1^2 + \frac{1}{2}B_2 u_2^2 + \frac{1}{2}B_3 u_3^2 + \frac{1}{2}B_4 u_4^2 \right] dt. \tag{7.11}$$

Subject to the terms of the model system (7.10). The constant $B_i$ measures the relative cost interventions associated with the control $u_i$ for $i = 1, 2, 3, 4$. The functions $\frac{1}{2}B_i u_i^2$ are the cost functions that correspond to the controls $u_i$, which is nonlinear (as in [120, 121]). In Equation (7.11), the values of $t_0$ and $t_f$ are taken as 0 and 20, respectively, to determine Ethiopia's 20-year (2019–2038) effective MDR-TB control strategy.

The main goal is to find the optimal controls $u_1^*$, $u_2^*$, $u_3^*$ and $u_4^*$ such that

$$Y(u_1^*, u_2^*, u_3^*, u_4^*) = \min\{Y(u_1, u_2, u_3, u_4) : u_1, u_2, u_3, u_4 \in U\}, \tag{7.12}$$

were $U = \{(u_1, u_2, u_3, u_4) \mid u_1, u_2, u_3$ and $u_4$ are Lebesgue integrable functions on the interval $[0,\infty)$, with $0 \le u_i \le 1$, $i = 1, 2, 3, 4\}$.

***Existence of an Optimal Control***

We show the existence of optimal control by using an approach as in [84]. The boundedness of the model's solution has already been established. The boundedness

of the solution is used to demonstrate that an optimal control exists. For detailed proof, see [122]. By using the maximum principle of Pontryagin [77], the Hamiltonian ($H$), which combines the state Equations (7.1) and the integrand of the objective functional (7.11), is given by

$$\begin{aligned} H\left(S,V,E,I,J,u_1,u_2,u_3,u_4,\lambda\right) = J &+ \frac{1}{2}B_1u_1^2 + \frac{1}{2}B_2u_2^2 + \frac{1}{2}B_3u_3^2 + \frac{1}{2}B_4u_4^2 \\ &+ \lambda_1\left[\left(1-u_1\right)\Lambda + \eta V + u_3rI + \left(1+u_4\right)\alpha J\right] \\ &- \lambda_1\left[\beta SI + \left(1-u_2\right)\theta SJ + \mu S\right] \\ &+ \lambda_2\left[u_1\Lambda - \left(\eta+\mu\right)V\ \right] \\ &+ \lambda_3\left[\beta SI - \left(k+\mu\right)E\right] \\ &+ \lambda_4\left[kE - (r+\delta+\mu)I\right] \\ &+ \lambda_5\left[\left(1-u_2\right)\theta SJ + \lambda_5\left(1-u_3\right)rI - \left(\left(1+u_4\right)\alpha+\mu+\delta\right)J\right]. \end{aligned}$$

Here, $\lambda = (\lambda_1,\lambda_2,\lambda_3,\lambda_4,\lambda_5) \in \mathbb{R}^5$ are the adjoint functions. The following result can be obtained by applying Pontryagin's maximum principle to the existence of the optimal control problem.

**Theorem 7.3.1.** *Let $u_1^*, u_2^*, u_3^*$, and $u_4^*$ be the control functions for the control problem given in the system (7.10), and $\overline{S},\overline{V},\overline{E},\overline{I}$, and $\overline{J}$ be the solutions of state variables. Then there are adjoint variables $\lambda_1$, $\lambda_2$, $\lambda_3$, and $\lambda_4$ 6 that satisfy the following Equations*

$$\begin{cases} \frac{d\lambda_1}{dt} = \left[\beta I + \mu + \theta J\left(1-u_2\right)\right]\lambda_1 - \beta I\lambda_3 - \theta J(1-u_2)\lambda_5 \\ \frac{d\lambda_2}{dt} = -\eta\lambda_1 + (\eta+\mu)\lambda_2 \\ \frac{d\lambda_3}{dt} = \left[k+\mu+\theta J\left(1-u_2\right)\right]\lambda_3 - k\lambda_4 - \theta J\left(1-u_2\right)\lambda_5 \\ \frac{d\lambda_4}{dt} = \left(\beta S - ru_3\right)\lambda_1 - \beta S\lambda_3 + \left(r+\delta+\mu\right)\lambda_4 - r\left(1-u_3\right)\lambda_5 \\ \frac{d\lambda_5}{dt} = -1 + \left[\theta S\left(1-u_2\right) - \alpha(1+u_4)\right]\lambda_1 \\ \qquad + \left[\delta+\mu-\theta S\left(1-u_2\right) + \alpha(1+u_4)\right]\lambda_5 \end{cases} \tag{7.13}$$

with transversality conditions

$$\lambda_1\left(t_f\right) = \lambda_2\left(t_f\right) = \lambda_3\left(t_f\right) = \lambda_4\left(t_f\right) = \lambda_5\left(t_f\right) = 0. \tag{7.14}$$

and

$$\begin{cases} u_1^* = \min\left\{\max\left\{0, \frac{\Lambda(\lambda_1-\lambda_2)}{B_1}\right\}, 1\right\} \\ u_2^* = \min\left\{\max\left\{0, \frac{\theta S(\lambda_5-\lambda_1)}{B_2}\right\}, 1\right\} \\ u_3^* = \min\left\{\max\left\{0, \frac{rI(\lambda_5-\lambda_1)}{B_3}\right\}, 1\right\} \\ u_4^* = \min\left\{\max\left\{0, \frac{\alpha J(\lambda_5-\lambda_1)}{B_4}\right\}, 1\right\} \end{cases} \tag{7.15}$$

**Proof:** The form of the adjoint system and the transversality conditions associated with this optimal control problem are obtained by applying Pontryagin's Maximum Principle [77]. For this purpose, we differentiate the formulated Hamiltonian function with respect to $S, V, E, I$, and $J$ as follows;

$$\frac{d\lambda_1}{dt} = -\frac{\partial H}{\partial S}, \frac{d\lambda_2}{dt} = -\frac{\partial H}{\partial V}, \frac{d\lambda_3}{dt} = -\frac{\partial H}{\partial E}, \frac{d\lambda_4}{dt} = -\frac{\partial H}{\partial I}, \frac{d\lambda_5}{dt} = -\frac{\partial H}{\partial J}, \tag{7.16}$$

with

$$\lambda_i\left(t_f\right) = 0, i = 1, 2, 3, 4, 5. \tag{7.17}$$

Finally, by applying the optimality condition

$$\frac{\partial H}{\partial u_1} = \frac{\partial H}{\partial u_2} = \frac{\partial H}{\partial u_3} = \frac{\partial H}{\partial u_4} = 0,$$

and using the bounds for the controls $u_1, u_2$, $u_3$ and $u_4$ we can derive the optimal control $(u_1^*,\ u_2^*,\ u_3^*, u_4^*)$ as in Equation (7.15). ■



Table 7.1: Initial values of the variables

| Symbols | Description | Units | Value | Reference |
|---|---|---|---|---|
| $N_0$ | Total population | *Humans* | $1.12\times10^8$ | [122] |
| $S_0$ | Susceptible | *Humans* | $3.404\times10^7$ | Estimated |
| $V_0$ | Vaccinated | *Humans* | $1.001 \times 10^6$ | [102] |
| $E_0$ | DS-TB latent | *Humans* | $1.83\times10^7$ | [122] |
| $I_0$ | DS-TB infected | *Humans* | $1.57\times10^5$ | [123] |
| $J_0$ | MDR-TB infected | *Humans* | $1.115\times10^3$ | [124] |

## 7.4 Numerical simulations

The forward-backwards sweeping method is used to solve the optimal control problem. The solution's algorithm is based on the approach suggested in [112]. The system (7.10) is simulated forward in time to achieve convergence, while the Hamiltonian function is

simulated backwards in time.

The unit of time used for the parameter values is one year. We calculate the initial number of vaccinated children as the product of the average number of newborns and the vaccination coverage, which is $V_0 = 1.001 \times 10^6$. In 2019, the incidence rate of MDR-TB in Ethiopia was 0.71% [124]. Hence, we take $J_0 = 0.0071 \times I_0 = 1115$. In the same year, 75% of MDR-TB patients in Ethiopia were treated successfully [125]. So, we take the value of $\alpha$ as 0.75.

A recent estimation indicated that 3.3% of MDR-TB cases worldwide occurred among new TB cases in 2019 [126]. We take 3.3% of $\beta$ to get the value of $\theta$. Hence $\theta = 5.43\times10^{-5}$. The values of the remaining parameters and the initial values of the variables used in our simulations are presented in Tables 7.1 and 7.2.

Table 7.2: parameter values.

| Symbols | Description | Units | Value | Reference |
|---|---|---|---|---|
| $\Lambda$ | Recruitment rate | $Humans/year$ | $1.4\times10^6$ | [122] |
| $\beta$ | Transmission rate for DS-TB | $1/year$ | $1.646\times10^{-7}$ | [122] |
| $\theta$ | Transmission rate for MDR-TB | $1/year$ | $5.43\times10^{-5}$ | Estimated |
| $\phi$ | Vaccination rate of new-borns | $1/year$ | 0.715 | [102] |
| $\eta$ | Loss of protection for vaccination | $1/year$ | 0.5 | [102] |
| $\mu$ | Natural mortality rate | $1/year$ | 0.016 | [105] |
| $k$ | Transfer rate from $E$ to $I$ | $1/year$ | 0.023 | [122] |
| $r$ | Treatment rate of $I$ | $1/year$ | 0.546 | [102] |
| $\omega$ | Recovery rate form DS-TB | $dimensionless$ | 0.832 | [126] |
| $\alpha$ | Recovery rate form MDR-TB | $1/year$ | 0.75 | [125] |
| $\delta$ | Death rate due to TB | $1/year$ | 0.17 | [125] |

### 7.4.1 Use of single control

For this control strategy, we have four alternatives:

Strategy A: $u_1$, only vaccination control,

Strategy B: $u_2$, only distancing control,

Strategy C: $u_3$, only treatment for DS-TB ,

Strategy D: $u_4$, only treatment for MDR-TB.

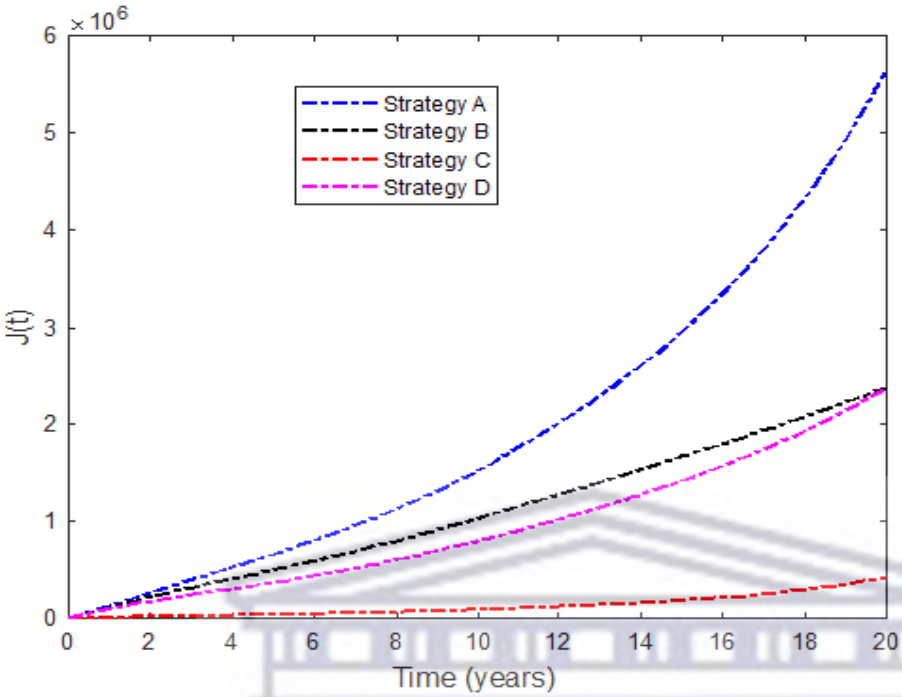


Figure 7.2: The MDR-TB infectious population trajectories under different single control strategies.

The simulation result of MDR-TB-infected individuals with different single control interventions is plotted in Figure 7.2. It can be observed that the number of MDR-TB-infected individuals can be significantly decreased when Strategy C (successful treatment for DS-TB) is applied. In contrast, Strategy A (only vaccination control) has the least impact on reducing the number of patients. This shows that it is beneficial to use treatment for DS-TB to prevent the MDR-TB.

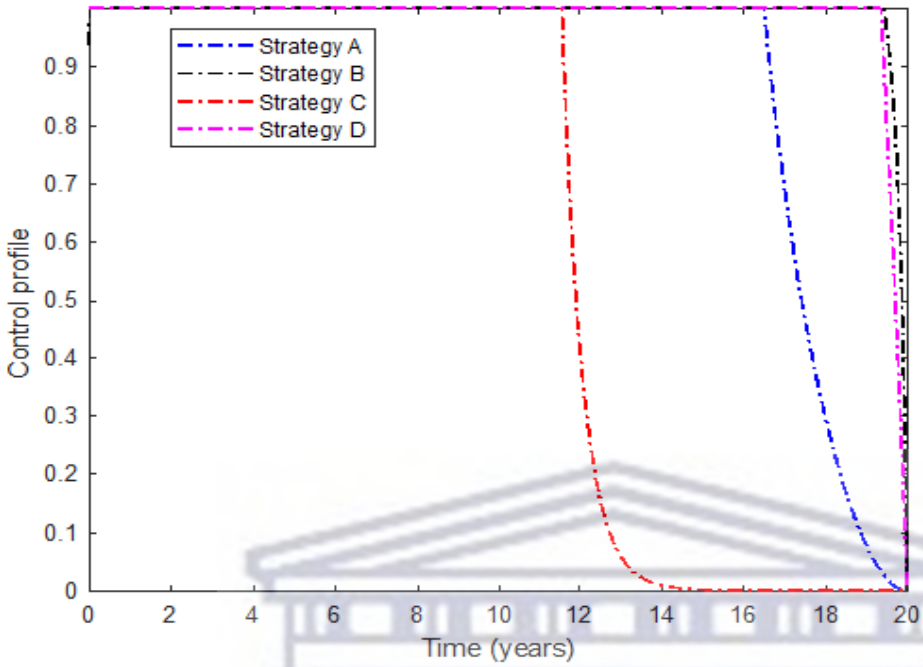


Figure 7.3: The control profiles of different single controls.

The control profiles in Figure 7.3 indicate that distancing and treatment for MDR-TB controls should be implemented at the maximum level until the end of the implementation. In contrast, the treatment for DS-TB and vaccination controls retained their highest bound for 13 and 18 years, respectively, then declined until they reached their minimum value.



### 7.4.2 Use of the dual controls

In this scenario, we consider a combination of two control functions, and we have six alternative strategies:

*Strategy E*: Vaccination ($u_1$) and distancing ($u_2$),

*Strategy F*: Vaccination ($u_1$) and treatment for DS-TB ($u_3$),

*Strategy G*: Vaccination ($u_1$) and treatment for MDR-TB ($u_4$),

*Strategy H*: Distancing ($u_2$) and treatment for DS-TB ($u_3$),

*Strategy I*: Distancing ($u_2$) and treatment for MDR-TB ($u_4$),

*Strategy J*: Treatment for DS-TB ($u_3$) and treatment for MDR-TB ($u_4$).

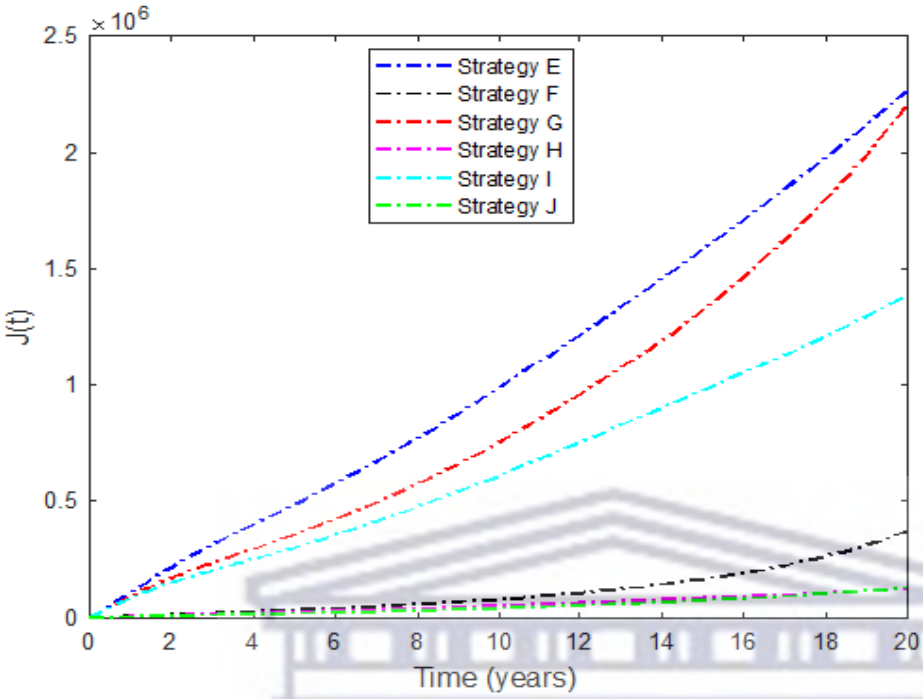


Figure 7.4: The MDR-TB infectious population trajectories under different double control strategies.

We noticed in Figure 7.4 that Strategy J has the highest number of MDR-TB infections averted, followed by Strategy *H, F, I, G*, and *E*. The control solution profile is shown in Figure 7.5.

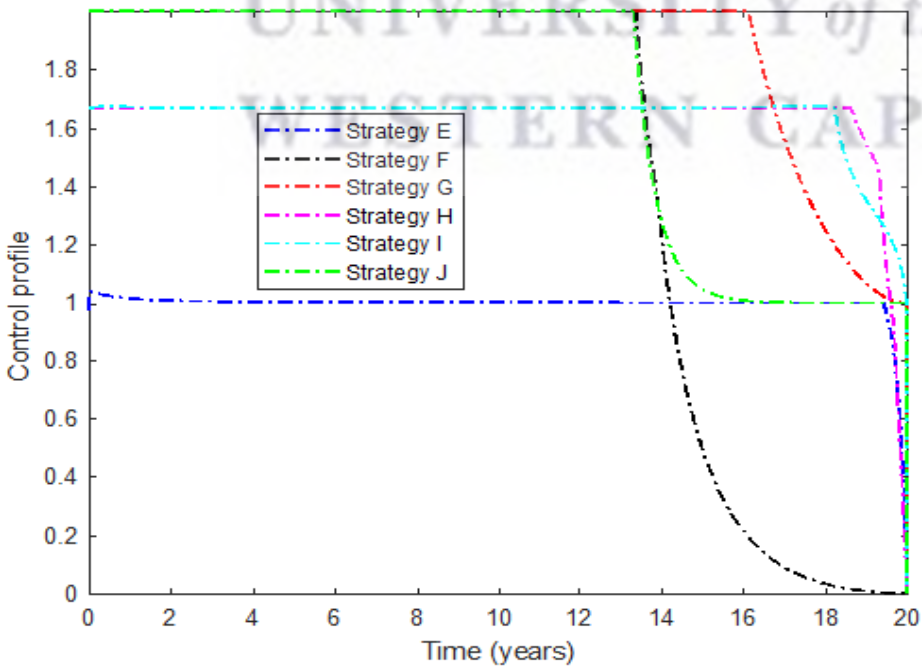


Figure 7.5: The control profiles of different double controls.

### 7.4.3 Use of the triple controls

In this section, we conduct numerical simulations by considering the application of triple control functions. For the combination of three different control practices, we have the following four alternative strategies:

*Strategy K*: Vaccination, distancing, and treatment for MDR-TB,

*Strategy L*: Vaccination, distancing, and treatment for DS-TB,

*Strategy M*: Vaccination, treatment for DS-TB, and treatment for MDR-TB,

*Strategy N*: Distancing, treatment for DS-TB, and treatment for MDR-TB.

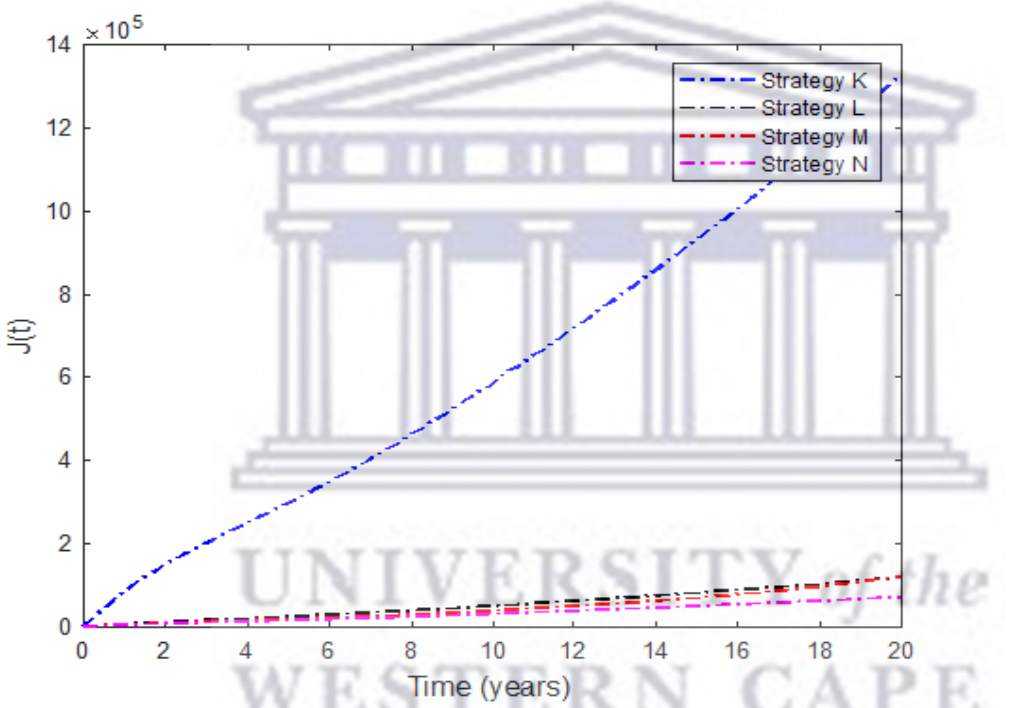


Figure 7.6: The MDR-TB infectious population trajectories under different triple control strategies.

Figure 7.6 presents simulation results for MDR-TB-infected individuals with different triple-control interventions. We can see that Strategy $N$ ( the combination of distancing, treatment for DS-TB, and treatment for MDR-TB) can significantly reduce the number of people infected with MDR-TB. In contrast, Strategy $K$ (the combination of Vaccination, distancing, and treatment for MDR-TB) has the least effect on reducing case numbers. The control function of this strategy is displayed in Figure 7.7.

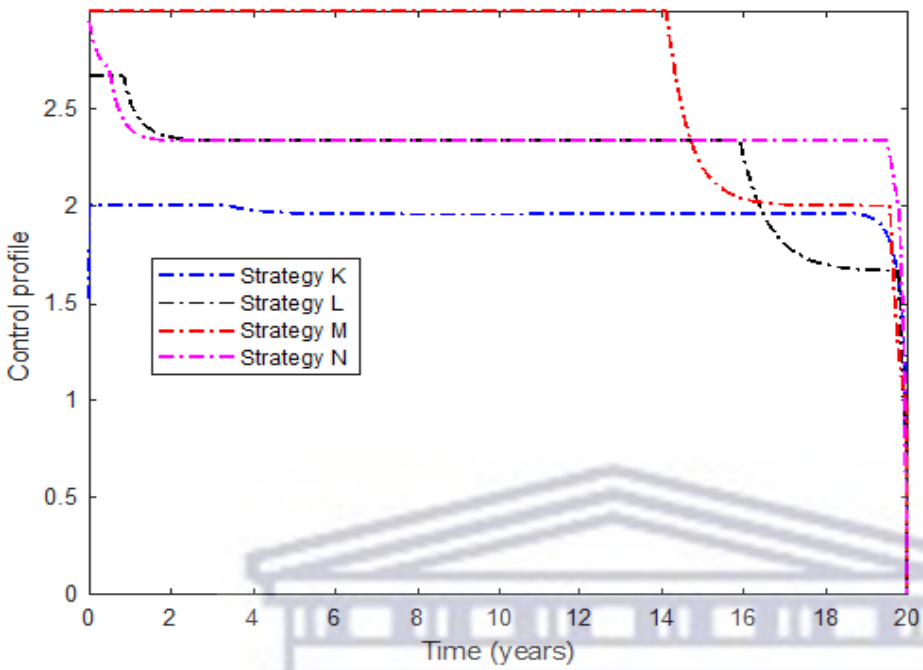


Figure 7.7: The control profiles of different triple controls.

## 7.5 Cost-Effectiveness Analysis

We used cost-effectiveness analysis to determine the most effective strategy to control MDR-TB in Ethiopia. This is performed by the incremental cost-effectiveness ratio (ICER) mentioned in [33, 123]. This ratio compares the differences between the total costs and the total decrement of MDR-TB patients for two alternative control strategies. The following formula obtains the ICER:

$$ICER(i,j) = \frac{The\ difference\ in\ costs\ between\ strategies\ i\ and\ j}{Difference\ in\ total\ number\ of\ infection\ averted\ in\ strategies\ i\ and\ j}.$$

Table 7.3: The number of MDR-TB infectious averted and the total cost of each single control strategy.

| Strategy | Total infection averted | Total cost ($) |
|---|---|---|
| B ($u_2$ ) | $3.85 \times 10^6$ | $3.86 \times 10^6$ |
| D ($u_4$ ) | $3.85 \times 10^6$ | $4.03 \times 10^6$ |
| A ($u_1$ ) | $5.7 \times 10^5$ | $6.85 \times 10^5$ |
| C ($u_3$ ) | $5.8 \times 10^6$ | $5.8 \times 10^6$ |

### 7.5.1 ICER for single control strategy

Based on the total number of people averted from MDR-TB infection, Strategies

$B, D, A$, and $C$ are ranked in increasing order as shown in Table 7.3. Based on this rank, we first compare the ICER of Strategy $B$ and Strategy $D$.

$$ICER\,(B) = \frac{3.86 \times 10^6}{3.8487 \times 10^6} = 1.0025.$$

$ICER$ (Strategy D with respect to Strategy B)$= \frac{4.03\times10^6 - 3.86\times10^6}{3.8497\times10^6 - 3.8487\times10^6} = 174.28.$

This shows that Strategy $B$ is less costly compared to strategy D. Strategy $D$ is then ignored, and the analysis continues by comparing Strategy $B$ with $A$:

$$ICER\,(B) = \frac{3.86 \times 10^6}{3.8487 \times 10^6} = 1.0025.$$

$ICER$(Strategy A with respect to Strategy B)$= \frac{6.85\times10^5 - 3.86\times10^6}{5.723\times10^5 - 3.8487\times10^6} = 0.97.$

It follows that Strategy $A$ is cheaper compared to Strategy $B$ and hence, strategy $B$ is ignored, and the analysis continues by comparing Strategy $A$ and Strategy $C$ as follows:

$$ICER\,(A) = \frac{6.85 \times 10^5}{5.723 \times 10^5} = 1.197.$$

$ICER$ (Strategy C with respect to Strategy A)$= \frac{5.8\times10^6 - 6.85\times10^5}{5.79\times10^6 - 5.723\times10^5} = 0.98.$

Eventually, Strategy $C$ is more cost-effective than Strategy $A$. Therefore, the control program that considers the application of Strategy $C$ (successful treatment of DS-TB) will achieve a more efficient result.

Table 7.4: The number of MDR-TB infectious averted and the total cost of each dual control strategy.

| Strategy | Total infection averted | Total cost ($) |
|---|---|---|
| $E$ ($u_1$ *and* $u_2$) | $3.95 \times 10^6$ | $4.07 \times 10^6$ |
| $G$ ($u_1$ *and* $u_4$) | $4.01 \times 10^6$ | $4.12 \times 10^6$ |
| $I$ ($u_2$ *and* $u_4$) | $4.83 \times 10^6$ | $5.02 \times 10^6$ |
| $F(u_1 and\ u_3)$ | $5.84 \times 10^6$ | $5.96 \times 10^6$ |
| $H$ ($u_2$ *and* $u_3$) | $6.003 \times 10^6$ | $6.02 \times 10^6$ |
| $J(u_3 and\ u_4)$ | $6.086 \times 10^6$ | $6.27 \times 10^6$ |

### 7.5.2 ICER for the dual control strategy

First, we must rank the strategies in order of increasing based on averted infections, as shown in Table 7.4. The incremental cost-effectiveness ratio for the dual control strategies is calculated in Table 7.5. From the table, we conclude that Strategy $H$ (i.e., the combi-

nation of distancing and the successful treatment of DS-TB) is the most cost-effective of all dual control strategies.

Table 7.5: The incremental cost-effectiveness ratio of the dual control strategies

| ICER | Decision |
|---|---|
| $ICER\,(E) = \frac{4.07\times10^6}{3.95\times10^6} = 1.03$ | ---- |
| $ICER\,(G,E) = \frac{4.12\times10^6-4.07\times10^6}{4.01\times10^6-3.95\times10^6} = 0.84$ | Strategy $G$ is less costly than Strategy $E$. Strategy $E$ is then ignored, and the analysis continues by comparing Strategy $I$ with $G$. |
| $ICER\,(G) = \frac{4.12\times10^6}{4.01\times10^6} = 1.03$ | ---- |
| $ICER\,(I,G) = \frac{5.02\times10^6-4.12\times10^6}{4.83\times10^6-4.01\times10^6} = 1.097$ | Strategy $I$ is cheaper and more effective than Strategy $G$ and hence, the analysis continues by comparing Strategy $I$ and Strategy $F$. |
| $ICER\,(I) = \frac{5.02\times10^6}{4.83\times10^6} = 1,04$ | ---- |
| $ICER(F,I) = \frac{5.96\times10^6-5.02\times10^6}{5.84\times10^6-4.83\times10^6} = 0.93$ | This comparison indicates that Strategy $F$ is cheaper than Strategy $I$, and the analysis continues by comparing Strategy $F$ and Strategy $H$. |
| $ICER\,(F) = \frac{5.96\times10^6}{4.83\times10^6} = 1.02$ | ---- |
| $ICER\,(H,F) = \frac{6.02\times10^6-5.96\times10^6}{6.003\times10^6-4.83\times10^6} = 0.35$ | Strategy $H$ is less costly and more effective than Strategy $F$. As a result, Strategy $F$ is eliminated from subsequent ICER computations. |
| $ICER\,(H) = \frac{6.02\times10^6}{6.003\times10^6} = 1,002$ | ---- |
| $ICER(J,H) = \frac{6.27\times10^6-6.02\times10^6}{6.086\times10^6-4.83\times10^6} = 3.07$ | Strategy $H$ is less costly and more effective than Strategy $J$. |



### 7.5.3 ICER for the triple control strategy

Using the simulation results, we rank the control strategies in increasing order of effectiveness based on infection averted. This ranking procedure shows that Strategy $K$ averted the least number of infections, followed by Strategy $M, L$ and $N$ (see Table 7.6). Based on this rank, we first compare the ICER of Strategy $K$ and Strategy $M$ as follows.

$$ICER\,(K) = \frac{5.19\times10^6}{4.89\times10^7} = 1.06.$$

$$ICER\,(M,K) = \frac{6.37\times10^6 - 5.19\times10^6}{6.09\times10^7 - 4.89\times10^7} = 0.996.$$

This implies that Strategy $K$ is more costly and less effective than Strategy $M$. Thus, we exclude Strategy $K$ from further consideration and continue to compare strategies $M$ and $L$.

$$ICER(M) = \frac{6.37 \times 10^6}{6.09 \times 10^7} = 1.05.$$

$$ICER(L, M) = \frac{6.22 \times 10^6 - 6.37 \times 10^6}{6.098 \times 10^7 - 6.09 \times 10^7} = -70.02.$$

This comparison indicates that Strategy $L$ is cheaper than Strategy $M$. Therefore, Strategy $M$ is rejected and continues to compare Strategy $L$ with Strategy $N$.

$$ICER(L) = \frac{6.22 \times 10^6}{6.098 \times 10^7} = 1.02.$$

$$ICER(N, L) = \frac{6.34 \times 10^6 - 6.22 \times 10^6}{6.14 \times 10^6 - 6.098 \times 10^7} = 2.48.$$

This indicates that Strategy $L$ is cheaper and more effective than Strategy $N$.

Finally, the comparison result reveals that Strategy $L$ is cheaper and more effective than Strategy $N$. Therefore, Strategy $L$ (combination of vaccination, distancing, and successful treatment of DS-TB) is the best of all triple control strategies.

Table 7.6: The number of MDR-TB infectious averted and the total cost of each triple control strategy.

| Strategy | Total infection averted | Total cost ($) |
|---|---|---|
| $K$ $(u_1,\ u_2, u_4)$ | $4.89 \times 10^7$ | $5.19 \times 10^6$ |
| $M$ $(u_1,\ u_3,\ u_4)$ | $6.09 \times 10^7$ | $6.37 \times 10^6$ |
| $L$ $(u_1\ , u_2, u_3)$ | $6.098 \times 10^7$ | $6.22 \times 10^6$ |
| $N$ $(u_2, u_3, u_4)$ | $6.14 \times 10^6$ | $6.34 \times 10^6$ |

## 7.6 Conclusions

In this chapter, we presented a compartmental model to understand the transmission dynamics of MDR-TB in Ethiopia. We first showed that the model is well-posed epidemiologically and mathematically. Then, we have described the conditions for the stability of the equilibrium points.

We applied preventive controls in the form of vaccination, distancing, and two treatment controls for DS-TB and MDR-TB. Theoretically, we proved the existence of optimal control and studied the characterization of optimal control by Pontryagin's Maximum Principle. In addition, the incremental cost-effectiveness ratio of single, coupled, and

triple combinations of control strategies was investigated to determine the most effective method to control the spread of MDR-TB in Ethiopia.

Among the four single controls, it is found that the successful treatment of DS-TB is the most effective strategy in curtailing the spread of MDR-TB. Therefore, the Ethiopian government should improve DS-TB therapy by reducing treatment failures in DS-TB patients if only one control strategy is used.

Within the six dual-control strategies, a combination of distancing and successful treatment of DS-TB is the most cost-effective strategy compared to others. Therefore, if dual control strategies are considered, we recommend the Ethiopian government focus on isolation policy, educational campaigns, and monitoring DS-TB patients to complete their treatment correctly.

Considering the combination of the triple control strategy, the combination of successful treatment of DS-TB with distancing and vaccination control is the most cost-effective strategy.

In this chapter, we employ just two compartments to represent the MD-TB strain, resulting in restricted accuracy. Therefore, we suggest further investigation that includes the latent stage for MD-TB.

# Chapter 8

# A model of the disease dynamics of Tuberculosis in a prison system: the case of Ethiopia

This chapter presents a model of tuberculosis dynamics in a crowded environment, which includes the influx of infected individuals into the population. The model is applied to the prison population of Ethiopia. First, we compare the TB epidemiology in the prison system with the situation in the ambient (open) population in terms of the numerical values of the basic reproduction numbers and the equilibrium points. Then, we compare the scenarios in terms of the equilibrium prevalence numbers for different levels of influx of infected individuals.



## 8.1 Introduction

Although tuberculosis is a common disease in many communities, it is more prevalent in densely populated areas and poorly ventilated buildings [127]. In particular, it has long been known that prisons have TB prevalence, which is relatively higher than in the ambient community [128].

Ethiopia has six federal and 120 regional detention centres; most prisoners live in a densely populated environment [129]. As a result, tuberculosis transmission among prisoners is a major public health concern in Ethiopia [130, 131]. Studies have shown that the prevalence of tuberculosis among Ethiopian prisoners ranges from 349 to 1913 per 100,000 [132, 133]. This high incidence of tuberculosis in prisons poses a serious threat to

both inmates and the general public. Therefore, significant attention should be paid to diagnosing and treating tuberculosis patients in prisons.

## 8.2 The model

The prison population at time $t$ is denoted by $N(t)$. We divided it into four epidemiological compartments: susceptible ($S$), high-risk latent ($E$), infectious ($I$ ), and treatment (low-risk latent) ($L$). The constant recruitment rate, $\Lambda$, is the number of new members arriving into the prison population in unit time. We assume that fraction $\theta$ of $\Lambda$ is infected with latent TB and another fraction $\eta$ of $\Lambda$ is infected with active TB. Then $0 \leq (\theta + \eta) \leq 1$. Furthermore, we assume that $(1-(\theta + \eta))\,\Lambda$ are free from the disease. Susceptible individuals get infected with active TB at a rate $\beta SI$. Individuals in the high-risk latent class will progress into the infectious stage at a rate of $kE$. Successfully treated infectious individuals from $I$ and $E$ are moved to the low-risk latent class at a rate of $prI$ and $\alpha E$, respectively. Since there is no permanent immunity to tuberculosis, some recovered (low latent risk) individuals may lose immunity and become latently infected with a relapse rate $\sigma$. We assume that death due to TB disease will happen only in the $I$-class with a rate $\delta$. In this model, the removal rate $\mu$ is a combination of the release rate from prison and the mortality rate of inmates.

The model flow diagram with the in-flow of infective prisoners is given in Figure 8.1. We derive the following system of non-linear ordinary differential Equations:

$$\begin{cases} \frac{dS}{dt} = (1 - (\theta + \eta))\,\Lambda - \beta SI - \mu S \\ \frac{dE}{dt} = \theta\Lambda + \beta SI + (1-p)rI + \sigma L - (k+\alpha+\mu)E \\ \frac{dI}{dt} = \eta\Lambda + kE - (\mu + r + \delta)\,I \\ \frac{dL}{dt} = prI + \alpha E - (\mu+\sigma)\,L \\ N(t) = S(t) + E(t) + I(t) + L(t)\,. \end{cases} \tag{8.1}$$

With the initial conditions $S_0, E_0, I_0, L_0 \geq 0$.

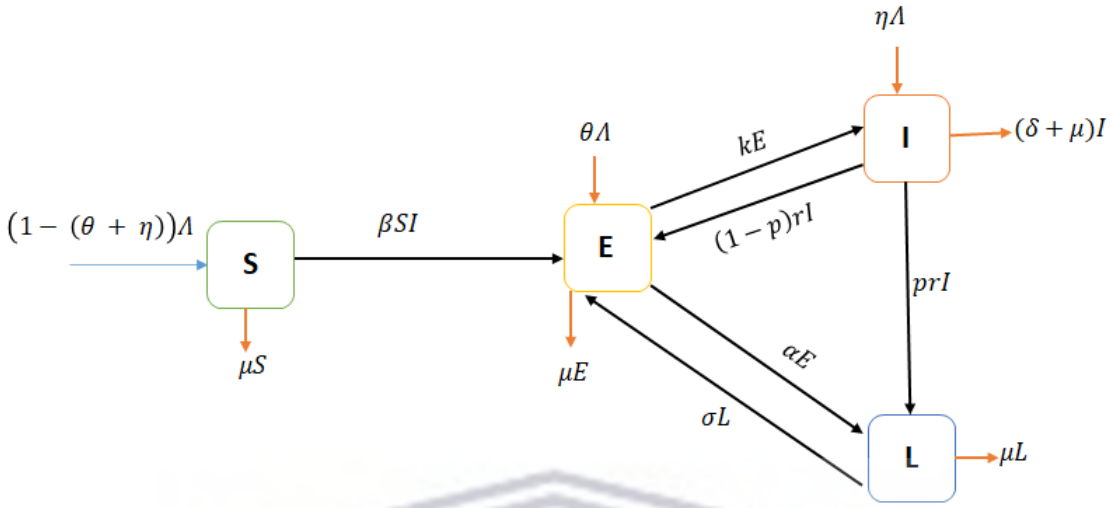


Figure 8.1: Flow chart for the model of TB transmission dynamics.

## 8.3 Model analysis

### 8.3.1 Positivity of the solutions

The variables in the system (8.1) represent human population numbers, which must be non-negative. Thus, we need to ensure that the model's solution is non-negative at any time. Methods used in [134, 135] made it possible to determine lower bounds for certain compartments in terms of the inflow of infected. The current paper follows the same methodology, enabling us to find lower bounds for the classes $E$, $I$, and $L$.

Let us introduce the numbers $B_1$, $B_2$ and $B_3$ as follows.

$B_1 = \frac{\theta\Lambda}{(k+\alpha+\mu)}$, $B_2 = \frac{\eta\Lambda+kB_1}{(\mu+r+\delta)}$, and $B_3 = \frac{\alpha B_1+prB_2}{(\mu+\sigma)}$

We define the set $G$ as below. $G = \left\{x \in \mathbb{R}^4_+ : x_2 > B_1, x_3 > B_2, x_4 > B_3, x_1+x_2+x_3+x_4 \leq \frac{\Lambda}{\mu}\right\}$.

**Theorem 8.3.1.** *Consider a fixed number $t_1 > 0$. Suppose that $X(t)$ is a local solution of the system (8.1) for which $X(s) \in \mathbb{R}^4_+$ while $0 < s < t_1$. If $N(0) \leq \Lambda/\mu$, then $N(t) \leq \Lambda/\mu$ for all $0 < t \leq t_1$.*

***Proof:*** Given any local solution with $X(t) \in \mathbb{R}^4_+$ for all $0 < t \leq t_0$, then we find that

$$\frac{d\left(N(t) - \frac{k}{\mu}\right)}{dt} = \Lambda - \mu N(t) - \delta I(t) \leq -\sigma L(t) \leq -\mu(N(t) - \frac{\Lambda}{\mu}.$$

Therefore $N(0) < \frac{k}{\mu}$ implies that $N(t) < \frac{k}{\mu}$ for all $0 < t \leq t_0$.

**Theorem 8.3.2.** *The set $G$ is a positively invariant set.*

***Proof***: Consider any point $y \in G$. Then there exists a local solution $X(t)$ in $G$ with the initial value $X(0) = y$. Suppose that $t_1$ is the time of exit of $X(t)$ from $G$ (and that $t_1$ is finite). We prove by contradiction that $t_1 = \infty$.

Let us write:

$$E_1(t) = E(t) - B_1, I_1(t) = I(t) - B_2 \text{ and } L_1 = L(t) - B_3.$$

Now we introduce the following function, for $0 \leq t \leq t_1$.

$$F_1(X(t)) = \ln\left(\frac{\Lambda}{\mu S(t)}\right) + \ln\left(\frac{\Lambda}{\mu E_1(t)}\right) + \ln\left(\frac{\Lambda}{\mu I_1(t)}\right) + \ln\left(\frac{\Lambda}{\mu L_1(t)}\right).$$

Note that each of the terms in the summation is a positive-valued function. Also, we know that for a constant $q > 0$,

$$\lim_{u \to 0^+} \ln(q/u) = \infty$$

Therefore, if any of the variables $S_1, E_1, I_1$ or $L_1$ tends to 0 as $t \to t_1$, then $F_1 \to \infty$. In the sequel, we shall prove to the contrary that if $t_1$ is finite, then $F_1$ is bounded over the interval $[0, t_1)$ and this will be the contradiction.

For $t \in [0, t_1)$, the following inequalities are derived:

$$\begin{aligned}
-\frac{\dot{E}_1(t)}{E_1(t)} &= \frac{-1}{E_1(t)}\left[\theta\Lambda + \beta S(t) I(t) + (1-p) r I(t) + \sigma L(t) - (\mu+\alpha+k) E(t)\right] \\
&\leq \frac{-1}{E_1(t)}\left[\theta\Lambda - (\mu+\alpha+k) E(t)\right] = \mu+\alpha+k. \\
-\frac{\dot{I}_1(t)}{I_1(t)} &= \frac{-1}{I_1(t)}\left[\eta\Lambda + kE - (\mu+\delta+r) I(t)\right] \\
&\leq \frac{-1}{I_1(t)}\left[\eta\Lambda + kB_1 - (\mu+\delta+r) I(t)\right] \\
&= \frac{1}{I_1(t)}\left[(\mu+\delta+r) I_1(t)\right] \\
&= \mu+\delta+r. \\
-\frac{\dot{L}_1(t)}{L_1(t)} &= \frac{-1}{L_1(t)}[prI(t) + (\alpha E(t) - (\mu+\sigma) L(t)] \\
&\leq \frac{-1}{L_1(t)}\left[prB_1 + \alpha B_2 - (\mu+\sigma) L(t)\right] \\
&= (\mu+\sigma)\frac{1}{L_1(t)}[L_1(t)] = \mu+\sigma.
\end{aligned}$$

We calculate the derivative:

$$\begin{aligned}
\frac{dF_1(X(t))}{dt} &= -\frac{1}{S}[(1-\theta-\eta)\Lambda - \beta S(t) I(t) - \mu S] - \frac{\dot{E}_1(t)}{E_1(t)} - \frac{\dot{I}_1(t)}{I_1(t)} - \frac{\dot{L}_1(t)}{L_1(t)} \\
&\leq \frac{1}{S}\left[-(1-\theta-\eta)\Lambda + \beta S(t) I(t) + \mu S(t)\right] \\
&\quad + (\mu+\alpha+k) + (\mu+\delta+r) + (\mu+\sigma) \\
&\leq \frac{1}{S}[\beta S(t) I(t) + \mu S(t)] + (\mu+\alpha+k) + (\mu+\delta+r) + (\mu+\sigma) \\
&\leq [\beta\Lambda/\mu + \mu] + (\mu+\alpha+k) + (\mu+\delta+r) + (\mu+\sigma) \\
&= F_0.
\end{aligned}$$

where

$$F_0 := [\beta\Lambda/\mu + \mu] + (\mu+\alpha+k) + (\mu+\delta+r) + (\mu+\sigma),$$

is a constant number, and in particular it is independent of $t_1$.

Then, for every $t \in [0, t_1)$ we have,

$$F_1(t) = \int_0^t \dot{F}_1(s)\, ds \leq tF_0 \leq t_1 F_0.$$

Therefore, over the bounded interval $[0, t_1)$, $F_1(t)$ is bounded. This is a contradiction, completing the proof.

### 8.3.2 Stability of equilibrium points

When $\theta = \eta = 0$, i.e., there is no infected inflow into the prison system, the disease-free equilibrium, in this case, is given by $P_0 = \left(\frac{A}{\mu}, 0, 0, 0\right)$. $R_0$ is obtained using the next-generation matrix method [25]. Thus, the matrices $\mathcal{F}$ and $\mathcal{M}$ are given by

$$\mathcal{F} = \begin{pmatrix} \frac{\beta SI}{1+bI} \\ 0 \\ 0 \end{pmatrix},$$

and

$$\mathcal{M} = \begin{pmatrix} -(1-p)rI - \sigma L + (k+\alpha+\mu)E \\ -kE + (\mu + r + \delta)I \\ -prI - \alpha E + (\mu+\sigma)L \end{pmatrix}.$$



Then we obtain

$$R_0 = \frac{k\beta\Lambda(\mu+\sigma)}{\mu\left(\mu\left(r+\delta+\mu\right)\left(\alpha+\mu+\sigma\right) + k\left(pr\mu + \left(\delta+\mu\right)\left(\mu+\sigma\right)\right)\right)}. \tag{8.2}$$

**Theorem 8.3.3.** *The disease-free equilibrium point $P_0^*$ of the system (8.1) is globally asymptotically stable in $\Omega$ if $R_0 \leq 1$.*

***Proof***: Let's define the function,$T(E, I, L)$, as follows

$$T(E, I, L) = (\mu+\sigma)E(t) + \frac{k(\mu+\sigma) + \mu(\alpha+\mu+\sigma)}{k} I(t) + \sigma L(t). \tag{8.3}$$

It is clear that $T$ is non-negative and $T(P_0^*) = 0$. Calculating the derivative of $T(t)$,

we obtain:

$$\begin{aligned}\dot{T} &= (\mu+\sigma)\,\dot{E} + \frac{k(\mu+\sigma)+\mu(\alpha+\mu+\sigma)}{k}\dot{I} + \sigma\dot{L},\\ &= (\mu+\sigma)\left[\frac{(1-\varepsilon+\theta\varepsilon)\,\beta SI}{1+bI} + (1-p)rI + \sigma L - (k+\alpha+\mu)\,E\right]\\ &+ \frac{k\,(\mu+\sigma)+\mu\,(\alpha+\mu+\sigma)}{k}\left\{kE-(\mu+r+\delta)\,I\right\} + \sigma\left\{prI+\alpha E-(\mu+\sigma)\,L\right\}.\end{aligned}$$

Using $S(t) \leq \frac{\Lambda}{\mu}$ and after simplification, we have

$$\dot{T} \leq \frac{\mu\,(r+\delta+\mu)\,(\alpha+\mu+\sigma)+k\,(pr\mu+(\delta+\mu)\,(\mu+\sigma))}{k}\,[R_0-1]\,I.$$

This implies that the largest compact invariant subset of $\{(S(t),E(t),I(t),L(t)) \in \Omega$: $\dot{T}=0\}$ is the singleton $P_0^*$. LaSalle's invariant principle [87] shows that $P_0^*$ is globally asymptotically stable in $\Omega$.

### 8.3.3 Existence of the endemic equilibrium point

**Theorem 8.3.4.** *If $R_0 > 1$, then the system (8.1) has a unique endemic equilibrium point.*

***Proof.*** the endemic equilibrium point of the system (8.1) satisfies the following system of algebraic Equations

$$\begin{cases} 0 = (1 - (\theta + \eta))\,A - \beta SI - \mu S,\\ 0 = \theta\Lambda + \beta SI + (1-p)rI + \sigma L - (k+\alpha+\mu)E,\\ 0 = \eta\Lambda + kE - (\mu+r+\delta)\,I,\\ 0 = prI + \alpha E - (\mu+\sigma)\,L. \end{cases} \tag{8.4}$$

Solving for $S^*$ from the first Equation in (8.4), we obtain

$$S^* = \frac{[1-(\eta+\theta)]\,\Lambda}{\beta I^* + \mu}. \tag{8.5}$$

Solving for $L^*$ from the last Equation in (8.4), we obtain

$$L^* = \frac{\alpha E^* + prI^*}{\mu+\sigma}. \tag{8.6}$$

Substituting $S^*$ and $L^*$ into the second Equation in (8.4) and solving for $E^*$, we obtain

$$E^* = \frac{rI^* \left(\beta I^* + \mu\right) \left[(1-p)\,\mu + \sigma\right] + \Lambda \left[\beta \left(1-\eta\right) I^* + \theta\mu\right] \left(\mu + \sigma\right)}{\left(\beta I^* + \mu\right) \left(k \left(\mu + \sigma\right) + \mu \left(\alpha + \mu + \sigma\right)\right)}. \tag{8.7}$$

Substituting $E^*$ into the third Equation in (8.4), we obtain

$$\begin{aligned} &\left[\eta\Lambda - I^* \left(r + \delta + \mu\right)\right] \left[\left(\beta I^* + \mu\right) \left(k \left(\mu + \sigma\right) + \mu \left(\alpha + \mu + \sigma\right)\right)\right] \\ &- \left[k \left(rI^* \left(\beta I^* + \mu\right) \left(\left(-1 + p\right)\mu - \sigma\right) + \Lambda \left(\beta \left(-1 + \eta\right) I^* - \theta\mu\right) \left(\mu + \sigma\right)\right)\right] = 0. \end{aligned} \tag{8.8}$$

Then, we get a quadratic Equation for $I^*$

$$AI^{*2} + BI^* + C = 0, \tag{8.9}$$

where

$$\begin{aligned} A &= -\beta \left[\mu \left(r + \delta + \mu\right) \left(\alpha + \mu + \sigma\right) + k \left(pr\mu + \left(\delta + \mu\right) \left(\mu + \sigma\right)\right)\right], \\ B &= \mu\beta\eta\Lambda \left(\alpha + \mu + \sigma\right) + \mu \left\{\mu \left(r + \delta + \mu\right) \left(\alpha + \mu + \sigma\right) + k \left(pr\mu + \left(\delta + \mu\right) \left(\mu + \sigma\right)\right)\right\} \left[R_0 - 1\right], \\ C &= \Lambda\mu \left(k \left(\eta + \theta\right) \left(\mu + \sigma\right) + \eta\mu \left(\alpha + \mu + \sigma\right)\right). \end{aligned}$$

Noting that $A$ is negative and $C$ is positive, then $AC < 0$ is negative. Similarly for $R_0 > 1$, $B$ is positive and $AB < 0$. Hence, by Descartes' Rule of Signs, there is exactly one positive real root to Equation (8.9).



## 8.4 Numerical values of variables and parameters of the model

This section estimates the value of the model's parameters and variables using epidemiological and demographic data from Ethiopia.

i According to a report by World Prison Brief (WPB) [136], in Ethiopia, an average of 16506 new suspects are incarcerated each year. Hence, taking $\Lambda$ =16506 is possible.

ii The total number of prisoners in Ethiopia in 2000 was 55209 [136]. Based on this, we can take the initial total population of our model as $N_0 = 55209$.

iii In the absence of the disease in the system, $\frac{\Lambda}{\mu}$ will be the total population. Hence

it is possible to take $\mu = \frac{\Lambda}{N} = 0.299$.

iv Generally, the prevalence of TB in Sub-Saharan African prisons is 6 to 30 times higher than in the general population [137]. The average Zambian prisoner, for example, is ten times more likely to develop TB than an individual in the free population [138]. In the case of Ethiopia, it would be plausible to assume that the transmission rate of TB in prisons is ten times greater than the general population. Hence, by taking the transmission rate of TB in the general population in Ethiopia from [105], we have $\beta = 1.646 \times 10^{-6}$.

v Prevalence studies from Ethiopian prisons suggest that the prevalence of TB among prisoners is 8.33 [139]. Hence, using this value, and with the initial total population $N_0$ =55209, we estimated $I_0 = 4599$.

vi In the paper [102], it is estimated that out of the total population in Ethiopia, 16.37% and 30% are latently TB infected at high risk and low risk, respectively. Hence, we estimated $E_0 = 9038$ and $L_0 = 16563$.

vii Then, the initial number of susceptible populations is estimated as $S_0 = N_0 - E_0 - I_0 - L_0 = 25009$.

viii The values of $\theta$ and $\eta$ can be taken as the ratio of $E$ and $I$ to the entire population, respectively [79]. Thus, we have $\theta = 0.164$ and $\eta = 0.083$.

## 8.5 Numerical results and discussion

We conducted a numerical simulation to investigate the impact of infective inflows quantitatively. This simulation uses real Ethiopian data, and the parameter values are presented in Table 8.1.

We first evaluate the system's dynamics without the inflow of infectives, and the curves are shown in Figure 8.2. Then, Figure 8.3 shows the system simulation with the inflow of infectives. Figure 8.4 shows the effect of the inflow of infectious individuals. From this figure, we can see that as the rate of flow of infective decreases, the number of infected individuals decreases significantly. A further simulation demonstrates that the disease-free equilibrium point $P_0^*$ is globally asymptotically stable for $R_0$ less than one (see Figure 8.5). That is, Theorem 8.3.3 holds in general.

Table 8.1: Values of the model variables and parameters

| **Variables** | **Description** | **Initial value** | **Sources** |
|---|---|---|---|
| $N_0$ | Initial total population | 67574 | [136] |
| $S_0$ | Susceptible | 35374 | Estimated |
| $E_0$ | High-risk latent | 9038 | [102] |
| $I_0$ | Infected | 4599 | [139] |
| $L_0$ | Low-risk latent | 16563 | [102] |
| **Parameters** | **Description** | **Value** | **Sources** |
| $\Lambda$ | Recruitment rate into the prison | 16506 | [136] |
| $\beta$ | Transmission rate | $1.646 \times 10^{-6}$ | [105, 138] |
| $\mu$ | The removal rate | 0.299 | Estimated |
| $k$ | Rate of moving from $E$ to $I$ | 0.023 | [105] |
| $r$ | Treatment rate of $I$ | 0.546 | [102] |
| $p$ | The treatment success rate of $I$ | 0.832 | [124] |
| $\alpha$ | Treatment rate of $E$ | 0.153 | [105] |
| $\delta$ | TB induced deaths rate | 0.17 | [14] |
| $\sigma$ | The relapse rate | 0.0013 | [102] |
| $\theta$ | Recruitment rate into $E$ | 0.164 | [79] |
| $\eta$ | Recruitment rate into $I$ | 0.083 | [79] |

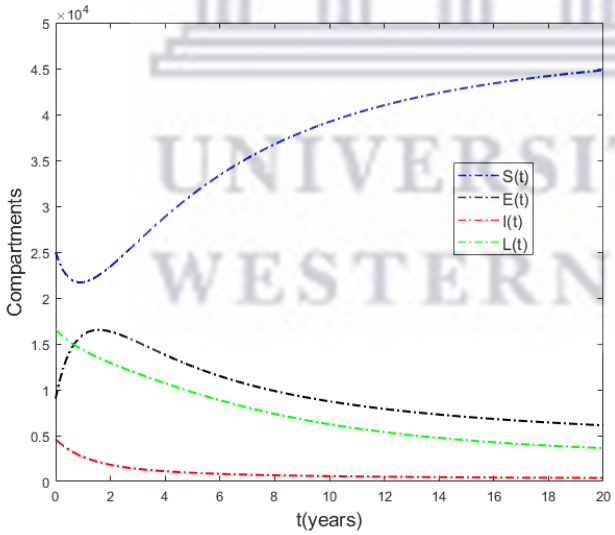


Figure 8.2: Prison population in different classes without the inflow of infectives and $R_0 = 1.128$.

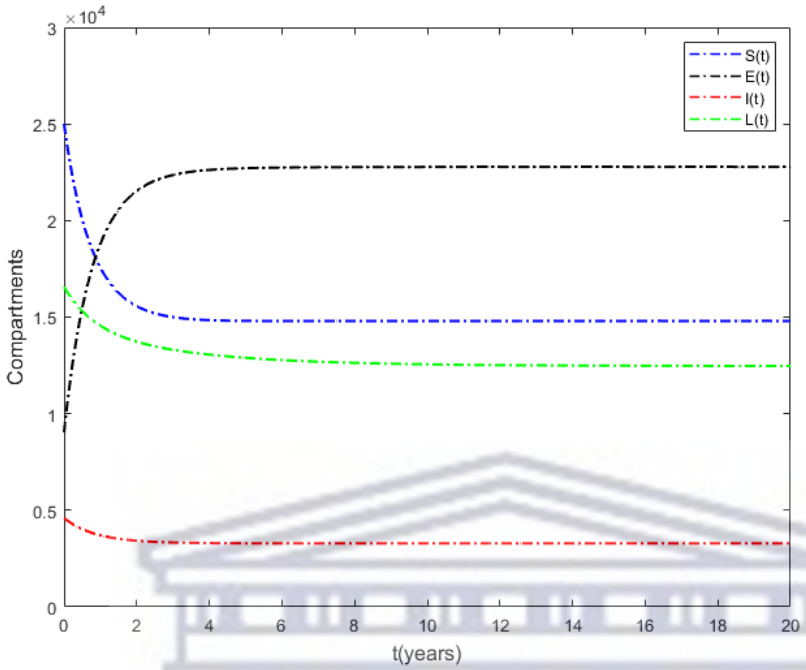


Figure 8.3: Prison population in different classes with the inflow of infectives $\theta = 0.164$ and $\eta = 0.083$ and $R_0 = 1.128$.

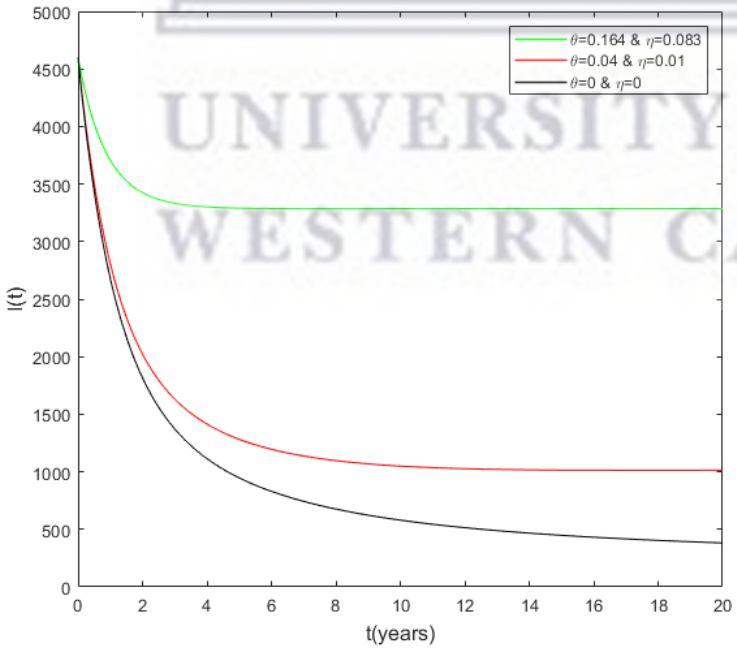


Figure 8.4: Comparison of Infective classes with different values of inflow of infectives.

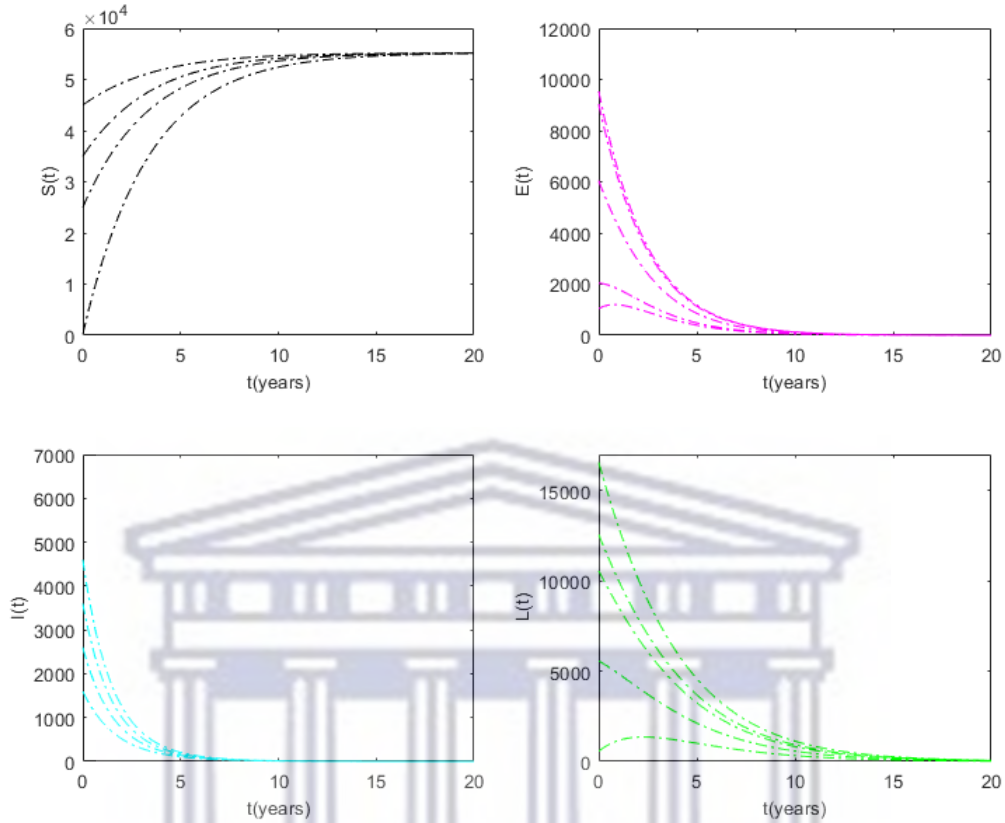


Figure 8.5: The stability of the DFE for the model (8.1) when $R_0 = 0.01$.



## 8.6 Conclusions

In this chapter, we developed a mathematical model for the spread of TB disease in the prison system. In addition to the inflow of healthy people into the susceptible class, we developed the model by considering the influx of infected individuals to high-risk latent and infected compartments. We estimated most of the model variables and parameters using Ethiopian prison health data, and the rest are taken from the literature.

We demonstrated the stability of the disease-free equilibrium point ($P_0^*$) using the basic reproduction number $R_0$. In the case of an absence of the infected individual and without the inflow of infected individuals into the prison, we found that $P_0^*$ is globally asymptotically stable when $R_0 < 1$ whereas, at $R_0 > 1$ it becomes unstable. However, we found a unique endemic equilibrium point when infected individuals inflow into the prison population, or for $R_0 > 1$. Moreover, it was found that if there is no inflow of infected inmates at a particular prison site, then the disease will be eliminated from the

prison provided that the numerical value of $R_0$ is below unity.

The numerical analysis of the model showed that the inflow of TB-infected individuals into the prison significantly increases the disease's spread. Therefore, eliminating the disease is impossible if there is an influx of latently infected (exposed) and infectious individuals into the prison. Based on our findings, we recommend that inmates be screened for tuberculosis before entering the prison. In addition, in prisons, the health status of inmates should be monitored regularly, and inmates diagnosed with tuberculosis should be treated separately.

# Chapter 9

# Conclusions and Future Work

## 9.1 Conclusions

This thesis presents four different nonlinear deterministic models that describe the transmission dynamics of tuberculosis. These models have been calibrated using reported TB-infected cases in Ethiopia from 2003 to 2017. In the given period, the basic reproduction number is estimated to be 2.13, indicating the disease's persistence.

Bacillus Calmette-Guerin (BCG) is the most widely administered vaccine and is usually given to newborns as part of their routine immunization schedule [140]. Hence, in this thesis, we develop and analyze a mathematical model for tuberculosis transmission dynamics by incorporating vaccination for newborns and treatment for TB patients. Our results quantify the positive influence of vaccination and the treatment of TB patients on tuberculosis control.

We derived and analyzed a deterministic model for the transmission of TB with vaccination and saturated incidence rate. The model is illustrated using parameters applicable to Ethiopia. Analysis of sensitivity indices for $R_0$ revealed that the transmission rate has a greater impact on TB spread in Ethiopia compared to other parameters. This finding aligns with the conclusions drawn in reference [141–143]. Towards curbing the spread of TB-disease, according to the model (4.1), the treatment rate for the latently infected shows higher sensitivity than the treatment rate for the active TB infectives. These observations are of course very useful for public health management.

The control study also revealed some very useful insights. It was observed that to effectively manage DS-TB disease in a cost-efficient manner, the Ethiopian government

should prioritize preventive measures such as isolating infectious individuals, early detection and treatment of TB patients, and implementing educational programs.

We have further considered an optimal control problem for the transmission dynamics of MDR-TB in Ethiopia. We found that the most cost-effective strategy to prevent the spread of drug-resistant TB is the successful treatment of DS-TB. This finding aligns with the result in [144] .

Finally, we propose a deterministic mathematical model to analyze the dynamics of TB disease in prison populations. The model includes the inflow of exposed and TB infective inmates. It is shown that the disease-free equilibrium point exists only when there is no inflow of infected into the prison population. We show that the model has a unique endemic equilibrium point. The model parameters are calibrated based on the epidemiological data of Ethiopia. Our findings show that inmates' health status should be monitored regularly, and those diagnosed with tuberculosis must be separated from the rest and treated.

## 9.2 Future Work

Our models do not consider some of the factors and approaches listed below that might affect the spread of tuberculosis. These factors may provide a better understanding of the disease and its control.

**Co-infection**: The impact of co-infection in infectious disease dynamics is undeniable today. This will allow us to study the dynamics of tuberculosis and HIV/AIDS co-infection in Ethiopia.

**Stochastic approach**: Stochasticity in the real world can be incorporated into ODE models by introducing stochastic perturbations. This means that ODEs can be replaced with stochastic differential Equations. It has been shown, for instance, how certain stochastic perturbations can enhance the stability of differential equations (e.g. [37, 85, 145, 146]). Therefore, it will be important to see the extent to which this phenomenon features in the models of this dissertation.

**Fractional order model**: The formulation of the fractional order model of tuberculosis is one of the factors that will be considered in future research. This is planned to determine which of the fractional and integer order models better describes the dynamics of TB.

# References


[1] J. B. Torrelles and L. S. Schlesinger, "Integrating lung physiology, immunology, and tuberculosis," *Trends in microbiology*, vol. 25, no. 8, pp. 688–697, 2017.

[2] P. Thorn, "Overcoming tuberculosis: A handbook for patients," *Geneva: Stop TB Partnership*, 2007.

[3] E. Michael and R. C. Spear, *Modelling parasite transmission and control*, vol. 673. Springer Science & Business Media, 2010.

[4] A. Cohen, V. D. Mathiasen, T. Schon, and C. Wejse, "The global prevalence of latent tuberculosis: a systematic review and meta-analysis," *European Respiratory Journal*, vol. 54, no. 3, 2019.

[5] B. Gore and K. Smith, "Tuberculosis infection control: a practical manual for preventing TB, 2011," *San Francisco (CA)*, vol. 16, 2011.

[6] Cedars, "Tuberculosis (TB)." https://www.cedars-sinai.org/health-library/diseases-and-conditions/t/tuberculosis-tb.html#:~:text=The%20stages%20of%20TB%20are%3A%201%20Exposure.%20This,%20symptoms%20of%20an%20active%20TB%20infection.%20, 2022.

[7] CDC, "Drug-resistant TB." https://www.cdc.gov/tb/topic/drtb/default.htm, 2022.

[8] M. Akl and A. Mahalli, "Drug resistant tuberculosis: Risk factors and resources-utilization at a chest disease clinic, Alexandria, Egypt," *J Am Sci*, vol. 8.

[9] J. Caminero, "Multidrug-resistant tuberculosis: epidemiology, risk factors and case finding," *The International Journal of Tuberculosis and Lung Disease*, vol. 14, no. 4, pp. 382–390, 2010.

[10] R. Prasad, N. Gupta, and A. Banka, "Multidrug-resistant tuberculosis/rifampicin-resistant tuberculosis: Principles of management," *Lung India: official organ of Indian chest society*, vol. 35, no. 1, p. 78, 2018.

[11] WHO, "Global tuberculosis report." https://www.who.int/teams/global-tuberculosis-programme/tb-reports/global-tuberculosis-report-2022, 2022.

[12] WHO, "Global tuberculosis report." https://www.who.int/publications/i/item/9789240037021, 2021.

[13] CDC, "Traveler's health Ethiopia." https://www.cdc.gov/globalhealth/countries/ethiopia/pdf/Ethiopia_Factsheet-p.pdf., 2018.

[14] WHO, "Global tuberculosis report." https://www.who.int/tb/publications/global_report/gtbr2018_main_text_28Feb2019.pdf, 2018.

[15] Q. Lin, S. Zhao, D. Gao, Y. Lou, S. Yang, S. Musa, M. Wang, Y. Cai, W. Wang, L. Yang, *et al.*, "A conceptual model for the outbreak of coronavirus disease 2019 (COVID-19) inwuhan, China with individual reaction and governmental action," *International journal of infectious diseases*, 2020.

[16] F. P. Rocha, H. S. Rodrigues, M. T. T. Monteiro, and D. F. Torres, "Coexistence of two dengue virus serotypes and forecasting for Madeira Island," *Operations Research for Health Care*, vol. 7, pp. 122–131, 2015.

[17] S. Choi and E. Jung, "Optimal tuberculosis prevention and control strategy from a mathematical model based on real data," *Bulletin of mathematical biology*, vol. 76, no. 7, pp. 1566–1589, 2014.

[18] D. Kereyu and S. Demie, "Transmission dynamics model of tuberculosis with optimal control strategies in Haramaya district, Ethiopia," *Advances in Difference Equations*, vol. 2021, no. 1, pp. 1–22, 2021.

[19] S. Kim, A. Aurelio, and E. Jung, "Mathematical model and intervention strategies for mitigating tuberculosis in the Philippines," *Journal of theoretical biology*, vol. 443, pp. 100–112, 2018.

[20] S. Ullah, M. A. Khan, M. Farooq, and T. Gul, "Modeling and analysis of tuberculosis (TB) in Khyber Pakhtunkhwa, Pakistan," *Mathematics and Computers in Simulation*, vol. 165, pp. 181–199, 2019.

[21] D. P. Moualeu, M. Weiser, R. Ehrig, and P. Deuflhard, "Optimal control for a tuberculosis model with undetected cases in Cameroon," *Communications in Nonlinear Science and Numerical Simulation*, vol. 20, no. 3, pp. 986–1003, 2015.

[22] H. Waaler, A. Geser, and S. Andersen, "The use of mathematical models in the study of the epidemiology of tuberculosis," *American Journal of Public Health and the Nations Health*, vol. 52, no. 6, pp. 1002–1013, 1962.

[23] U. D. Purwati, F. Riyudha, H. Tasman, *et al.*, "Optimal control of a discrete age-structured model for tuberculosis transmission," *Heliyon*, vol. 6, no. 1, p. e03030, 2020.

[24] S. Lee, H.-Y. Park, H. Ryu, and J.-W. Kwon, "Age-specific mathematical model for tuberculosis transmission dynamics in South Korea," *Mathematics*, vol. 9, no. 8, p. 804, 2021.

[25] Y. Zhao, M. Li, and S. Yuan, "Analysis of transmission and control of tuberculosis in Mainland China, 2005–2016, based on the age-structure mathematical model," *International journal of environmental research and public health*, vol. 14, no. 10, p. 1192, 2017.

[26] Y. Yang, S. Tang, X. Ren, H. Zhao, and C. Guo, "Global stability and optimal control for a tuberculosis model with vaccination and treatment," *Discrete & Continuous Dynamical Systems-B*, vol. 21, no. 3, p. 1009, 2016.

[27] L. N. Nkamba, T. T. Manga, F. Agouanet, and M. L. Mann Manyombe, "Mathematical model to assess vaccination and effective contact rate impact in the spread of tuberculosis," *Journal of Biological Dynamics*, vol. 13, no. 1, pp. 26–42, 2019.

[28] D. Aldila, Z. A. S. Ryanto, and A. Bustamam, "A mathematical model of TB control with vaccination in an age-structured susceptible population," in *Journal of Physics: Conference Series*, vol. 1108, p. 012050, IOP Publishing, 2018.

[29] R. Naresh, D. Sharma, and A. Tripathi, "Modelling the effect of tuberculosis on the spread of HIV infection in a population with density-dependent birth and death rate," *Mathematical and computer Modelling*, vol. 50, no. 7-8, pp. 1154–1166, 2009.

[30] T. D. Awoke and S. M. Kassa, "Optimal control strategy for TB-HIV/AIDS co-infection model in the presence of behaviour modification," *Processes*, vol. 6, no. 5, p. 48, 2018.

[31] A. Mallela, S. Lenhart, and N. K. Vaidya, "HIV–TB co-infection treatment: Modeling and optimal control theory perspectives," *Journal of Computational and Applied Mathematics*, vol. 307, pp. 143–161, 2016.

[32] Y. Liu, Z. Sun, G. Sun, Q. Zhong, L. Jiang, L. Zhou, Y. Qiao, and Z. Jia, "Modeling transmission of tuberculosis with MDR and undetected cases," *Discrete Dynamics in Nature and Society*, vol. 2011, 2011.

[33] M. A. Kuddus, M. T. Meehan, L. J. White, E. S. McBryde, and A. I. Adekunle, "Modeling drug-resistant tuberculosis amplification rates and intervention strategies in Bangladesh," *Plos one*, vol. 15, no. 7, p. e0236112, 2020.

[34] J. M. Trauer, J. T. Denholm, and E. S. McBryde, "Construction of a mathematical model for tuberculosis transmission in highly endemic regions of the Asia-Pacific," *Journal of theoretical biology*, vol. 358, pp. 74–84, 2014.

[35] Z.-W. Jia, G.-Y. Tang, Z. Jin, C. Dye, S. J. Vlas, X.-W. Li, D. Feng, L.-Q. Fang, W.-J. Zhao, and W.-C. Cao, "Modeling the impact of immigration on the epidemiology of tuberculosis," *Theoretical population biology*, vol. 73, no. 3, pp. 437–448, 2008.

[36] H. Guo and J. Wu, "Persistent high incidence of tuberculosis among immigrants in a low-incidence country: impact of immigrants with early or late latency," *Mathematical Biosciences & Engineering*, vol. 8, no. 3, p. 695, 2011.

[37] S. Maku Vyambwera and P. Witbooi, "A stochastic TB model for a crowded environment," *Journal of Applied Mathematics*, vol. 2018, 2018.

[38] B. Buonomo and D. Lacitignola, "Analysis of a tuberculosis model with a case study in Uganda," *Journal of Biological Dynamics*, vol. 4, no. 6, pp. 571–593, 2010.

[39] D. Shaweno, J. M. Trauer, J. T. Denholm, and E. S. McBryde, "The role of geospatial hotspots in the spatial spread of tuberculosis in rural ethiopia: a mathematical model," *Royal Society Open Science*, vol. 5, no. 9, p. 180887, 2018.

[40] S. Sintayehu, *Modeling the Transmission of Drug Resistant Tuberculosis in Ethiopia.* PhD thesis, Master Thesis, Addis Ababa University, Addis Ababa, Ethiopia, 2013.

[41] S. Banerjee, *Mathematical modeling: models, analysis and applications.* Chapman and Hall/CRC, 2021.

[42] M. Y. Li, *An introduction to mathematical modeling of infectious diseases*, vol. 2. Springer, 2018.

[43] Y. Sabbar, *Mathematical Analysis of Some Stochastic Infectious Disease Models with White Noises and Lévy Jumps.* PhD thesis, Université Sidi Mohamed Ben Abdellah de Fès (Maroc), 2021.

[44] G. Birkhoff and G.-C. Rota, *Ordinary Differential Equations.* John Wiley and Sons, 1989.

[45] B. B. Gerstman, *Epidemiology kept simple: an introduction to traditional and modern epidemiology.* John Wiley & Sons, 2013.

[46] O. Diekmann and J. A. P. Heesterbeek, *Mathematical epidemiology of infectious diseases: model building, analysis and interpretation*, vol. 5. John Wiley & Sons, 2000.

[47] K. Okosun, *Mathematical epidemiology of Malaria disease transmission and its optimal control analyses.* PhD thesis, University of the Western Cape, South Africa, 2010.

[48] P. Van den Driessche and J. Watmough, "Reproduction numbers and sub-threshold endemic equilibria for compartmental models of disease transmission," *Mathematical Biosciences*, vol. 180, no. 1-2, pp. 29–48, 2002.

[49] O. Diekmann, J. A. P. Heesterbeek, and J. A. Metz, "On the definition and the computation of the basic reproduction ratio R0 in models for infectious diseases in heterogeneous populations," *Journal of Mathematical Biology*, vol. 28, no. 4, pp. 365–382, 1990.

[50] H. J. Marquez, *Nonlinear control systems: analysis and design*, vol. 161. John Wiley Hoboken^ eN. JNJ, 2003.

[51] D. Arrowsmith and C. M. Place, *Dynamical systems: differential equations, maps, and chaotic behaviour*, vol. 5. CRC Press, 1992.

[52] L. J. Allen, *Introduction to mathematical biology*. Pearson/Prentice Hall, 2007.

[53] W. Hahn *et al.*, *Stability of motion*, vol. 138. Springer, 1967.

[54] C. Chicone, *Ordinary Differential Equations with Applications*. Springer New York, NY, 1999.

[55] J. LaSalle, "Some extensions of Liapunov's second method," *IRE Transactions on circuit theory*, vol. 7, no. 4, pp. 520–527, 1960.

[56] N. Krasovskii, "Problems in the theory of stability of motion, Moscow: Gosudarstv," *Izdat. Fiz.-Mat. Lit*, 1959.

[57] A. Saltelli, M. Ratto, T. Andres, F. Campolongo, J. Cariboni, D. Gatelli, M. Saisana, and S. Tarantola, *Global sensitivity analysis: the primer*. John Wiley & Sons, 2008.

[58] M. G. Buhnerkempe, R. J. Eisen, B. Goodell, K. L. Gage, M. F. Antolin, and C. T. Webb, "Transmission shifts underlie variability in population responses to yersinia pestis infection," *PloS one*, vol. 6, no. 7, p. e22498, 2011.

[59] N. Chitnis, J. M. Hyman, and J. M. Cushing, "Determining important parameters in the spread of malaria through the sensitivity analysis of a mathematical model," *Bulletin of mathematical biology*, vol. 70, pp. 1272–1296, 2008.

[60] R. G. McLeod, J. F. Brewster, A. B. Gumel, and A. Slonowsky, "Sensitivity and uncertainty analyses for a sars model with time-varying inputs and outputs," *Mathematical Biosciences and Engineering*, vol. 3, no. 3, p. 527, 2006.

[61] D. A. Rand, "Mapping global sensitivity of cellular network dynamics: sensitivity heat maps and a global summation law," *Journal of The Royal Society Interface*, vol. 5, no. suppl_1, pp. S59–S69, 2008.

[62] S. Marino, I. B. Hogue, C. J. Ray, and D. E. Kirschner, "A methodology for performing global uncertainty and sensitivity analysis in systems biology," *Journal of theoretical biology*, vol. 254, no. 1, pp. 178–196, 2008.

[63] D. M. Hamby, "A review of techniques for parameter sensitivity analysis of environmental models," *Environmental monitoring and assessment*, vol. 32, pp. 135–154, 1994.

[64] J. Yang, "Convergence and uncertainty analyses in monte-carlo based sensitivity analysis," *Environmental Modelling & Software*, vol. 26, no. 4, pp. 444–457, 2011.

[65] J. Wu, R. Dhingra, M. Gambhir, and J. V. Remais, "Sensitivity analysis of infectious disease models: methods, advances and their application," *Journal of The Royal Society Interface*, vol. 10, no. 86, p. 20121018, 2013.

[66] S. Gubbins, S. Carpenter, M. Baylis, J. L. Wood, and P. S. Mellor, "Assessing the risk of bluetongue to uk livestock: uncertainty and sensitivity analyses of a temperature-dependent model for the basic reproduction number," *Journal of the Royal Society Interface*, vol. 5, no. 20, pp. 363–371, 2008.

[67] S. M. Blower and H. Dowlatabadi, "Sensitivity and uncertainty analysis of complex models of disease transmission: an hiv model, as an example," *International Statistical Review/Revue Internationale de Statistique*, pp. 229–243, 1994.

[68] M. D. Morris, "Factorial sampling plans for preliminary computational experiments," *Technometrics*, vol. 33, no. 2, pp. 161–174, 1991.

[69] F. Campolongo, J. Cariboni, and A. Saltelli, "An effective screening design for sensitivity analysis of large models," *Environmental modelling & software*, vol. 22, no. 10, pp. 1509–1518, 2007.

[70] A. Saltelli, S. Tarantola, F. Campolongo, M. Ratto, *et al.*, *Sensitivity analysis in practice: a guide to assessing scientific models*, vol. 1. Wiley Online Library, 2004.

[71] J. C. Helton, R. L. Iman, and J. B. Brown, "Sensitivity analysis of the asymptotic behavior of a model for the environmental movement of radionuclides," *Ecological modelling*, vol. 28, no. 4, pp. 243–278, 1985.

[72] M. D. McKay, R. J. Beckman, and W. J. Conover, "A comparison of three methods for selecting values of input variables in the analysis of output from a computer code," *Technometrics*, vol. 42, no. 1, pp. 55–61, 2000.

[73] J. C. Helton and F. J. Davis, "Latin hypercube sampling and the propagation of uncertainty in analyses of complex systems," *Reliability Engineering & System Safety*, vol. 81, no. 1, pp. 23–69, 2003.

[74] I. M. Sobol, "Global sensitivity indices for nonlinear mathematical models and their monte carlo estimates," *Mathematics and computers in simulation*, vol. 55, no. 1-3, pp. 271–280, 2001.

[75] M. Domijan and D. A. Rand, "Balance equations can buffer noisy and sustained environmental perturbations of circadian clocks," *Interface Focus*, vol. 1, no. 1, pp. 177–186, 2011.

[76] W. H. Fleming and R. W. Rishel, *Deterministic and stochastic optimal control*, vol. 1. Springer Science & Business Media, 2012.

[77] L. S. Pontryagin, *Mathematical theory of optimal processes*. CRC press, 1987.

[78] R. M. Neilan and S. Lenhart, "An introduction to optimal control with an application in disease modeling.," in *Modeling paradigms and analysis of disease trasmission models*, pp. 67–81, 2010.

[79] P. Witbooi and S. M. Vyambwera, "A model of population dynamics of TB in a prison system and application to South Africa," *BMC research notes*, vol. 10, no. 1, pp. 1–8, 2017.

[80] A. Ssematimba, J. Mugisha, and L. Luboobi, "Mathematical models for the dynamics of tuberculosis in density-dependent populations: The case of internally displaced peoples' camps (IDPCS) in Uganda," *Journal of Mathematics and Statistics*, vol. 1, no. 3, pp. 217–224, 2005.

[81] S. Athithan and M. Ghosh, "Mathematical modelling of TB with the effects of case detection and treatment," *International Journal of Dynamics and Control*, vol. 1, no. 3, pp. 223–230, 2013.

[82] I. M. Wangari, J. Trauer, and L. Stone, "Modelling heterogeneity in host susceptibility to tuberculosis and its effect on public health interventions," *PloS one*, vol. 13, no. 11, p. e0206603, 2018.

[83] G. A. Colditz, T. F. Brewer, C. S. Berkey, M. E. Wilson, E. Burdick, H. V. Fineberg, and F. Mosteller, "Efficacy of BCG vaccine in the prevention of tuberculosis: meta-analysis of the published literature," *Jama*, vol. 271, no. 9, pp. 698–702, 1994.

[84] H. M. Yang, "The basic reproduction number obtained from Jacobian and next generation matrices–A case study of dengue transmission modelling," *Biosystems*, vol. 126, pp. 52–75, 2014.

[85] P. Witbooi, "Stability of a stochastic model of an SIR epidemic with vaccination," *Acta Biotheoretica*, vol. 65, no. 2, pp. 151–165, 2017.

[86] P. J. Witbooi, "An SEIRS epidemic model with stochastic transmission," *Advances in Difference Equations*, vol. 2017, no. 1, pp. 1–16, 2017.

[87] J. P. La Salle, *The stability of dynamical systems*. Society for Industrial and Applied Mathematics, 1976.

[88] World-Bank, "Life expectancy at Birth." https://data.worldbank.org/indicator/SP.DYN.LE00.FE.IN?end=2018&name_desc=false&start=2018&view=map, 2018.

[89] WHO, "WHO TB burden estimates." https://www.who.int/tb/country/data/download/en/, 2018.

[90] WHO, "WHO vaccine-preventable diseases: monitoring system. 2019 global summary." https://apps.who.int/immunization_monitoring/globalsummary/estimates?c=ETH, 2019.

[91] WHO, "Treatment success data by country." http://apps.who.int/gho/data/node.main.602?lang=en, 2018.

[92] R. Xu and Z. Ma, "Global stability of a delayed SEIRS epidemic model with saturation incidence rate," *Nonlinear Dynamics*, vol. 61, no. 1-2, pp. 229–239, 2010.

[93] M. E. Alexander and S. M. Moghadas, "Bifurcation analysis of an SIRS epidemic model with generalized incidence," *SIAM Journal on Applied Mathematics*, vol. 65, no. 5, pp. 1794–1816, 2005.

[94] V. Capasso and G. Serio, "A generalization of the Kermack-McKendrick deterministic epidemic model," *Mathematical biosciences*, vol. 42, no. 1-2, pp. 43–61, 1978.

[95] M. Gomes, A. Margheri, G. Medley, and C. Rebelo, "Dynamical behaviour of epidemiological models with sub-optimal immunity and nonlinear incidence," *Journal of mathematical biology*, vol. 51, pp. 414–430, 2005.

[96] L.-M. Cai, X.-Z. Li, and M. Ghosh, "Global stability of a stage-structured epidemic model with a nonlinear incidence," *Applied Mathematics and Computation*, vol. 214, no. 1, pp. 73–82, 2009.

[97] H. Zhang, L. Yingqi, and W. Xu, "Global stability of an SEIS epidemic model with general saturation incidence," *International Scholarly Research Notices*, vol. 2013, 2013.

[98] G. P. Sahu and J. Dhar, "Analysis of an SVEIS epidemic model with partial temporary immunity and saturation incidence rate," *Applied Mathematical Modelling*, vol. 36, no. 3, pp. 908–923, 2012.

[99] I. A. Baba, R. A. Abdulkadir, and P. Esmaili, "Analysis of tuberculosis model with saturated incidence rate and optimal control," *Physica A: Statistical Mechanics and its Applications*, vol. 540, p. 123237, 2020.

[100] T. K. Kar and S. Jana, "A theoretical study on mathematical modelling of an infectious disease with application of optimal control," *Biosystems*, vol. 111, no. 1, pp. 37–50, 2013.

[101] P. Van den Driessche, "Reproduction numbers of infectious disease models," *Infectious Disease Modelling*, vol. 2, no. 3, pp. 288–303, 2017.

[102] A. Kelemu Mengistu and P. J. Witbooi, "Modeling the effects of vaccination and treatment on tuberculosis transmission dynamics," *Journal of Applied Mathematics*, vol. 2019, 2019.

[103] C. Bhunu, S. Mushayabasa, and J. Tchuenche, "A theoretical assessment of the effects of smoking on the transmission dynamics of tuberculosis," *Bulletin of mathematical biology*, vol. 73, no. 6, pp. 1333–1357, 2011.

[104] Z. S. Kifle and L. L. Obsu, "Mathematical modeling for COVID-19 transmission dynamics: A case study in Ethiopia," *Results in Physics*, vol. 34, p. 105191, 2022.

[105] A. K. Mengistu and P. J. Witbooi, "Mathematical analysis of TB model with vaccination and saturated incidence rate," in *Abstract and Applied Analysis*, vol. 2020, Hindawi, 2020.

[106] D. La Torre, H. Kunze, M. Ruiz-Galan, T. Malik, and S. Marsiglio, "Optimal control: theory and application to science, engineering, and social sciences," in *Abstract and Applied Analysis*, vol. 2015, Hindawi, 2015.

[107] D. p. Gao and N. j. Huang, "Optimal control analysis of a tuberculosis model," *Applied Mathematical Modelling*, vol. 58, pp. 47–64, 2018.

[108] C. J. Silva and D. F. M. Torres, "Optimal control strategies for tuberculosis treatment: A case study in Angola," *Numerical Algebra, Control and Optimization*, vol. 2, no. 3, pp. 601–617.

[109] K. Hattaf, M. Rachik, S. Saadi, Y. Tabit, and N. Yousfi, "Optimal control of tuberculosis with exogenous reinfection," *Applied Mathematical Sciences*, vol. 3, no. 5, pp. 231–240, 2009.

[110] D. K. Das, S. Khajanchi, and T. K. Kar, "The impact of the media awareness and optimal strategy on the prevalence of tuberculosis," *Applied Mathematics and Computation*, vol. 366, p. 124732, 2020.

[111] K. Adnaoui, I. Elberrai, A. E. A. Laaroussi, and K. Hattaf, "A spatiotemporal SIR epidemic model two-dimensional with problem of optimal control," *Bol. Soc. Paran. Mat*, 2020.

[112] S. Lenhart and J. T. Workman, *Optimal control applied to biological models*. Chapman and Hall/CRC, 2007.

[113] L. Cesari, *Optimization—theory and applications: problems with ordinary differential equations*, vol. 17. Springer Science & Business Media, 2012.

[114] WHO, "WHO TB Burden Estimates. Global Tuberculosis Report." https://www.who.int/teams/global-tuberculosis-programme/data, 2021.

[115] S. B. Cantor and T. G. Ganiats, "Incremental cost-effectiveness analysis: the optimal strategy depends on the strategy set," *Journal of clinical epidemiology*, vol. 52, no. 6, pp. 517–522, 1999.

[116] Y. Liu, A. A. Gayle, A. Wilder-Smith, and J. Rocklöv, "The reproductive number of COVID-19 is higher compared to SARS coronavirus," *Journal of travel medicine*, 2020.

[117] Z. Hu, C. Song, C. Xu, G. Jin, Y. Chen, X. Xu, H. Ma, W. Chen, Y. Lin, Y. Zheng, *et al.*, "Clinical characteristics of 24 asymptomatic infections with COVID-19 screened among close contacts in Nanjing, China," *Science China Life Sciences*, vol. 63, pp. 706–711, 2020.

[118] C. Bhunu, "Mathematical analysis of a three-strain tuberculosis transmission model," *Applied mathematical modelling*, vol. 35, no. 9, pp. 4647–4660, 2011.

[119] S. Ullah, O. Ullah, M. A. Khan, and T. Gul, "Optimal control analysis of tuberculosis (TB) with vaccination and treatment," *The European Physical Journal Plus*, vol. 135, pp. 1–27, 2020.

[120] T. D. Keno, L. L. Obsu, and O. D. Makinde, "Modeling and optimal control analysis of malaria epidemic in the presence of temperature variability," *Asian-European Journal of Mathematics*, vol. 15, no. 01, p. 2250005, 2022.

[121] G. T. Tilahun, O. D. Makinde, and D. Malonza, "Co-dynamics of pneumonia and typhoid fever diseases with cost effective optimal control analysis," *Applied Mathematics and Computation*, vol. 316, pp. 438–459, 2018.

[122] A. K. Mengistu and P. J. Witbooi, "Tuberculosis in Ethiopia: Optimal intervention strategies and cost-effectiveness analysis," *Axioms*, vol. 11, no. 7, p. 343, 2022.

[123] K. O. Okosun, O. Rachid, and N. Marcus, "Optimal control strategies and cost-effectiveness analysis of a malaria model," *BioSystems*, vol. 111, no. 2, pp. 83–101, 2013.

[124] WHO, "Global tuberculosis report." https://www.who.int/tb/data/en/, 2020.

[125] WHO, "Global tuberculosis report 2018." https://www.who.int/tb/publications/global_report/gtbr2018_main_text_28Feb2019.pdf, 2019.

[126] WHO, "Treatment success data by country." http://apps.who.int/gho/data/node.main.602?lang=en, 2020.

[127] I. Baussano, B. G. Williams, P. Nunn, M. Beggiato, U. Fedeli, and F. Scano, "Tuberculosis incidence in prisons: a systematic review," *PLoS medicine*, vol. 7, no. 12, p. e1000381, 2010.

[128] J. O'Grady, M. Hoelscher, R. Atun, M. Bates, P. Mwaba, N. Kapata, G. Ferrara, M. Maeurer, and A. Zumla, "Tuberculosis in prisons in sub-saharan africa–the need for improved health services, surveillance and control," *Tuberculosis*, vol. 91, no. 2, pp. 173–178, 2011.

[129] Y. Merid, Y. Woldeamanuel, M. Abebe, D. Datiko, T. Hailu, G. Habtamu, G. Assefa, R. R. Kempker, H. M. Blumberg, and A. Aseffa, "High utility of active tuberculosis case finding in an Ethiopian prison," *The International Journal of Tuberculosis and Lung Disease*, vol. 22, no. 5, pp. 524–529, 2018.

[130] S. A. Mohammed, *M. tuberculosis among jail inmates of Ethiopian prisons: risk factors, molecular epidemiology and drug resistance*. PhD thesis, lmu, 2017.

[131] M. Gizachew Beza, E. Hunegnaw, and M. Tiruneh, "Prevalence and associated factors of tuberculosis in prisons settings of East Gojjam Zone, Northwest Ethiopia," *International Journal of Bacteriology*, vol. 2017, 2017.

[132] J. Chakaya, M. Khan, F. Ntoumi, E. Aklillu, R. Fatima, P. Mwaba, N. Kapata, S. Mfinanga, S. E. Hasnain, P. D. Katoto, *et al.*, "Global tuberculosis report 2020–reflections on the global TB burden, treatment and prevention efforts," *International Journal of Infectious Diseases*, vol. 113, pp. S7–S12, 2021.

[133] B. Moges, B. Amare, F. Asfaw, W. Tesfaye, M. Tiruneh, Y. Belyhun, A. Mulu, and A. Kassu, "Prevalence of smear positive pulmonary tuberculosis among prisoners in North Gondar Zone Prison, northwest Ethiopia," *BMC infectious diseases*, vol. 12, no. 1, pp. 1–7, 2012.

[134] P. J. Witbooi, "An SEIR model with infected immigrants and recovered emigrants," *Advances in Difference Equations*, vol. 2021, no. 1, pp. 1–15, 2021.

[135] P. Witbooi, G. Abiodun, and M. Nsuami, "A model of malaria population dynamics with migrants," 2021.

[136] WPB, "World prison brief data." ttps://www.prisonstudies.org/country/ethiopia, 2020.

[137] A. Zumla, "Tuberculosis in prisons in sub-Saharan Africa-a potential time bomb," *South African Medical Journal*, vol. 101, no. 2, 2011.

[138] P. Moszynski, "Zambian prisons " threaten public health" because of high rates of TB and HIV," *BMJ: British Medical Journal (Online)*, vol. 340, 2010.

[139] A. Melese and H. Demelash, "The prevalence of tuberculosis among prisoners in Ethiopia: a systematic review and meta-analysis of published studies," *Archives of Public Health*, vol. 75, no. 1, pp. 1–9, 2017.

[140] WHO, "BCG vaccine." https://www.who.int/teams/health-product-and-policy-standards/standards-and-specifications/vaccines-quality/bcg, 2024.

[141] M. M. Ojo, O. J. Peter, E. F. D. Goufo, H. S. Panigoro, and F. A. Oguntolu, "Mathematical model for control of tuberculosis epidemiology," *Journal of Applied Mathematics and Computing*, vol. 69, no. 1, pp. 69–87, 2023.

[142] S. Kasereka Kabunga, E. F. Doungmo Goufo, and V. Ho Tuong, "Analysis and simulation of a mathematical model of tuberculosis transmission in democratic republic of the congo," *Advances in Difference Equations*, vol. 2020, no. 1, p. 642, 2020.

[143] U. T. Mustapha, B. Idris, S. S. Musa, and A. Yusuf, "Mathematical modeling and analysis of mycobacterium tuberculosis transmission in humans with hospitalization and reinfection," 2022.

[144] F. Biadglegne, U. Sack, and A. C. Rodloff, "Multidrug-resistant tuberculosis in Ethiopia: efforts to expand diagnostic services, treatment and care," *Antimicrobial Resistance and Infection Control*, vol. 3, no. 1, pp. 1–10, 2014.

[145] M. U. Nsuami and P. J. Witbooi, "Stochastic dynamics of an HIV/AIDS epidemic model with treatment," *Quaestiones Mathematicae*, vol. 42, no. 5, pp. 605–621, 2019.

[146] P. J. Witbooi, G. E. Muller, and G. J. Van Schalkwyk, "Vaccination control in a stochastic SVIR epidemic model," *Computational and Mathematical Methods in Medicine*, vol. 2015, 2015.